FORMULATION AND CHARACTERIZATION OF BEESWAX/ROSEMARY OIL NANOSTRUCTURED LIPID CARRIER FOR DRUG DELIVERY SYSTEM

FARHANIM BINTI MOHD LATIF

FACULTY OF SCIENCE
UNIVERSITI MALAYA
KUALA LUMPUR

2021

FORMULATION AND CHARACTERIZATION OF BEESWAX/ROSEMARY OIL NANOSTRUCTURED LIPID CARRIER FOR DRUG DELIVERY SYSTEM

FARHANIM BINTI MOHD LATIF

DISSERTATION SUBMITTED IN FULFILMENT OF THE REQUIREMENTS FOR THE DEGREE OF MASTER OF SCIENCE

DEPARTMENT OF CHEMISTRY
FACULTY OF SCIENCE
UNIVERSITI MALAYA
KUALA LUMPUR

2021

UNIVERSITI MALAYA

ORIGINAL LITERARY WORK DECLARATION

Name of Candidate: **FARHANIM BINTI MOHD LATIF**

Matric No: **SGR 150022 / 17057498/1**

Name of Degree: **MASTER OF SCIENCE**

Title of Dissertation ("this Work"): **FORMULATION AND CHARACTERIZATION OF BEESWAX/ROSEMARY OIL NANOSTRUCTURED LIPID CARRIER FOR DRUG DELIVERY SYSTEM**

Field of Study: **BIOCOLLOID**

I do solemnly and sincerely declare that:

(1) I am the sole author/writer of this Work;
(2) This Work is original;
(3) Any use of any work in which copyright exists was done by way of fair dealing and for permitted purposes and any excerpt or extract from, or reference to or reproduction of any copyright work has been disclosed expressly and sufficiently and the title of the Work and its authorship have been acknowledged in this Work;
(4) I do not have any actual knowledge nor do I ought reasonably to know that the making of this work constitutes an infringement of any copyright work;
(5) I hereby assign all and every rights in the copyright to this Work to the University of Malaya ("UM"), who henceforth shall be owner of the copyright in this Work and that any reproduction or use in any form or by any means whatsoever is prohibited without the written consent of UM having been first had and obtained;
(6) I am fully aware that if in the course of making this Work I have infringed any copyright whether intentionally or otherwise, I may be subject to legal action or any other action as may be determined by UM.

Candidate's Signature Date:

Subscribed and solemnly declared before,

Witness's Signature Date:

Name:

Designation:

FORMULATION AND CHARACTERIZATION OF BEESWAX/ROSEMARY OIL NANOSTRUCTURED LIPID CARRIER FOR DRUG DELIVERY SYSTEM

ABSTRACT

A stable colloidal suspension of nanostructured lipid carriers (NLCs) was synthesized from natural source of lipid. The toxicity and insolubility of drugs in water remain a significant problem and has led to the development of food-grade drug delivery systems such as nanostructured lipid carriers (NLCs). NLCs composing various amount of beeswax (BW), rosemary oil (RO) and poloxamer 188 (P188) were prepared by melt-emulsification combined with ultrasonication method. The physicochemical properties of NLC also were determined. Optimization of the formulation (F) was performed based on the criteria of stability. Formulation with the smallest particle size and highest magnitude of zeta potential was selected to be loaded with terbinafine hydrochloride (TBHC1) and hydrophilic molecule, which is calcein. Drug separation methods that applied in this study were centrifugal ultrafiltration and size exclusion chromatography method. The percentage of encapsulation efficiency, drug loading efficiency and drug release were evaluated. The optimized formulation composing 3.75 % BW, 1.25 % RO, 3 % P188 and 92 % deionized water. The mean of particle size and zeta potential for optimize NLC were (174 ± 2) nm and (-36 ± 5) mV, respectively. By using x-ray diffractometer (XRD) and differential scanning calorimeter (DSC), the optimized formulation of NLC showed a lower degree of crystallinity and melting enthalpy compared to solid lipid nanoparticle (SLN) of BW. The morphology of NLC was observed as spherical shape with a dense appearance in the transmission electron microscope (TEM) images. The encapsulation efficiency and loading efficiency were found dependent on the amount of TBHCl and calcein. The release of TBHC1 and calcein from the optimized formulation were (62.87±

0.04) % and (41.70 ± 0.09) % respectively. It can be concluded that NLC prepared from natural source of lipid may serve as a potential carrier for drug delivery.

Keywords: colloidal, beeswax, lipid, nanostructured lipid carrier

RUMUSAN DAN PENCIRIAN LILIN LEBAH/MINYAK ROSMARI PEMBAWA LIPID NANOSTRUKTUR UNTUK SISTEM PENGHANTAR DADAH

ABSTRAK

Ampaian koloid yang stabil bagi pembawa lipid nanostruktur (NLC) telah disintesis dari sumber semula jadi lipid. Ketoksikan dan ketidaklarutan dadah dalam air merupakan masalah utama yang menjurus kepada pembangunan sistem penghantar dadah seperti pembawa lipid nanostruktur (NLC). NLC yang dirumus mengandungi pelbagai jumlah lilin lebah (BW), minyak rosmari (RO) dan poloxamer 188 (P188) yang telah disediakan melaui kaedah pengemulsian cair yang digabungkan bersama ultrasonikasi. Sifat fizikokimia NLC juga dinilai. Pengoptimuman rumusan (F) dilakukan berdasarkan kriteria kestabilan. Rumusan dengan saiz zarah terkecil dan magnitud keupayaan zeta tertinggi telah dipilih untuk dimuatkan dengan terbinafin hidroklorida (TBHC1) dan molekul hidrofilik, yang merupakan calcein. Kaedah pemisahan dadah yang digunakan untuk kajian ini adalah kaedah pengultraturasan emparan dan kromatografi penyisihan saiz. Peratusan kecekapan pengkapsulan, kecekapan pemuatan dan pembebasan dadah dinilai. Perumusan yang dioptimumkan merangkumi 3.75% BW, 1.25% RO, 3% P188 dan 92% air ternyahion. Purata saiz zarah dan keupayaan zeta untuk rumusan optimum NLC ialah (174 ± 2) nm dan (-36 ± 5) mV. Dengan menggunakan pengukur pembelauan sinar-x (XRD) dan kalorimeter pengimbasan perbezaan (DSC), perumusan NLC yang dioptimumkan memperlihatkan darjah kehabluran dan entalpi lebur yang lebih rendah berbanding dengan nanopartikel lipid pepejal (SLN) dari lilin lebah. Morfologi NLC dapat diperhatikan sebagai berbentuk sfera dengan penampilan padat dalam imej mikroskop penghantaran electron (TEM). Kecekapan pengkapsulan dan pemuatan telah didapati bergantung kepada jumlah TBHC1 dan calcein. Kadar pelepasan TBHC1 dan calcein dari rumusan optimum masing-masing adalah (62.87 ± 0.04) % dan (41.70 ± 0.09)

%. Dapat disimpulkan bahawa, NLC yang disediakan dari sumber semula jadi lipid boleh berpotensi berfungsi sebagai pembawa penghantaran dadah.

Kata Kunci: koloid, lilin lebah, lipid, pembawa lipid nanostruktur

ACKNOWLEDGEMENTS

I am grateful to Allah for his blessings in giving me the strength and guidance in order for me to complete this dissertation. I would like to express my deepest appreciation to my supervisor, Dr. Teo Yin Yin for guiding me throughout the process of completing this master. She was very patient throughout this process. Every knowledges, suggestions, advices and motivations that she gave me are so valuable and useful for me to use in the future. The given opportunity, I have used to become a research assistant and finally postgraduate student from University of Malaya. Also, I would like to say my gratitude to my co-supervisor Prof. Misni Misran for his ideas and suggestions in improving my research's data.

Special thank you to University of Malaya for offering me Graduate Research Assistant Scheme (GRAS) for my first two semesters. Besides, my deepest gratitude to "Kementerian Pengajian Tinggi Malaysia" (KPTM) for the sponsored scholarship for me for last two semesters. My heartfelt gratitude also goes out to all lecturers and staffs in the Department of Chemistry for their assistance as well as the University of Malaya management.

My special thanks also to all colloid and surfaces laboratory colleagues. They are so kind, high tolerance and give the valuable encouragement and assistance throughout the research journey. Especially to Dr. Vicit Rizal Eh Suk, Dr. Premanayani Menon, Dr. Anita Marliana, Nurshafiqa Mohamed Sidin, Dr. Shahid Bashir Baig, Lim Qian Ying, Dr. Yew Han Choi, Dr. Sumaira Naem, Tiew Shu Xian, Rabiatul Adawiyah Mohd Ali, Assiela Aiman Lukhman and Tang Nyiak Tao. In this opportunity, I would like to express my thank you to those who involved directly or indirectly in helping me completing this research master.

Finally, I would like to express my biggest appreciation to my beloved parents and family for their encouraging, sacrificing and inspiring me throughout the research journey.

TABLE OF CONTENTS

ABSTRACT ..... **iii**

ABSTRAK ..... **v**

ACKNOWLEDGEMENTS ..... **vii**

TABLE OF CONTENTS ..... **ix**

LIST OF FIGURES ..... **xiii**

LIST OF TABLES ..... **xviii**

LIST OF SYMBOLS AND ABBREVIATIONS ..... **xix**

LIST OF APPENDICES ..... **xxi**

CHAPTER 1: INTRODUCTION **1**

1.1 Background Study 1

1.2 Problem Statement 2

1.3 Significance of Study 4

1.4 Scope of Study 4

1.5 Objectives 5

1.6 Thesis Outline 5

CHAPTER 2: LITERATURE REVIEW **6**

2.1 Drug Delivery System 6

2.1.1 Liposomes 6

2.1.2 Microemulsion 7

2.1.3 Solid Lipid Nanoparticles (SLNs) 7

2.2 Nanostructured lipid carrier (NLCs) 7

2.2.1 Types of NLCs 8

2.2.1.1 Imperfect Type (Imperfectly Structured Solid Matrix) 8

2.2.1.2 Amorphous Type (Structureless Solid Amorphous Matrix) 8
2.2.1.3 Multiple type (multiple oil in fat in water (O/F/W) carrier)..... 9
2.3 Materials used in the formulation of NLCs 9
2.3.1 Lipid 14
2.3.1.1 Beeswax (BW) 14
2.3.1.2 Rosemary oil (RO) 16
2.3.2 Surfactant..... 17
2.3.2.1 Poloxamer 188 (P188)..... 19
2.4 Preparation methods of NLCs 22
2.4.1 High pressure homogenization 22
2.4.2 Ultrasonication and/or high-speed homogenization..... 24
2.4.3 Solvent emulsification-evaporation technique 24
2.4.4 Melt-emulsification combined with Ultrasonication Method 25
2.5 Characterization of NLCs..... 25
2.5.1 Photon correlation spectroscopy (PCS)..... 25
2.5.1.1 Particle size and polydispersity index 26
2.5.1.2 Stability and zeta potential 27
2.5.2 Differential scanning calorimeter (DSC) 29
2.5.3 X-ray diffractometer (XRD)..... 31
2.5.4 Field emission scanning electron microscope (FESEM) and transmission electron microscope (TEM)..... 32
2.6 Optimization study of NLCs..... 35
2.7 Terbinafine hydrochloride (TBHC1)..... 36
2.8 Calcein. 38
2.9 Separation of non-encapsulated drug from NLCs 40
2.10 Drug release of NLCs 43

2.11 Applications of NLCs 47

CHAPTER 3: MATERIALS AND METHODOLOGY 52

3.1 Chemicals 52

3.2 Formulation NLCs and SLNs 52

3.2.1 Melt-emulsification combined with ultrasonication method 52

3.2.2 Design of experiments 53

3.2.3 Long-term stability studies 56

3.3 Encapsulation of TBHC1 or calcein in NLCs 56

3.4 Freeze-drying of NLCs and SLNs dispersion 57

3.5 Physico-chemical properties characterization 57

3.5.1 Particle size and zeta potential measurement 57

3.5.2 Differential scanning calorimeter (DSC) 58

3.5.3 X-ray diffractometer (XRD) 59

3.5.4 Field emission scanning electron microscope (FESEM) 60

3.5.5 Transmission electron microscope (TEM) 61

3.6 Preparation of standard calibration curve of TBHC1 in DW for encapsulation and drug loading efficiency study 63

3.7 Preparation of calcein standard calibration curve in DW for encapsulation and drug loading efficiency study 64

3.8 Encapsulation and drug loading efficiency of TBHC1 65

3.9 Encapsulation and drug loading efficiency of calcein 68

3.10 Preparation of TBHC1 standard calibration curve in 1:1 (v/v) ethanol: phosphate buffer saline for *In vitro* release study 69

3.11 Preparation of calcein standard calibration curve in 1:1 (v/v) ethanol: PBS solution for *In vitro* release study 70

3.12 *In vitro* drug release studies of TBHC1 and calcein 71

CHAPTER 4: RESULTS AND DISCUSSION 74

4.1 Solubility study of TBHC1 in solid and liquid lipid 74

4.2 Mixture Design 75

4.2.1 Modelling of the mixture design response 75

4.3 Particle Size 77

4.3.1 The effect of sonication time and amplitude percentage 77

4.3.2 The effect of lipid and surfactant composition on the particle size of NLCs and SLNs and Polydispersity Index (PDI) 79

4.4 Stability 84

4.4.1 Particle size and polydispersity Index (PDI) 84

4.4.2 Zeta Potential 95

4.5 Optimization of The Responses for NLC Formulations 101

4.6 Thermal properties analysis 103

4.7 Crystallinity of NLCs 107

4.8 Morphology of NLCs 110

4.9 Drug encapsulation and drug loading efficiency of TBHC1 in NLCs 111

4.10 Drug encapsulation and drug loading efficiency of calcein in NLCs 112

4.11 *In Vitro* drug release studies of TBHC1 from NLCs 114

4.12 *In Vitro* drug release studies of calcein from NLCs 118

CHAPTER 5: CONCLUSION 120

References 121

List of Publications and Papers Presented 138

Appendices 141

LIST OF FIGURES

Figure 1.1: Illustration of NLCs 2

Figure 2.1: Molecular structure of BW 16

Figure 2.2: Constituents of RO (1,8-cineole, α-pinene, champene) 16

Figure 2.3: The general structure of surfactant 18

Figure 2.4: Molecular structure of P188 20

Figure 2.5: High pressure homogenization 23

Figure 2.6 :(a) Coating NLC sample (b) Non-coating NLC sample 33

Figure 2.7: SEM micrograph of NLC prepared from modified beeswax, medium chain triglycerides oil, alkylpolyglucoside and ethanol (reprinted permission has obtained from Elsevier) 34

Figure 2.8: TEM micrograph of NLC prepared from triglycerides of caprylic/capric acid, glycerol monostearate type 1 EP and lauroyl macrogol-6-glycerides EP (reprinted permission has obtained from Elsevier) 35

Figure 2.9: Molecular structure of TBHC1 37

Figure 2.10: Molecular structure of calcein 40

Figure 2.11: Illustration of set-up for *in vitro* release from microspheres using the Float-a-Lyzer 45

Figure 3.1: Malvern Nano series Zetasizer (Malvern Instrument, UK) 58

Figure 3.2: Capillary cell 58

Figure 3.3: Differential scanning calorimeter 59

Figure 3.4: XRD sample 59

Figure 3.5 :(a) Sputter coater (b) Platinum coating process of sample 61

Figure 3.6: Diagram of TEM 62

Figure 3.7: UV-VIS absorption spectrum of TBHC1 in DW 63

Figure 3.8: Standard calibration curve of TBHC1 in DW 64

Figure 3.9: UV-VIS absorption spectrum of various calcein concentration in DW 65

Figure 3.10: Standard calibration curve of calcein in DW 65

Figure 3.11: Centrifuge (Dynamica, Velocity 18R) 67

Figure 3.12: (a) Centrifugal filter tube before centrifuge and (b) centrifugal filter tube after centrifuge 67

Figure 3.13: Calcein encapsulated in NLCs introduced dropwise onto the column 68

Figure 3.14: UV-VIS absorption spectrum of TBHC1 in 1:1 (v/v) ethanol: PBS solution 69

Figure 3.15: Standard calibration curve of TBHC1 in 1:1 (v/v) ethanol: PBS solution . 70

Figure 3.16: UV-VIS absorption spectrums of calcein in 1:1 (v/v) ethanol: PBS solution 71

Figure 3.17: Standard calibration Curve of calcein in 1:1 (v/v) ethanol: PBS solution.. 71

Figure 3.18: Franz diffusion cells (Hanson MicroettePlus™) 72

Figure 3.19: Vertical clear glass diffusion cell 73

Figure 3.20: Cary® 50 UV-Visible spectrophotometer 73

Figure 4.1: The influence of sonication time and amplitude percentage on particles size and polydispersity index of NLCs. 78

Figure 4.2: Particle size of NLCs and SLNs versus the percentage of P188 80

Figure 4.3: Polydispersity index (PDI) value of NLCs and SLNs versus of the percentage of P188 81

Figure 4.4: Particle size of NLCs and SLNs versus Percentage of RO 82

Figure 4.5: Size of particle and viscosity versus percentage of BW in SLNs. The SLNs displayed were F9 (BW (5%), RO (0%), P188 (5%), DW (90%)), F3 (BW (7.5%), RO (0%), P188 (5%), DW (87.5%)) and F13 (BW (10%), RO (0%), P188 (5%) DW (85%)). 83

Figure 4.6: (a) F17 (BW (3.75%), RO (1.25%), P188 (1%), DW (94%)), F16 (BW (3.75%), RO (1.25%), P188 (3%), DW (92%)) and F20 (BW (3.75%), RO (1.25%), P188 (5%), DW (90%)). 85

Figure 4.7: (a) Stable nanoparticles with the higher concentration of P188 (b) Less stable of nanoparticles with the lower concentration of P188. 86

Figure 4.8: Size of particle and polydispersity index versus time of storage (day). The NLCs displayed were F27 (BW (2.5%), RO (2.5%), P188 (1%), DW (94%)), F21 (BW (2.5%), RO (2.5%), P188 (3%), DW (92%)) and F12 (BW (2.5%), RO (2.5%), P188 (5%), DW (90%)). 87

Figure 4.9: Size of particle and polydispersity index versus time of storage (day). The NLCs displayed were F26 (BW (3.75%), RO (3.75%), P188 (1%), DW (91.5%)), F4 (BW (3.75%), RO (3.75%), P188 (3%), DW (89.5%)) and F15 (BW (3.75%), RO (3.75%), P188 (5%), DW (87.5%)). 88

Figure 4.10: Size of particle and polydispersity index versus time of storage (day). The NLCs displayed were F17 (BW (3.75%), RO (1.25%), P188 (1%), DW (94%)), F16 (BW (3.75%), RO (1.25%), P188 (3%), DW (92%)) and F20 (BW (3.75%), RO (1.25%), P188 (5%), DW (90%)). 89

Figure 4.11: Size of particle and polydispersity index versus time of storage (day). The NLCs displayed were F2 (BW (5%), RO (5%), P188 (1%), DW (895)), F6 (BW (5%), RO (5%), P188 (3%), DW (87%)) and F1 (BW (5%), RO (5%), P188 (5%), DW (85%)). 90

Figure 4.12: Size of particle and polydispersity index versus time of storage (day). The SLNs displayed were F11 (BW (5%), RO (0%), P188 (1%), DW (94%)), F14 (BW (5%), RO (0%), P188 (3%), DW (92%)) and F9 (BW (5%), RO (0%), P188 (5%), DW (90%)). 91

Figure 4.13: Size of particle and polydispersity index versus time of storage (day). The NLCs displayed were F5 (BW (5.625%), RO (1.875%), P188 (1%), DW (91.5%)), F19 (BW (5.625%), RO (1.875%), P188 (3%), DW (89.5%)) and F18 (BW (5.625%), RO (1.875%), P188 (5%), DW (87.5%)). 92

Figure 4.14: Size of particle and polydispersity index versus time of storage (day). The SLNs displayed were F25 (BW (7.5%), RO (0%), P188 (1%), DW (91.5%)), F24 (BW (7.5%), RO (0%), P188 (3%), DW (89.5%)) and F3 (BW (7.5%), RO (0%), P188 (5%), DW (87.5%)). 93

Figure 4.15: Size of particle and polydispersity index versus time of storage (day). The SLNs displayed were F8 (BW (10%), RO (0%), P188 (1%), DW (89%)), F22 (BW (10%), RO (0%), P188 (3%), DW (87%)) and F13 (BW (10%), RO (0%), P188 (5%), DW (85%)). 94

Figure 4.16: Value of zeta potential versus time of storage (day). The NLCs displayed were F27 (BW (2.5%), RO (2.5%), P188 (1%), DW (94%)), F21 (BW (2.5%), RO (2.5%), P188 (3%), DW (92%)) and F12 (BW (2.5%), RO (2.5%), P188 (5%), DW (90%)). 96

Figure 4.17: Value of zeta potential versus time of storage (day). The NLCs displayed were F26 (BW (3.75%), RO (3.75%), P188 (1%), DW (91.5%)), F4 (BW

(3.75%), RO (3.75%), P188 (3%), DW (89.5%)) and F15 (BW (3.75%), RO (3.75%), P188 (5%), DW (87.5%)). 96

Figure 4.18: Value of zeta potential versus time of storage (day). The NLCs displayed were F17 (BW (3.75%), RO (1.25%), P188 (1%), DW (94%)), F16 (BW (3.75%), RO (1.25%), P188 (3%), DW (92%)) and F20 (BW (3.75%), RO (1.25%), P188 (5%), DW (90%)). 97

Figure 4.19: Value of zeta potential versus time of storage (day). The NLCs displayed were F2 (BW (5%), RO (5%), P188 (1%), DW (89%)), F6 (BW (5%), RO (5%), P188 (3%), DW (87%)) and F1 (BW (5%), RO (5%), P188 (5%), DW (85%)). 97

Figure 4.20: Value of zeta potential versus time of storage (day). The SLNs displayed were F11 (BW (5%), RO (0%), P188 (1%), DW (94%)), F14 (BW (5%), RO (0%), P188 (3%), DW (92%)) and F9 (BW (5%), RO (0%), P188 (5%), DW (90%)). 98

Figure 4.21: Value of zeta potential versus time of storage (day). The NLCs displayed were F5 (BW (5.625%), RO (1.875%), P188 (1%), DW (91.5%)), F19 (BW (5.625%), RO (1.875%), P188 (3%), DW (89.5%)) and F18 (BW (5.625%), RO (1.875%), P188 (5%), DW (87.5%)). 98

Figure 4.22: Value of zeta potential time of storage (day). The SLNs displayed were F25 (BW (7.5%), RO (0%), P188 (1%) DW, (91.5%)), F24 (BW (7.5%), RO (0%), P188 (3%), DW (89.5%)) and F3 (BW (7.5%), RO (0%), P188 (5%), DW (87.5%)). 99

Figure 4.23: Value of zeta potential versus time of storage (day). The SLNs displayed were F8 (BW (10%), RO (0%), P188 (1%), DW (89%)), F22 (BW (10%), RO (0%), P188 (3%), DW (87%)) and F13 (BW (10%), RO (0%), P188 (5%), DW (85%)). 99

Figure 4.24: Value of zeta potential versus time of storage (day). The NLCs displayed F21 (BW (2.5%), RO (2.5%), P188 (3%), DW (92%)), F4 (BW (3.75%), RO (3.75%), P188 (3%), DW (89.5%)) and F6 (BW (5%), RO (5%), P188 (3%), DW (87%)). 100

Figure 4.25: Ternary contour plot showing the effect of mixture on the particle size (red lines) and zeta potential (blue lines) of the formulated lipid carriers fixed at 92% water content. 102

Figure 4.26: F16 (3.75% (BW), 1.25% (RO), 3% (P188), 92% (DW)) 102

Figure 4.27: Endothermic thermogram of starting materials, (a) BW, (b) RO and (c) P188. 103

Figure 4.28: Endothermic thermogram of (a) NLCs, F4, (BW:RO, 3.75:3.75), (b) NLCs, F16, (BW:RO, 3.75:1.25), (c) SLNs, F14, (BW:RO, 5:0)..... 104

Figure 4.29: DSC thermogram of (a) Optimized NLCs loaded with TBHC1, (b) TBHC1 106

Figure 4.30: Diffractogram of (a) BW, (b) P188, (c) SLNs, F14, (BW:RO, 5:0) (d) NLCs, F16, (BW:RO, 3.75:1.25) 107

Figure 4.31: Diffractogram of (a) Optimized NLCs encapsulated with TBHC1, (b) TBHC1 108

Figure 4.32: Diffractogram of (a) Optimized NLCs encapsulated with calcein, (b) Calcein 109

Figure 4.33: TEM Micrograph of NLCs (F16) (scale bar denotes size of 500 nm) 110

Figure 4.34: FESEM Micrograph of NLCs (F16)..... 111

Figure 4.35: The effects of TBHC1 concentration on encapsulation efficiency (solid square) and drug loading efficiency (empty triangle)..... 112

Figure 4.36: Encapsulation efficiency (%) versus concentration of calcien..... 113

Figure 4.37: Comparative in vitro release of TBHC1 in optimized NLCs, SLNs and free drug solution 115

Figure 4.38: Illustrated diagram for in vitro release mechanism of NLCs and SLNs with active ingredients in Franz diffusion cell..... 116

Figure 4.39: Comparative in vitro release of calcien in optimized NLCs, SLNs and free drug solution 119

LIST OF TABLES

Table 2.1: Examples of NLCs 10

Table 2.2: Marketed NLCs in cosmetic products 13

Table 2.3: Examples of homolipids 14

Table 2.4: Toxicity studies of P188 21

Table 2.5: List of NLCs preparation methods 22

Table 2.6: TBHC1 incorporated in drug delivery systems 37

Table 2.7: Toxicity studies of TBHC1 38

Table 2.8: Calcein in drug delivery system 39

Table 2.9: Equations of Mathematical Models 46

Table 2.10: Applications of NLCs 48

Table 3.1: Ranges and constraints of the mixture proportions 53

Table 3.2: The designed matrix and responses 54

Table 3.3: Formulations for the comparison of RO composition 55

Table 4.1: TBHC1 solubility in solid and liquid lipids 74

Table 4.2: Estimated regression coefficients for particle size and zeta potential 76

Table 4.3: Thermal properties of BW, P188, SLNs and NLCs 104

Table 4.4: Kinetic data obtained by using a different mathematical model for the release of TBHC1 117

Table 4.5: Kinetic data obtained by using a different mathematical model for the release of calcein 117

LIST OF SYMBOLS AND ABBREVIATIONS

°	:	Degree
℃	:	Degree celcius
μm	:	Micrometer
%	:	Percent
BW	:	Beeswax
CCD	:	Charge-coupled device
Da	:	Dalton
DSC	:	Differential scanning calorimeter
DL	:	Drug loading
DLE	:	Drug loading efficiency
EE	:	Encapsulation efficiency
F	:	Formulation
FESEM	:	Field emission scanning electron microscope
GRAS	:	Generally recognized as safe
g	:	Gram
g/mL	:	Gram/milliliter
HPLC	:	High performance liquid chromatography
J/g	:	Joule/gram
kDa	:	Kilodalton
LDDS	:	Lipid-based drug delivery systems
mL	:	Milliliter
mg/kg	:	Milligram/kilogram
mg/mL	:	Milligram/milliliter
mm	:	Millimeter

MWCO	:	Molecular weight-cut off
NLC	:	Nanostructured lipid carrier
NLCs	:	Nanostructured lipid carriers
P188	:	Poloxamer 188
PDI	:	Polydispersity index
HTCC	:	Positively charged chitosan derivative
R^2	:	Regression coefficient value
n	:	Release exponent value
RO	:	Rosemary oil
SEM	:	Scanning electron microscope
SLN	:	Solid lipid nanoparticle
SLNs	:	Solid lipid nanoparticles
cm^2	:	Square centimeter
TBHC1	:	Terbinafine hydrochloride
TEM	:	Transmission electron microscope
UV	:	ultraviolet
v/v	:	Volume/volume
w/v	:	Weight/volume
w/w	:	Weight/weight
XRD	:	X-ray diffractometer
ZP	:	Zeta potential

LIST OF APPENDICES

Elsevier License (reprinted permission)……. 141

Elsevier License (reprinted permission)……. 148

CHAPTER 1: INTRODUCTION

1.1 Background Study

Drug toxicity is one of the factors that contributes to the development of colloidal drug carriers. The evolution of colloidal drug carrier is prominent to improve drug safety and minimize the toxicity (Lim et al., 2012). Besides, colloidal drug carrier is able to enhance its bioavailability, avoid from chemical degradation, and reduce the bitterness taste of drug (Garg et al., 2017). The expansion of nanoscale drug delivery system including lipid-based nanoparticles also has been emerged as an alternative. It has the power of being a less chronic toxic for *in vivo* application and the ingredients usually are lipids of biocompatible and biodegradable (Ganesan & Narayanasamy, 2017).

NLCs is one type of lipid-nanoparticles that was firstly formulated at the end of the 1990s (Tamjidi et al., 2013; Granja et al., 2017). It was evolved from SLNs system. NLCs has attracted much attention in past decades as an alternative dosage form because of their biocompatibility, biodegradable, high bioavailability and good shelf-life. Besides, it can be readily produced in a large scale using certain tools at economical cost (Okonogi & Riangjanapatee, 2015). NLCs consists a mixture of solid lipid and liquid lipid (oil) (Weber et al., 2014). However, the solid lipid is the major component with the suggested amount in the range of 70 % to 99 %. In addition, solid lipids are existed in the form of solid phase at room and body temperature such as triglycerides, phospholipids and waxes (Doktorovova et al., 2014; Woo et al., 2014). The end product of NLCs has been represented as a cosmetic excipient and pharmaceutical product in the market. The example of marketed NLCs will be described in the literature review's chapter later (Pardeike et al., 2009; Saez et al., 2018). The Illustration diagram of NLCs has been displayed in the figure 1.1 (Livney, 2015).

Characterization of NLCs is an essential procedure due to the complexity of NLCs formulation system. It is fundamental to supervise its quality, stability and release kinetics (Rizwanullah et al., 2016).

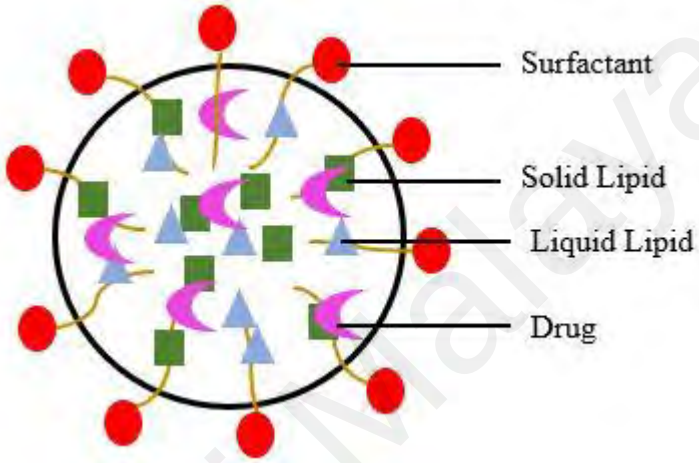

Figure 1.1: Illustration of NLCs

1.2 Problem Statement

The toxicity and insolubility of drug in water has been a main problem that lead to the development of drug delivery system like NLCs (Chime & Onyishi, 2013). BW and RO were chosen as solid and liquid lipid respectively in this research. Although many works have been reported on the preparation of NLCs but there is no study on the mixture between BW and RO. RO has been chosen in this experiment due to the antioxidant, antimicrobial and anticarcinogenic properties that possessed in this oil. Many studies have investigated the preparation of NLCs using a variety of lipid materials, for instance, fatty acids, triglycerides, phospholipids, and waxes (that are found as solid lipids at both room and body temperature); however, only a limited number of these reports have involved food-grade lipids that are generally recognised as safe (GRAS) that approved by Food and Drug Administration (FDA). Good applicability of NLCs from edible sources has

been demonstrated in the agricultural, food, and pharmaceutical industries (Nguyen et al., 2012; Lasoń et al., 2013).

The use of natural remedies as food preservative in the preparation of nanocarriers will create an inexpensive, renewable system with high acceptability among consumers (Keivani Nahr et al., 2018). Nowadays, the awareness among consumers regarding the connection between their nutritional habits and general health is increasing; hence, they are looking for foods containing multifunctional ingredients besides those necessary nutrients (Babazadeh et al., 2016). NLCs are also a potential encapsulation system in food science, which could be achieved using food-grade components. NLCs composed of food-grade drug and nutraceutical delivery formulations are a novel prospect of nanotechnology in nanodelivery science. The safety standard of food science is considered as important as pharmaceutical standards; however, it will have more serious consequences due to the long-term use of food as compared with drugs. Drugs are taken occasionally, while foods are consumed regularly; hence, health and safety standards used in food science could certainly be practiced in pharmaceutical sciences. NLCs can also aid oral delivery of bioactive food components that can protect and improve their functionality (Babazadeh et al., 2016).

Lipids are the major components of NLCs that can affect the stability, drug loading capacity and maintained the release behavior of the formulations. There also exist a few studies related to wax-based NLCs. Wax-based NLCs are believed to become a more stable system and display good particle size distribution (Soleimanian et al., 2018).

In this study, NLCs was prepared by using melt-emulsification combined with ultrasonication method. This preparation method is simple and environmental friendly due to no organic solvent used throughout their preparation. It is a current trend in NLC preparation. Organic solvent is use to solubilize the lipid. (Ganesan & Narayanasamy, 2017).

1.3 Significance of Study

SLNs has highly ordered crystal lattice due to the only solid lipid using in preparation. As a result, accommodation of drug in SLNs is limited. In order to enhance the drug loading capacity, liquid lipid is introduced in the formulation. The presence of liquid lipid creates the imperfection of crystal lattice which provides more space to accommodate drug. So, this is the reason to blend two different states of lipids to produce the best drug delivery system (Wissing et al., 2004).

NLCs can improve the stability of chemically-sensitive lipophilic ingredients (Yadav et al., 2013). In this context, the degradation rate of the active ingredients is slowed in the solid matrix as compared with the liquid matrix. The micro-phase separation between the active ingredients and carrier lipid, and within individual particles, can be managed to avoid the accumulation of active compounds at the surface of lipid particles where degradation used to take place. In addition, NLCs can maintain their solid state at room temperature by tuning the proportion of liquid lipid, aiding controlled release of the drug (Fu-Qiang Hu, 2005). Besides, NLCs can reduced the risks of drug leakage during storage by mixing the solid and liquid lipid in NLC formulations (Cirri et al., 2012).

1.4 Scope of Study

NLCs varying in composition of BW, RO and P188 were prepared. The physicochemical properties of the formulated NLCs such as particle size, zeta potential, crystallinity and morphology were investigated. The optimized formulation was determined according to the particle size and zeta potential values. Then, two types of drug were encapsulated in this optimized NLCs, which are TBHC1 as a hydrophobic drug, and calcein as a hydrophilic drug. The encapsulation and drug loading efficiency were determined from the encapsulated NLCs. Lastly, the drug release was evaluated.

1.5 Objectives

The objectives of this research are:

1) To formulate a physically stable NLCs from BW, RO and P188.
2) To study the physicochemical properties of the formulated NLCs.
3) To evaluate encapsulation, drug loading efficiency and drug release of NLCs

1.6 Thesis Outline

This thesis is structured into five chapters.

Chapter 1 presents a general review on NLCs that able to work as a good drug delivery system. The significance and scope of study also has been clearly described along with the objectives of work.

Chapter 2 highlights on the review of drug delivery system, materials that used in the preparation of NLCs, preparation methods and physico-chemical properties of NLCs. The separation method, drug release and applications of NLCs also has been reviewed.

Chapter 3 explains methodology that involved in this research works. Such as formulation of NLCs, encapsulation of TBHC1 and calcein. Then, characterization of physico-chemical properties also has been presented.

Chapter 4 reports and discuss on the result obtained from experiment itself.

Chapter 5 concludes all the research works that has been done. In this chapter, the results have been summarized while future works also has been structured.

CHAPTER 2: LITERATURE REVIEW

2.1 Drug Delivery System

Drug delivery systems can help to introduce foreign substances into our body through various techniques and generate the desired effect for disease treatments. In addition, this system is able to transport medicines to the exact location (illness area) in our body where a drug is released into the body. It is capable in reducing or even eliminating the side effects of drugs and the damage of surrounding tissue at treatment site.

Drug delivery system or colloidal drug carrier is very crucial to help the delivery process of active ingredient (drug) into a human body efficiently. In general, most drugs have poor water solubility and high toxicity characteristics that can lead to enzymatic deterioration. These posed a great challenge in drug delivery systems due to the limited absorption process of drugs in human body. Thus, development of new formulation strategies is escalating over the years to overcome this limitation. Many researchers have joined hands to create the excellent drug carrier that able to incorporate and shield the drug to transport it to the action site. There are many types of lipid-based drug delivery systems (LDDS) including liposomes, microemulsion, SLNs and NLCs have been created and capable to solve the current problems (Chime & Onyishi, 2013).

2.1.1 Liposomes

Liposomes is a spherical vesicle that produced by the hydration of surfactant that mixed with water under a low shear force. It comprises membrane that consists of one or more lipid bilayer. Usually, the bilayer is formed from phospholipid. Liposome is a flexible carrier that has the ability to entrap water-soluble and water-insoluble ingredients (Tamjidi et al., 2013). The encapsulated drug liposome can prevent the toxicity of drug and capable to target the drug delivery to the site of action. Unfortunately, the main

limitation of liposomes is instability during storage. It has high tendency to aggregate and fuse during storage (Meland et al., 2014).

2.1.2 Microemulsion

Microemulsions is a transparent, thermodynamically stable and isotropic liquid dispersion. The basic materials needed to prepare microemulsion are oil, surfactant, co-surfactant and dispersed phase (Güngör et al., 2013). A ternary phase diagram is commonly prepared in the formulation of microemulsion. It represents the behavior of dispersed phase, oil, surfactant and co-surfactant. The properties of microemulsion can be investigated through its solubility, and viscosity. During the changes of environmental condition, they are disposed to disintegrate. Eventually, they are regularly difficult to encapsulate large lipophilic molecules in particle structure due to the optimum curvature of the surfactant monolayer (Tagavifar et al., 2018).

2.1.3 Solid Lipid Nanoparticles (SLNs)

SLNs is an oil in water emulsion containing solid lipids as the oil phase. This system is produced from a single or blends of solid lipid. It is an alternative formulation to unite all the advantages of others drug delivery systems and to avoid some of their deficiencies. It has a highly ordered crystalline structure due to the solid nature of lipid. However, there is a restricted space remains for drug incorporation. Drug leakage may occur during storage due to the lipid transformation from high energy modification into more ordered modification (β) (Uner, 2006; Fathi et al., 2018).

2.2 Nanostructured lipid carrier (NLCs)

NLCs is a new generation of drug delivery system that has been developed to overcome the limitations of SLNs. NLCs was prepared from the combination of solid and liquid lipid. This lipids combination generates an imperfect matrix that enable incorporation and protection of the bioactive compounds efficiently. In addition, benefits of NLCs including

high encapsulation efficiency, good stability, non-toxicity, suitability for industrial processing and higher drug release compared to the SLNs. Besides, it also can reduce the drug expulsion during storage and avoid the risk of gelation in formulations (Tetyczka et al., 2017).

2.2.1 Types of NLCs

Different types of NLC can be obtained based on the preparation method and composition of lipids blend. There are imperfect type (imperfectly structured solid matrix), amorphous type (structureless solid amorphous matrix) and multiple type (multiple oil in fat in water (O/F/W) carrier).

2.2.1.1 Imperfect Type (Imperfectly Structured Solid Matrix)

It can be prepared by mixing solid lipids with sufficient amount of liquid lipids (oil) in NLC formulation. The formation of imperfect NLCs can be achieved by the using of caprylocaproylmacrogol-8-glycerides (Labrasol®) and oleoyl macrogol-6-glycerides (Labrafil® M 1944 CS) (Liu et al., 2014; Safwat et al., 2017). With the addition of glycerides that contained different fatty acid chain length, the NLCs matrix is not able to form a highly ordered structure. Therefore, it created an available space and imperfect solid matrix with many voids that enable incorporation of active ingredient (Ganesan & Narayanasamy, 2017).

2.2.1.2 Amorphous Type (Structureless Solid Amorphous Matrix)

This type of NLCs can be accessed by combining solid lipids for examples hydroxyl octacosanyl hydroxy stearate, isopropyl myristate, isopropyl palmitate and dibutyl adipate. Lipid matrix of NLCs is existed in the non-crystalline (amorphous state) lipid nanoparticles. In addition, it is capable to reduce the crystallinity properties of NLCs after homogenization and cooling process. As known, drug expulsion will be happened from

the process of lipid crystallization during storage. So, it can be prevented by adding the special structure of lipid in NLC formulations (Singhal et al., 2011).

2.2.1.3 Multiple type (multiple oil in fat in water (O/F/W) carrier)

Multiple type of NLCs can be prepared by mixing the higher amount of liquid lipid compared to the solid lipid in the formulation. Nano-compartment oil is formed inside the solid lipid matrix of NLCs. From that, the drug will be more solubilize in the liquid lipid compared to the solid lipid. Drug expulsion also can be avoided by preventing the crystallinity of solid lipid with the addition of higher amount of liquid lipid in it (Rizwanullah et al., 2016).

2.3 Materials used in the formulation of NLCs

The basic materials required to prepare NLCs are lipid, surfactant and water. NLCs can be produced by using a different starting material. Table 2.1 displayed the examples of NLCs in the past research, while marketed NLCs applied in cosmetic products are listed in the table 2.2

Table 2.1: Examples of NLCs

Solid Lipids	Liquid Lipids	Drugs	Surfactants	References
Stearic acid	Oleic acid	Donepezil	Lecithin and sodium taurodeoxycholate	(Mendes et al., 2019)
		Aceclofenac	P188	(Patel et al., 2012)
		Clobetasol propionate	Sodium dodecyl sulfate	(Hu et al., 2005)
		Fluconazole	Span 80 and Tween 80	(Kelidari et al., 2017)
		Progesterone	Tween 20, monostearin & polyethylene glycol monostearate	(Yuan et al., 2007)
		Simvastatin	Pluronic F-68 and lecithin	(Fathi et al., 2018)
Glyceryl monostearate	Labrasol	TBHC1	Pluronic F-127	(Gaba et al., 2015)

Table 2.1: Continued

Solid Lipids	Liquid Lipids	Drugs	Surfactants	References
Hydrogenated soybean lecithin	Castor oil	-	P188	(Dora et al., 2012)
Cetyl palmitate	Capmul® MCM (mono-diglyceride of medium chain fatty acid)	Resveratrol	P188, tween 80 and acrysol K150	(Rajput & Butani, 2019)
1)Fully hydrogenated sunflower oil 2)Fully hydrogenated rapeseed oil	1) Soybean oil 2) Medium chain triglycerides (MCT)	Conjugated linoleic acid	Tween 80	(M. Zheng et al., 2013)
Glyceryl monostearate	Castor oil	Bromonidine tartrate	P188 (pluronic F68)	(El-Salamouni et al., 2015)
Glycerol monostearate	Oleic acid	Simvastatin	Poloxamer 407	(Tiwari & Pathak, 2011)
Orange Wax	Rice bran Oil	Lycopene	Eumulgin SG	(Kaur et al., 2015)
Glyceryl palmitostearate	Medium chain triglycerides	Betasitosterol	Poloxamer 407 and Tween 80	(Bagherpour et al., 2017)
Saturated fatty acid of C18 and glyceryl behenate	Castor oil and caprylic/capric triglycerides	Flurbiprofen	Tween 80	(González-Mira et al., 2011)
Glyceryl palmitostearate	Triacetin and phosal® 53 MCT	Bicalutamide	Poloxamer 407	(Kumbhar & Pokharkar, 2013)
Glyceryl palmitostearate	Squalene	Triamcinolone acetonide	P188	(Araújo et al., 2011)

Table 2.1: Continued

Solid Lipids	Liquid Lipids	Drugs	Surfactants	References
Glyceryl monostearate and stearic acid	Media chain triglyceride	Quercetin	Soy lecithin	(Chen-yu et al., 2012)
Glycerin monostearate	Oleic acid	Oleanolic acid and gentiopicrin	P188	(Zhang et al., 2013)
Tristearin	Oleic acid	Minoxidil	P188	(Uprit et al., 2013)
Glycerol monostearate	Medium triglyceride chain	Oridonin	P188, polyethylene glycol monostearate and lecithin	(Jia et al., 2012)
Glyceryl palmitostearate	Sunflower oil	Astaxanthin	Tween 40 and poloxamer 407	(Rodriguez-Ruiz et al., 2018)

Table 2.2: Marketed NLCs in cosmetic products

Product name	Producer/distributor	Main active ingredients	Year
Cutanova cream Nanorepair Q 10	Dr. Rimpler	Q 10, polypeptide, hibiscus extract, ginger extract, ketosugar	2005
SURMER Elixir du Beauté Nano-Vitalisant	Isabelle Lancray	Coconut oil, Monoi Tiare Tahiti®, pseudopeptide, milk extract from coconut, wilder ginger, Noni extract	2006
Supervital	Amore Pacific	Coenzyme Q 10, co-3 and co-6 unsaturated fatty acids	2007
NanoLipid Basic CLR	Dr. Kurt Richer, CLR Berlin	Caprylic/capric triglycerides	2006
Reconstruction Serum hexapeptide-8, highly active oligosaccharides	Beate Johnen	Q10, actyl	2007
Olivenöl Anti Falten Pflegekonzentrat	Dr. Theiss	Olea, europaea oil, panthenol, acacia Senegal, tocopheryl	2008
Regenerationscreme Intensive	Scholl	Macadamia ternifolia seed oil, avocado oil, urea, black currant seed oil	2007

(Müller et al., 2007; Pardeike et al., 2009; Kaul et al., 2018; Battaglia & Ugazio, 2019)

2.3.1 Lipid

Lipid is an organic compound that consists of fatty acid and its derivatives. Some of lipids may soluble in alcohol. Carboxylic acid of fatty acid offers a good interaction between fatty acid and alcohol via ester linkage. Solid lipids can be divided into several classes depend to their chemical composition, which are homolipids, heterolipids and complex lipids (Attama et al., 2012).

Homolipids are esters of fatty acid with alcohols. This type of lipid consists of carbon (C), hydrogen (H) and oxygen (O). So, it is referred to as a simple lipid. The number of carbon in the long-chain fatty acid is usually range between 14 to 24 carbons. It is found typically in a common fat. Besides, the medium-chain fatty acid possesses 6 to 12 carbons. Homolipids is regularly found in coconut oil and palm kernel oil in the form of triacylglycerol. Examples of homolipids are explained in the table 2.3.

Table 2.3: Examples of homolipids

Types	Examples
cerides – Simple lipids that are esters of higher monohydroxy alcohols and fatty acids.	waxes: beeswax, carnauba wax,
glycerides – Ester of glycerol especially with fatty acids.	fat and oils
steride	esters of cholesterol with fatty acids

2.3.1.1 Beeswax (BW)

BW is obtained from the honeycombs of bees after removal of honey by centrifugation. The combs are melted with hot water, steam or exposed to solar heat to remove insoluble impurities. Insoluble impurities were possibly come from brood comb. After that, the liquid wax is sent for further purification by re-melting and treatment with activated carbon, aluminium, magnesium silicates or diatomaceous earth. Then, the treated melt is

eventually submitted to the pressure filtration to obtain a food-grade yellow BW. Bleaching the BW is also available to yield a white BW by using hydrogen peroxide, sulphuric acid or sunlight.

Yellow BW became brittle when cold and appears as dull, granular and non-crystalline fracture when broken. It has a properties of honey odor. BW is insoluble in water and moderately soluble in alcohol. However, it is very soluble in chloroform, ether, hydrocarbon solvent and volatile oils. It is partially soluble in a cold carbon disulphide and completely soluble in it at the temperature of 30 °C and above. BW contains flavonoids, antioxidant, antibacterial and antifungal compound. These compounds capable to treat dermatitis, psoriasis and skin fungal infections. BW also has been used in food application. It adopted as a component in dietary food supplements (soft gelatine capsules and tablets), glazing and coatings, chewing gum, flavoured drinks and as a carrier for food additive (Al-Waili, 2005).

BW is made up from combination of organic substances. It mainly composed of palmitate, palmitoleate, hydroxypalmitate and oleate esters of long chain (C30-C32) aliphatic alcohol. It's usually existed as an ester with long hydrocarbon chains as displayed in figure 2.1. Hydrolysis of BW yields a straight chain of carboxylic acid and alcohol. The presence of significant amount of free fatty acids contributes to the viscoelastic behaviour of BW (Fabra et al., 2009). However, the composition of BW is depending to some extent on the subspecies of the bees, the age of wax and the climatic circumstances of its production. This variation in composition occurs mainly in the relative amounts of the different components present, rather than in their chemical identity (Negri et al., 2000).

BW has been used in the colloidal systems as drug delivery vehicles. From the past research, BW and carnauba wax were used to produce SLNs that encapsulated ketoprofen

(drug) (Kheradmandnia et al., 2010). As mentioned by Rosita and the group, SLNs has been produced from BW and glyceryl monostearate that loaded with para methoxy cinnamic acid (drug) (Rosita et al., 2014). Moreover, lipid matrices also has been formulated from BW and goat fat by Attama and the team (Attama et al., 2007). The same group researches also have developed a lipid matrices between theobroma oil and BW (Attama et al., 2006).

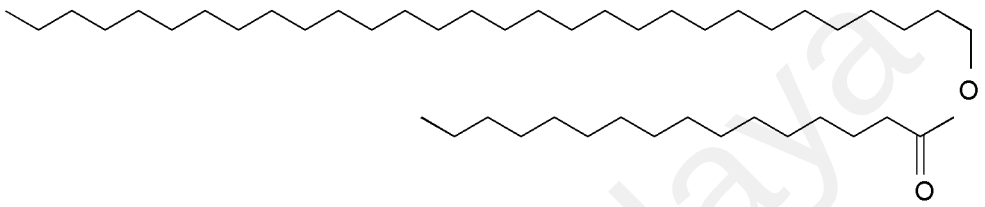

Figure 2.1: Molecular structure of BW

2.3.1.2 Rosemary oil (RO)

RO is a long-lasting evergreen aromatic herb that extensively spread and cultivated in the Mediterranean region. It consists of phenolic constituents mainly monoterpenes such as 1,8 -cineole, α-pinene, camphor and camphene as shown in the figure 2.2. It possess various therapeutically effects include antioxidant, antimicrobial and anticarcinogenic (Turasan et al., 2015). Hence, RO is a suitable candidate in the formulation of NLCs for topical application.

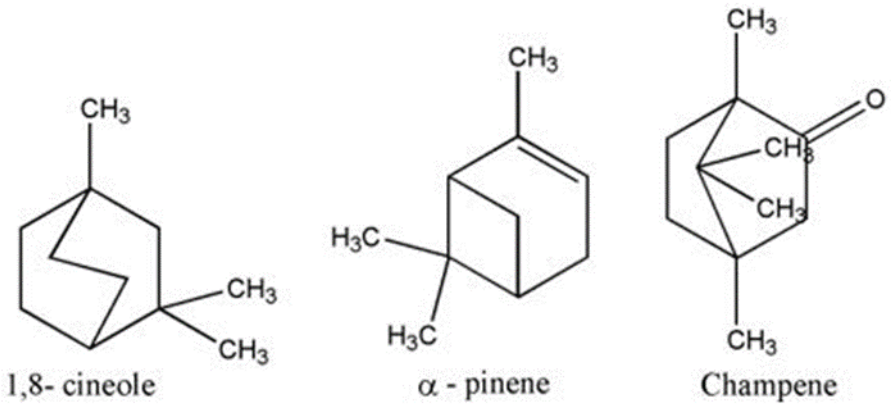

Figure 2.2: Constituents of RO (1,8-cineole, α-pinene, champene)

RO also has been formulated with cetyl palmitate, glyceryl oleate and polyoxyethylene-20-oleyl ether in the preparation of NLCs (Montenegro & Pasquinucci, 2017). However, RO also has been implemented in the other drug delivery systems, which were emulsion, nano-liposome, gel, SLNs and nanocapsules (Akbari et al., 2015; Turasan et al., 2015; Aarabi, 2017; Montenegro & Pasquinucci, 2017; Rubenick et al., 2017).

2.3.2 Surfactant

Surfactant is 'surface-active' molecule, that usually existed in aqueous solutions. This surface-active molecule will adsorb at the interfaces. The adsorption action can be occurred as a response to the solvent used (dispersed phase like DW and phosphate buffer saline solution) and chemical structure of the surfactant itself. The structure of surfactant is a combination of both polar and non-polar group in a single molecule, which is called an amphiphile. So, it has both of hydrophilic and hydrophobic moieties or "head" and "tail", respectively that enable adsorption of the molecule at interfaces effectively.

Figure 2.3 showed a general structure of surfactant (surface-active material). It includes hydrophilic head group and hydrophobic tail. Hydrophilic head or lyophilic group having a high affinity towards water or solvent. While, hydrophobic tail or lyophobic group having low affinity towards water or solvent.

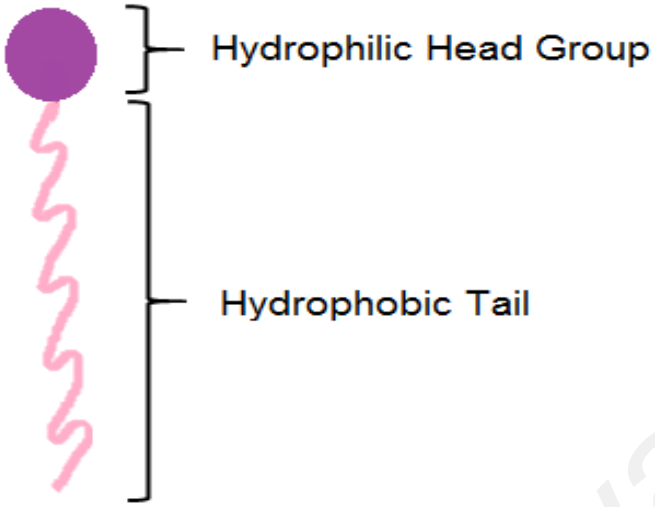

Figure 2.3: The general structure of surfactant

Type of surfactants is depending to its structure, which is head and tail group of surfactants. The head group can be charged or neutral in with a small or compact size. Normally, the hydrophilic part responsible for its solubility in a solvent through the formation of ionic interaction or hydrogen bonding. Generally, the tail group can be existed in a single or double chain. Furthermore, it can be straight or branched hydrocarbon chain. However, it may also be existed as a fluorocarbon, siloxane or aromatic groups.

Surfactant should be used in the formulation of NLCs to stabilize the lipid dispersion. Variety of emulsifiers different in charge and molecular weight could be used. Without the presence of surfactant in NLCs, it is impossible to reach a stable NLCs formulation. It also helps in manipulating the size of NLCs into nanometer range. In certain condition, blending of two or more surfactants will form a sufficient coverage viscosity that can promote stability in NLCs (Trotta et al., 2003). As mentioned by Mendes and the group, the mixture between lecithin and sodium taurodeoxycholate can produced a more stable NLCs formulation than the use of only lecithin (Mendes et al., 2019).

Cationic surfactants like linear alkyl-amines and alkyl-ammoniums are more toxic compared to anionic surfactants like soaps and other carboxylates. However, nonionic surfactants such as P188, polysorbates, polyethylene glycol (PEG) and polyvinyl alcohol are investigated as a safest surfactant compared to the others surfactant. This is because nonionic surfactant was reported as a non-toxic within certain specific limit. (Rizwanullah et al., 2016).

2.3.2.1 Poloxamer 188 (P188)

P188 is a non-ionic surfactant with hydrophile-lypophile balance (HLB) number ~29. The other name of P188 is Pluronic F-68. It does not ionize in aqueous solutions. Therefore, it is less sensitive to electrolyte compared to the ionic surfactants. Furthermore, it was found compatible with the other colloidal carriers and has been used in the formulation of pharmaceuticals, cosmetics and food products. It exhibits minimum toxicity that able to control a release and targeted a delivery applications (Tamjidi et al., 2013). Clinical testing presented that P188 would cure the constipation disease by increase the hydration of faeces for easier passage during defecation. Furthermore, it could increase the membrane repair capacity in various cell and tissues. It also can work as an antimicrobial agent for certain species of microbes. Besides, P188 can caused a declined of bacterial growth to the below of control cultures level.

P188 can sterically stabilize the NLCs by covering the surface of NLCs. Figure 2.4 showed the molecular structure of P188 (Singh-Joy & McLain, 2007). It is a triblock copolymer that consisted central polyoxypropylene molecule, which is connected by two hydrophilic POE chains. They are ethylene oxide and propylene glycol (PEG) (Singh-Joy & McLain, 2007). Refer to the molecular structure of P188, there is no charges for the triblock copolymer in it. Thus, it has less interaction towards the lipids. Toxicity studies of P188 also has been tableted in the table 2.4.

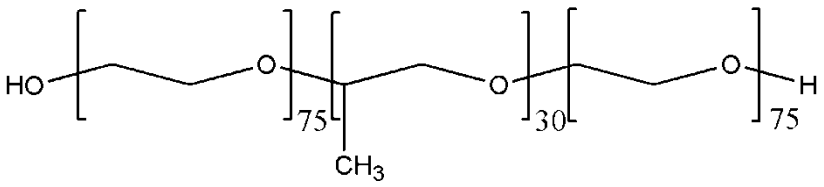

Figure 2.4: Molecular structure of P188

Table 2.4: Toxicity studies of P188

Toxicity studies			References
Amount applied	Samples (Human/Animal)	Results	
-	Humans - 10 volunteer's forearms	No skin irritation was observed. After 10 days rest, no skin sensitization data had realized in any volunteers.	(Singh-Joy & McLain, 2007)
10%	Rabbit	0.5% hemolysis	(Lowe et al., 1995)
More than 4%	Rat blood	Minor hemolysis	
10%	Rat blood	(4.7 ± 1.5) % mean hemolysis.	
10%	Rat	Mean of hemolysis was noticed only at (0.5 ± 0.3) %. The researchers conclude that the using of purified P188 may be preferable for intravascular applications formulation.	
-	Red blood cell	It could decrease a red blood cell aggregation.	(Armstrong et al., 2001)
(30, 100, 300, 720, 2400 or 72000 mg/kg/day) were given continuously via intravenous infusion for 30 days	Twenty male and female dogs	Afterwards, plasma samples were taken during and after infusion. At the day 7, it reached a safe state for all dose group and remained stable throughout the administration. In conclusion, it displayed no effect of dose and gender of the P188 concentration on the plasma concentration.	(Grindel et al., 2002)

2.4 Preparation methods of NLCs

A numerous attractive chemical method has been evolved for the formulation of NLCs. It is very challenging in order to optimize the green preparation method of NLCs. A variety of methods have been developed in NLCs as shown in the table 2.5.

Table 2.5: List of NLCs preparation methods

No.	Methods	References
1)	High Pressure Homogenization	(Hung et al., 2011; Tetyczka et al., 2017)
2)	Ultrasonication/ High Speed Homogenization	(Nnamani et al., 2014; Kelidari et al., 2017; Khurana et al., 2017)
3)	Solvent Emulsification- Evaporation Technique	(Sjöström et al., 1995; Dubes et al., 2003; Shahgaldian et al., 2003; Wissing et al., 2004)
4)	Solvent Emulsification-Diffusion Technique	(Yuan et al., 2007)
5)	Supercritical fluid method	(Chattopadhyay et al., 2007; Chen et al., 2009)
6)	Microemulsion based method	(Lin et al., 2007)
7)	Spray Drying Method	(X. Zhang et al., 2008; Livney, 2015; Xia et al., 2016)
8)	Double Emulsion Method	(Häuser et al., 2015; Pelegri-O'Day & Maynard, 2016)
9)	Solvent Injection Technique	(Pandita et al., 2009)
10)	Membrane Contractor Method	(Charcosset et al., 2005)

2.4.1 High pressure homogenization

There are two general methods to achieve high pressure homogenization, which are hot homogenization and cold homogenization (Jain et al., 2017). The benefits of this method are low in capital cost and can be demonstrated at the lab scale. However, this method required intensive process energy, produce unproven scalability, polydisperse distribution of particle size and can cause biomolecule damage. The procedure of this technique can be referred in the figure 2.5.

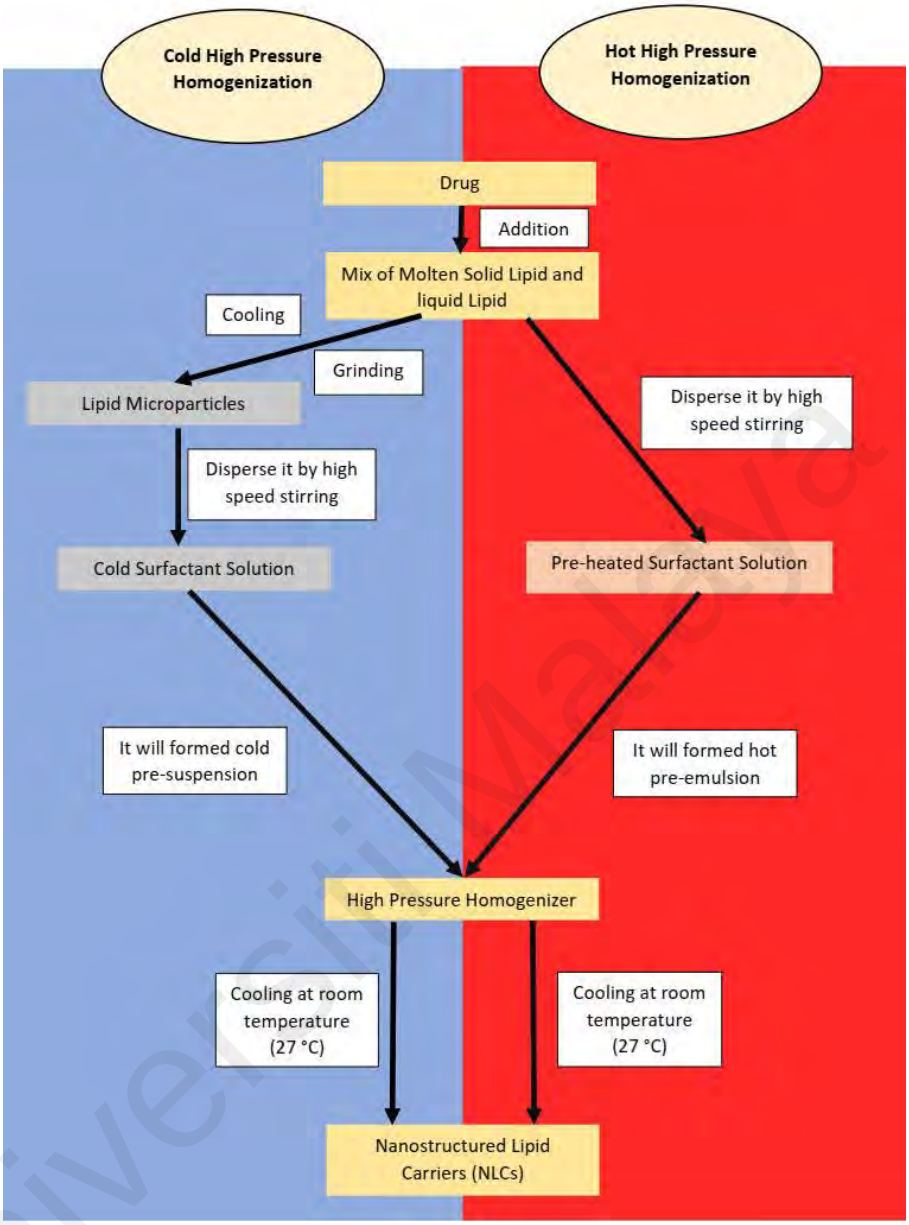

Figure 2.5: High pressure homogenization

For hot high pressure homogenization, drug was added to the mixture of the molten solid and liquid lipid. Then, it was dispersed in pre-heated surfactant solution by high speed stirring. Next, it formed a hot pre-emulsion. Later, this hot pre-emulsion was homogenized by high pressure homogenizer. After that, the NLCs was formed by cooling it at room temperature.

In addition, for cold high pressure homogenization, drug was blended to the mixture of molten solid and liquid lipid. After that, this active mixture was cooled down and ground it to form lipid microparticles. Afterwards, this lipid microparticles was dispersed in a cold surfactant solution by high-speed stirring to form cold pre-suspension. Subsequently, the sample must be cooled at room temperature before subjected to high pressure homogenizer to produce NLCs.

2.4.2 Ultrasonication and/or high-speed homogenization

Small size NLCs can be acquired by using combination of these two methods, which are ultrasonication and high-speed homogenization. These techniques are easy to be carried out and accessible in most of the laboratory. The mixture of lipids is melted at temperature higher than 5 °C to 10 °C from its melting point. Then, hot surfactant solution is dispersed in lipids mixture at the same temperature under high-speed homogenization. Then, NLCs is formed by cooling down the pre-emulsion to room temperature (Uner, 2006).

Comparing with the other technique, the advantage of this technique is can reduce a shear stress, which is tending to cause deformation of material by slippage along a plane or planes parallel to the imposed stress. However, metal contamination may occur in NLCs product and unproven scalability will be produced (Ganesan & Narayanasamy, 2017).

2.4.3 Solvent emulsification-evaporation technique

In this preparation technique, the lipophilic material and hydrophobic drug were dissolved in water immiscible organic solvents (for example cyclohexane, dichloromethane, toluene and chloroform). Then, it was emulsified in an aqueous emulsifier solution by using high speed homogenizer. Next, the pre-emulsion was directly passed through the microfluider to enhance the efficiency of fine emulsification process.

After that, the organic solvent was evaporated through a mechanical stirring at room temperature (Singhal et al., 2011). However, this method will produced a low concentration of final NLCs in a solvent residue (Tamjidi et al., 2013).

2.4.4 Melt-emulsification combined with Ultrasonication Method

This method was chosen for this work. Firstly, the mixture of lipids will be melted at 10 °C higher than the solid lipid's melting point. Then, a hot surfactant solution will be poured into the molten lipids. It will be homogenized and sonicated after the addition of surfactant by using homogenizer or probe sonicator. Finally, this emulsion will be poured into cold water to form NLCs. The advantages of this method are simple, and no organic solvent required in the preparation.

2.5 Characterization of NLCs

Characterization of the prepared NLC formulations is very important. It is also essential procedure due to the complexity of NLC formulation system. It is fundamental to supervise its quality, stability and release kinetics (Rizwanullah et al., 2016). The physicochemical properties are also necessary to control the quality and monitor the stability of formulated NLCs. The physicochemical properties will be studied by using various instruments, which are:

2.5.1 Photon correlation spectroscopy (PCS)

Photon correlation spectroscopy (PCS) or zetasizer is used to study the particle size, zeta potential and polydispersity index of NLCs. It is also known as dynamic light scattering instrument. The fluctuation of scattered light intensity caused by particles movement is measured. This technique could measure the diffusion of particles that move under the brownian motion principle and correlate with hydrodynamic particle size.

2.5.1.1 Particle size and polydispersity index

The physical stability of NLCs is very crucial in determine the potential product application. NLCs are heterogeneous system and thermodynamically unstable. It tends to lose their physical stability during storage. So, it is important to monitor the NLCs size within certain period of time to ensure the formation of a stable dispersion with limited or no aggregation. Changes of particle size can be used as an instability characteristics because the size is possible to rise before a macroscopic changes appear (Heurtault et al., 2003). The particle size of NLCs can be influenced by variety parameters, such as lipid matrix, surfactant, production methods, conditions and the storage period (K. Zheng et al., 2013).

The NLC formulation with high surfactant concentration will promote a complete emulsification process and more produce formation of NLCs with rigid structure. Thus, the size of NLCs can be modified. The small size of NLCs tends to form a stable dispersion and against sedimentation. Based on the past research, the size of NLCs was seen decreased with the increasing amount of surfactant (Heurtault et al., 2003). The presence of surfactant reduced the interfacial tension between lipid and solvent which increases the surface area of the dispersed solvent-lipid droplets that start to form a smaller particle. Furthermore, the insufficient of surfactant concentration may lead to instability of NLCs dispersion (Michael et al., 2009).

The particle size of NLCs previously prepared from various synthetic and petroleum type of lipids are in the range of (1090 ± 6) nm to (165 ± 6) nm. Garcia-Orue and the team produced NLCs in the size of (220 ± 54) nm. They prepared NLCs from Precitol® ATO 5 (solid lipid), Miglyol® 812 N (liquid lipid), P188 and Tween® 80 (surfactant) (Garcia-Orue et al., 2016). Besides, Beloqui and the group formulated NLCs in the range of size (1090 ± 6) nm and (165 ± 6) nm (Beloqui et al., 2013). In addition, the size of NLCs was

found at (231.3 ± 15.7) nm and (212.9 ± 26.7) nm by Mendes and the group. They synthesized NLCs from a different composition of glyceryl behenate, triglyceride of capric/caprylic acids and Tween® 80 (Mendes et al., 2013). Zhang and friends have prepared NLCs in the size of (208 ± 4.52) nm and (209.5 ± 2.53) nm from a different ratio of isopropyl myristate (solid lipid), stearyl alcohol (liquid lipid), poloxamer 407 and sodium hydrogen N-(-1-oxooctadecyl)-L-glutamate) (Zhang et al., 2017).

Polydispersity index (PDI) is a parameter for analysis of particle size homogeneity. The PDI varied from 0 to 1 value. If the PDI value is near to zero, it indicates a high homology size of NLCs. If the PDI value is close to 1, the size of particle are polydisperse. With the low PDI value, the NLCs size distribution is uniform and presented a good reproducibility. Ammar and the team prepared NLCs in the range of PDI value from 0.13 until 0.39 (Ammar et al., 2016). Based on the past research, all formulation of NLCs exhibited a similar value of PDI in the range value of 0.2 (Baek et al., 2015).

2.5.1.2 Stability and zeta potential

Zeta potential (Taymouri et al.) is a parameter to estimate the stability of a colloidal system. It is an essential aspect that acknowledges the prediction physical stability of a colloidal dispersion. The higher magnitude of zeta potential, either positive or negative, tends to produce a stable formulation. In general, a colloidal suspension is considered as a stable system when ZP value is higher than the absolute value of 30 mV (Iqbal et al., 2012). Normally, particle aggregation is less likely to happen among charged particles (high zeta potential) due to electrostatic repulsion. It has been reported that, the reduction of zeta potential value will reduce the physical stability in NLCs (Fan et al., 2014).

Stability of NLCs can be explored with the existence of steric effect from nonionic surfactant. From the past experiment, self-associated micelles due to polyoxyethylene chains in Tween 80 and alkene oxide derivatives in poloxamer 407. These micelles

formed on the surfaces of nanoparticles where the core of micelles is surrounded by the soft “brush” of highly hydrated in polar region that start to an extension of the diffuse layer. Hence, depression of the ZP value happen (Tan et al., 2010).

Negative charge of ZP value reflects the negative surface charge of a particle. The surface charge of a particle is contributed by the charged head group of anionic surfactants and/ or the non-ionic surfactant by the polarization of its head group and adsorption of polarized water molecules at the surface of a particle (Karthik et al., 2016). As studied by Khurana and the team, ZP value of NLCs was found between -10.41 mV to -42.1 mV. This can be attributed from the interaction of PEG-esters and glycerides fraction with lipid and nonionic surfactant in NLCs (Khurana et al., 2017). From the others literature, ZP value of NLC formulations were reported in the range of -30 mV. It showed that, the NLCs particles were stable in dispersion with no tendency to aggregate due to the repulsion forces that promoted by their surface charge (González-Mira et al., 2011; Granja et al., 2017). However, ZP value of NLCs with ionic surfactant (sodium cholate and sodium lauryl sulphate) was stated lower compared to the NLCs with a nonionic surfactant (Tween 80 and poloxamer 127) (Tan et al., 2010).

In addition, the sample concentration of NLCs could affect the ZP value. As stated by Mendes and the team, ZP value increased when increased the sample dilution. ZP value was found nearly zero (≈ -2.62 mV) without dilution and increased up to a +50 mV after a sample dilution correspond to sample concentrations that lower than 10 % (v/v) with the presence of cationic surfactant (benzalkonium chloride). This is due to the high concentration of NLCs sample causes high light absorption or scattering to the sample. (Medrzycka, 1991; Lage et al., 2012; Mendes et al., 2013).

Moreover, the value of ZP was reported decreased when increasing the surfactant concentration in NLC formulation due to the reduced thickness of diffuse layer on the

particle (Tan et al., 2010; Emami et al., 2012) At certain level, the adsorption of surfactant just enough to saturate a monolayer at the stern layer that produces the highest achievable ZP value for NLCs system. However, concentrations of surfactant beyond the requirement will saturate the stern layer and reducing the ZP as a result of expanding diffuse layer (Duro et al., 1998).

Furthermore, the amount of liquid oil did not influence the value of ZP (Mitrea et al., 2014). However, some liquid oil has shown their influence on the ZP value. For example, the increasing amount of oleic acid from 15 % to 30 % in NLC formulations will decreased the absolute value of zeta potential from (-19.7 ± 0.23 mV) to (-12.7 ± 0.19 mV) (Emami et al., 2012). Similar to corn oil, ZP value of NLCs became more negative from -44 mV to -55 mV when increased the amount of corn oil from 0 % to 100 % due the smaller particle size that had the higher surface charge density (Nguyen et al., 2012).

The value of ZP is affected by pH. As discussed by Choi and group, ZP value showed an almost zero mV at pH 2 and 4. The carboxyl group of oleic acid (liquid lipid used) in this formulation was protonated at low pH. However, gradual increase of pH resulted in a decreased of ZP to negative value. This is due to deprotonation of carboxylic acid at high pH to carboxylate that causes a negative ZP value. Furthermore, NLCs that coated with chitosan and positively charged chitosan derivative (HTCC) also displayed a highly positive ZP value at low pH. It's due to the protonation of amino group for chitosan and quaternized ammonium group from HTCC (Choi et al., 2016).

2.5.2 Differential scanning calorimeter (DSC)

DSC is used to identify the thermal properties such as melting point and melting enthalpy. It is also used to obtain the crystallization behavior of NLCs. The degree of crystallinity can be calculated from the ratio of NLCs enthalpy to the bulk lipid enthalpy, which is calculated from the basis of total weight. DSC is a thermo-analytical technique

in which different amount of heat as a function of temperature was applied to increase the temperature of sample and reference (empty aluminium pan). Both sample and reference are maintained at the same temperature throughout the experiment. The temperature program for DSC analysis is designed that, the sample holder temperature increases linearly as a function of time. The reference sample should have a well-defined heat capacity over the range of temperatures scanned. The technique was developed by E. S. Watson and M. J. O'Neill in 1962. It was introduced commercially in 1963 at Pittsburgh Conference on Analytical Chemistry and Applied Spectroscopy.

The connection between solid and liquid lipid in NLCs can be illustrated by DSC thermograms. As mentioned by Pan and team, the melting temperature, melting peak height and melting enthalpy were decreased when the percentage of liquid lipid is increasing in NLC formulations. Moreover, the solidification temperature, solidification peak height and solidification enthalpy decreased when increasing the percentage of glyceryl trioctanoate (liquid lipid) in the production of NLCs. It also could minimize the formation of eicosane (solid lipid) crystals with the presence of liquid lipid composition (Pan et al., 2016). It indicated a change in the polymorphic state of lipid from crystalline to amorphous with more deficiency in the crystal lattice which can provide space for drug loading (Sadati Behbahani et al., 2019). According to Zhao and friends, the addition of oleic acid as liquid lipid will formed more liquid nanocompartments of oil in the solid matrix and did not change the structure of NLCs (Zhao et al., 2016).

The presence of surfactant in NLCs influence the appearance of DSC thermogram. As mentioned by Lin and Duh, NLCs that composing sodium dodecyl sulfate (surfactant) in the aqueous phase, had the low enthalpy of fusion. It is because the sodium dodecyl sulfate hindered the recrystallization rate of lipids in NLCs. The similar result were reported by Kalam and group, the reduction in recrystallization rate of mixed lipids was

noticed with the presence of P188 as a surfactant in NLC formulation (Kalam et al., 2010; Lin & Duh, 2016).

DSC profiles are applied to determine if drug is dispersed and encapsulated in NLCs completely. Lin and Duh used lansoprazole as an active ingredient to be encapsulated in NLCs. The endothermic melting peak of lansoprazole was disappeared in NLCs. This observation indicated that, lansoprazole was solubilized in the lipids (Lin & Duh, 2016). Similarly, the melting point of pure doxorubicin hydrochloride (drug) was disappeared in the thermogram of doxorubicin hydrochloride loaded NLCs. Therefore, it indicated that doxorubicin hydrochloride did not form precipitated on the surface of NLCs but remained as a molecular dispersion in NLCs (Zhao et al., 2016).

2.5.3 X-ray diffractometer (XRD)

In XRD, the monochromatic beam is diffracted at a specific angle by the spacing of the planes in the crystals. The type and arrangement of the atoms will be recorded by a detector as a certain pattern. The intensity and position of the diffraction peaks are exclusive to each type of crystalline materials.

XRD diffractogram is applied to determine the arrangement of lipid molecule, phase behavior and the structure of lipid. XRD is an important analysis to study the length of long and short spacing of the lipid lattice. The crystallinity of NLCs can be identified by using XRD. The polymorphism status of NLCs also can be detected by XRD diffractogram.

It has been reported that, XRD diffractogram is capable to explain the phase behavior and describe the structure of drug molecules in NLCs. From the past literature, the docetaxel (drug) was loaded in formulated NLCs. The high crystalline characteristic peaks of pure docetaxel can be detected in the 2θ scattered angle at 11°, 13°, 14°, 16°, and

17° in XRD diffractogram. However, the blank NLCs and docetaxel loaded in NLCs only showed one significant peak at 24°. The crystallinity properties of pure docetaxel disappeared after being loaded in NLCs. So, it was assumed that docetaxel had been fully dispersed and encapsulated in NLCs (Qiua et al., 2012; Chen et al., 2014).

Quercetin was used as an active ingredient by Sun and group. Quercetin exhibited a high crystalline structure from the immense peak produced in XRD diffractogram. Then, quercetin was completely disappeared in the XRD pattern of quercetin loaded NLCs. It was discovered that the molecule of quercetin was dispersed in the hydrophobic core region and formed an amorphous complex with the matrix of NLCs (Sun et al., 2014).

As stated by Behbahani and team, the sharp intensity of stearic acid (solid lipid) in the 2θ scattered angle at 7.01, 11.72, 21.54 and 23.84 was reduced with the presence of caprylic/capric triglyceride (liquid lipid) in NLC formulation. Thus, it is indicating a lower crystallinity of NLCs with the reduced intensity of stearic acid in it. (Sadati Behbahani et al., 2019).

2.5.4 Field emission scanning electron microscope (FESEM) and transmission electron microscope (TEM)

The surface morphology and shape of NLCs can be observed from these two microscopy techniques. There is not much difference between SEM and FESEM except the type of beam gun. SEM used electromagnetic, while thermionic for FESEM. FESEM is capable to produce micrograph with high magnification and resolution. It will have a better quality compared to the SEM micrograph. FESEM employs the concept of electrons scattered from the surface of samples. The appearance of NLCs sample can be in the form of lyophilized or non-lyophilized to be viewed under FESEM. However, NLCs sample need to be dried before viewing its surface morphology. NLCs is placed on the aluminum specimen stubs that covered with the carbon double-sided tape or carbon

paste. Then, NLCs sample is submitted to a gold or palladium coating by using sputtering system at certain current for several minutes under a vacuum condition.

Coating is a very important for non-conducting samples like NLCs. It will minimize the electron charging within the sample during viewing. The specimen is irradiated with an electron beam. For non-conducting sample, it causes accumulation of static electric charges on the specimen surface and charging effects can be arise from it. This static charge can influence the electron signals and lead to disintegrate of image information.

Figure 2.6 illustrated the differences of secondary electron emission during FESEM analysis between coating and non-coating NLCs sample. Figure 2.6 (a) represented a coating sample of NLCs. The charges are passed to the ground via conducting layer. Hence, negative charges are not accumulated over the sample. On the other hand, figure 2.6 (b) representing a non-coating sample of NLCs. Secondary electrons emitted from the sample may be less due to the decrease of incident electron that can be landed on the sample. The electron just sticks on the sample's surface and does not passed through the layer. This form a negative charge of sample that will reject the electrons and causing them to distort in paths and show a deteriorated image.

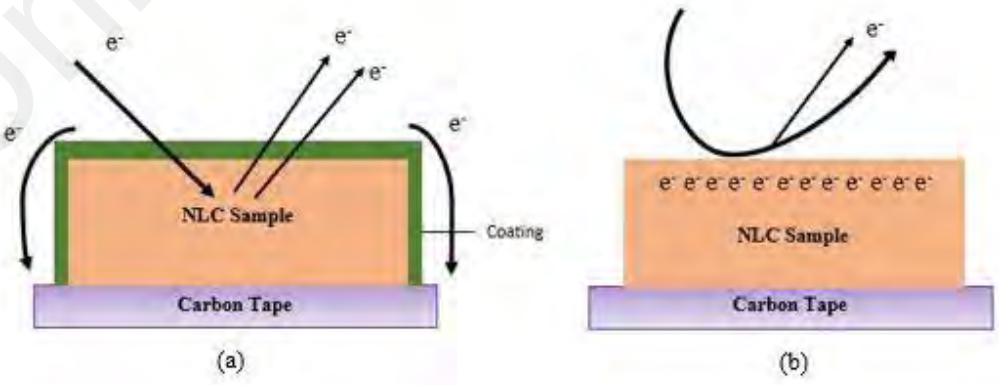

Figure 2.6 :(a) Coating NLC sample (b) Non-coating NLC sample

Figure 2.7 showed the SEM micrographs from the previous research for modified beeswax, medium chain triglycerides oil, alkylpolyglucoside and ethanol sample. Refer to the past experiments, most of the micrographs indicated spheroid-like particles spread on the rough surface. In addition, some micrograph represented the agglomeration of NLCs that may be due to the lipid nature of carrier and the drying process during sample preparation before FESEM analysis (Kuo & Chung, 2011).

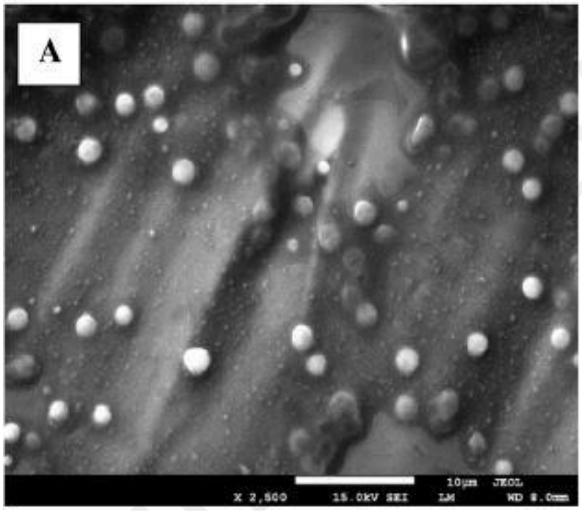

Figure 2.7: SEM micrograph of NLC prepared from modified beeswax, medium chain triglycerides oil, alkylpolyglucoside and ethanol (reprinted permission has obtained from Elsevier)

(Lasoń et al., 2016)

TEM is capable to capture image at higher resolution compared to light microscopes. This enables TEM to snap a fine detail image even as small as a single column of atoms, which is thousand times smaller than a resolvable object seen in a light microscope. Negative staining towards the NLCs specimen is necessary for contrasting a thin specimen with an optically opaque fluid. Once the background is stained, the actual specimen is left untouched, thus it became visible. Phosphotungstic acid and uranyl acetate are the examples of negative staining agent. The concentration of negative staining agent should be adjusted until it reaches the suitable transparency to display the micrograph on the computer (Bello et al., 2010). Figure 2.8 represented the micrographs

of TEM from the previous research. Most of them showed a non-aggregated particle with a spherical shape.

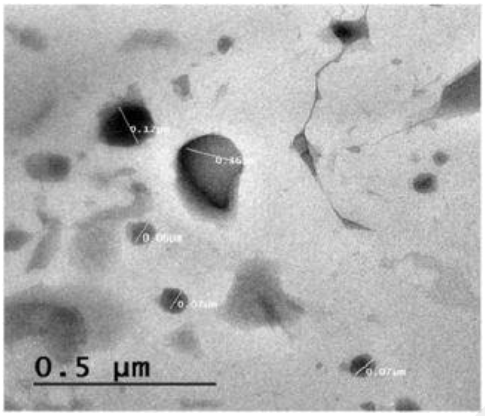

Figure 2.8: TEM micrograph of NLC prepared from triglycerides of caprylic/capric acid, glycerol monostearate type 1 EP and lauroyl macrogol-6-glycerides EP (reprinted permission has obtained from Elsevier)

(Ammar et al., 2016)

2.6 Optimization study of NLCs

Optimization is the method that capable to explore and determine the problem of minimizing or maximizing an objective function that connect the variable to optimize the design and operating variables. In this experiment, optimization of NLCs formulation is very important in order to get the best formulation before proceeds with the encapsulation efficiency and drug release study. Most of the optimized formulations will be selected based on the particle size, zeta potential value and also PDI value (Araújo et al., 2011; Hejri et al., 2013; Baig et al., 2020)

Various NLC Formulations had been optimized from the previous works. As stated by Lakhani and friends, three level response surface design (Box-Behnken Design) was applied to optimize the PEGylated NLC for maximum drug loading, minimum particle size and polydispersity index (PDI). The experiment design was produced and interpreted by using Design Expert® version 8 (Stat-Ease, INC, MN, US). From this experiment, the

optimized formulation was found to be 218 ± 5 nm and 0.3 ± 0.02 for particle size and PDI respectively (Lakhani et al., 2019).

Besides, NLC formulations loaded with retinoids (drug) had optimized by using the software STATISTICA 10 (StatSoft, Inc., 2010, EUA). The optimized formulation will be chosen based on the three responses which are particle size, zeta potential and encapsulation efficiency. In this experiment NLC Particles sizes of 134.5 ± 5.4 nm and zeta potential value of -57.0 ± 2.8 mV were obtained as optimized formulation (Pinto et al., 2019).

According to the past research, Baig and the group was optimized NLC formulations by operating Box Behnken design method (BBD). In this experiment, they found the optimized NLC formulation in the range of 98.04 to 230.12 nm, 0.144 to 0.351 and 12.83 to 26.65 mV for particle size, PDI and zeta potential value respectively (Baig et al., 2020).

2.7 Terbinafine hydrochloride (TBHC1)

TBHC1 is a synthetic allylamine drug commonly used as antifungal. It has a comprehensive activity against yeast, fungi, molds and dermatophytes. It is a poor water-soluble drug and highly lipophilic (log P 3.3) in nature. Figure 2.9 represented the molecular structure of TBHC1.

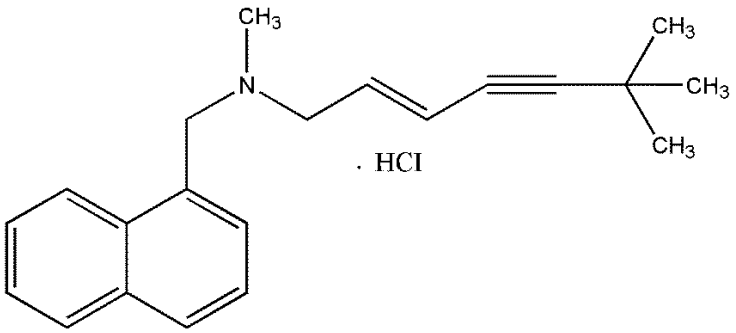

Figure 2.9: Molecular structure of TBHC1

In the past research, TBHC1 had been encapsulated in NLCs that contained glyceryl monostearate, Labrasol® and poloxamer 407 for topical delivery. In this experiment, the entrapment efficiency and drug loading of optimized NLC formulation were determined at (80.24 ± 4.56) % and (14.26 ± 1.82) % , respectively (Gaba et al., 2015). The other drug delivery systems as listed in the table 2.6. The dosage and administration of TBHC1 to the adult was 250 mg per day (Karthik et al., 2016). Toxicity studies of TBHC1 has been recorded in the table 2.7.

Table 2.6: TBHC1 incorporated in drug delivery systems

Drug delivery system	Remarks	References
Chitosan hydrogel	Drug content in chitosan hydrogel was detected between 88.8 and 93.5 %.	(Sen et al., 2000; Özcan et al., 2009)
SLNs	Entrapment efficiency of TBHC1 in SLNs was presented at 74.56 ± 1.41 %, while drug content was found to be 0.98 ± 0.04 %.	(Vaghasiya et al., 2013)
Liposome	Entrapment efficiency of TBHC1 in liposome was determined at 84.38 ± 2.13 %.	(Tanriverdi & Ozer, 2013)
Ethosomes	Entrapment efficiency of TBHC1 in ethosomes was reported at 59.25 ± 1.9 %.	(AbdelSamie et al., 2016)

Table 2.7: Toxicity studies of TBHC1

Toxicity studies			References
Amount applied	Samples (Human/Animal)	Results	
120 mg/kg orally once a day	Red-tailed hawks	Exhibited regurgitation (undigested food) within 3 hours of administration.	(Bechert et al., 2010)
97 mg/kg orally once a day for 1 year	Rats	Without death or organ toxicity.	(Schmitt et al., 1990)
100 mg/kg and 200 mg/kg gave orally at the once day	Rabbits	Infected with the coccidiomycosis (valley fever) and aspergillosis (disease caused by the infection of fungi). They had no significant effect on the disease progression.	(Sorensen et al., 2000; Kirkpatrick et al., 2005)
20 mg/kg orally once a day	Horses	Adverse effects (like pawing at the ground, curling of the lips, head shaking and anxiety) were detected in 1 out 6 horses	(Williams et al., 2011)

2.8 Calcein

Calcein also known as fluorexon or fluorescein complex. It is a water-soluble polyanionic fluorescein derivative with photosensitizing properties. It has an orange crystals appearance. It has been used as an indicator in drug release studies of lipid vesicle and as a contrast agent in retinal angiography (Kopechek et al., 2008). Furthermore, it is traditionally employed as a complexometric indicator for titration of calcium ions with EDTA and for fluorometric determination of calcium. Calcein was also applied as a model of hydrophilic drug in a variety of drug delivery systems as reported in table 2.8. The molecular structure of calcein is shown in the figure 2.10 (Gao et al., 2017).

Table 2.8: Calcein in drug delivery system

Drug Delivery Systems	Functions	Results	References
Liposome	Hydrophilic marker (interaction study between drug and liposome)	It was found to permeate into liposomal membrane in response to osmotic pressure gradient that created across the membrane.	(Kopechek et al., 2008; Maherani et al., 2013)
Hydrogel	Model drug	The calcein encapsulation efficiency in hydrogel was reported between 20.0 to 80.1 %.	(Han et al., 2005)
Metal-organic framework	Hydrophilic molecule in metal organic framework	The drug loading was determined between 1.0 − 15.2 %.	(Orellana-Tavra et al., 2015; Orellana-Tavra et al., 2016)
Bacterial ghost platform	Water-soluble substance	By using fluorescence microscope, 27 % of bacterial ghost platform was filled well with calcein.	(Paukner et al., 2003)
Mesoporous silica nanoparticles	Model drug	Total loaded of calcein was revealed between 1136.48 − 1950.80 μ g.	(Huang et al., 2014)
Microneedle	Hydrophilic molecule	The skin permeability of calcein was reported highest when 0.1 g of calcein gel was coupled to the 500 µm-depth microneedle (154 ea/cm^2). It showed an approximately 5- and 3.6-fold increase in calcein permeation into the rat skin.	(Oh et al., 2008)

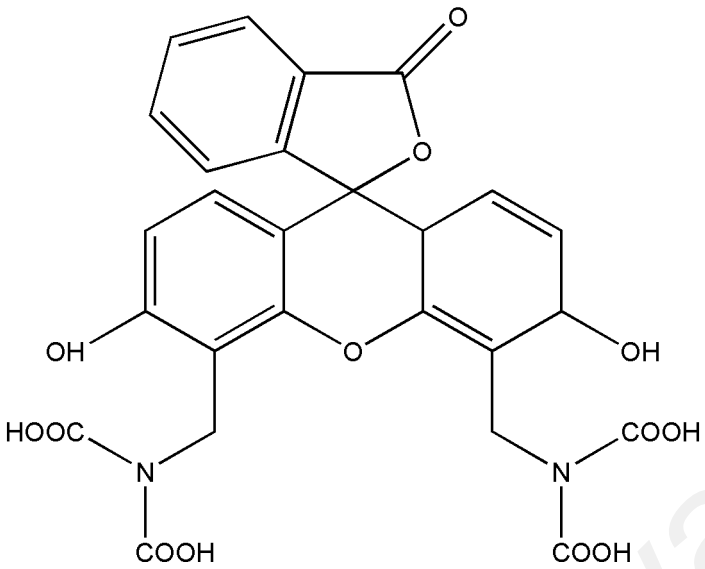

Figure 2.10: Molecular structure of calcein

2.9 Separation of non-encapsulated drug from NLCs

There are diverse methods can be applied to separate the non-loaded drug from those drug loaded in NLCs. The hydrophobic drug molecules homogeneously diffuse in the lipid matrix or enrich in the lipid core. Inversely, aqueous and interfacial phases are the main locations for encapsulation of hydrophilic drug (Fang et al., 2013).

Centrifugation method is widely used to separate the drug loaded in NLCs from those non-loaded. From the past research, NLCs dispersion was acidified with 0.1 N hydrochloric acid for aggregation and isolation of lipid nanoparticles. It was then submitted to a high-speed centrifuge at 10,000 rpm (5590×g) for 30 minutes. Supernatant decanted and the pellets were resuspended in 10 mL methanol and analyzed via high performance liquid chromatography (HPLC). The Encapsulation efficiency (EE) obtained was in the range of 66 % to 95 %, while Drug loading efficiency (DLE) was in the range between 6.5 % and 9.4 % (Khan et al., 2016; Swidan et al., 2016).

Filtration is another method that was employed to discrete drug from NLCs. According to Nguyen and team, NLCs dispersion was filtered using a cellulose ester membrane of 1 mm pore size to remove non-encapsulated drug that has been precipitated in the solution.

After that, NLCs dispersion was diluted 5-fold with distilled water followed by dissolving in organic solvents. The encapsulated drug was determined by using HPLC at certain wavelength. EE of NLC formulations was found between 41.1 % and 83.6 % (Nguyen et al., 2012). The other result indicated that, by filtering NLCs with 0.45 μm cellulose nitrate membrane, the EE obtained was in the range of 86. 73 % and 92.96 % (Li et al., 2016). As studied by Bondi and group, the freeze-dried of NLCs were dissolved in 1:1, acetonitrile: chloroform solution. Next, it was filtered with 0.45 μm polytetrafluoroethylene (PTFE) filters before analyzed by HPLC. The EE of tyrphostin AG-1478 (drug loaded NLCs) was obtained in the range of 28 % and 70 %, while in the range of 1.7 % and 24.0 % for DLE respectively (Bondì et al., 2014).

The combination between filtration and centrifugation method also has been practiced for the same purpose. According to the previous research, NLCs filtrate was diluted to 100-folds with acetone. The drug was extracted completely from lipid to acetone by using cyclomixer. Then, drug content was determined by using HPLC. The amount of non-encapsulated drug was measured by ultrafiltration. It used centrifugal filter tubes with molecular weight cut off 300 kDa (Millipore, Ireland). Then, it was centrifuged at 5827×g for 10 minutes. Amount of drug in aqueous phase was determined by using HPLC. The EE and DLE were found to be 93 % and 1.06 % respectively (X. Zhang et al., 2008). By using the same technique with a different setting, NLCs exhibited EE in the range of 89.1 % and 93.6 % (Kelidari et al., 2017). Ammar and the team (2013) conducted the experiment by using this separation method. The supernatant was filtered and diluted with methanol after centrifuge about 1 hour in 7000 rpm at -4 °C. Then, the free drug was determined spectrophotometrically. NLCs was presented a high EE that above 95 %. Commonly, a high EE is obtained in NLCs due to the high lipophilicity and low water solubility of drug (Ammar et al., 2016).

Centrifugal ultrafiltration method has been employed to separate non encapsulated drug from NLCs dispersion. NLCs dispersion was placed into the upper chamber of centrifugal tubes. After that, it was centrifuged for a certain period of time and speed. Then, the concentration of free drug in supernatant was determined spectrophotometrically. From the past research, by using the same method, EE for triamcinolone acetonide (drug) obtained by Araújo and friends were at 94. 82 %, while 0.26 % for DLE (Araújo et al., 2011). Beloqui and team (2013) analyzed that, NLC formulations displayed an almost ~100 % for EE, while 0.9 % for DLE (Beloqui et al., 2013). This method is convenient and able to separate the free drug without damage the carrier (Shi et al., 2013).

Lastly, size exclusion chromatography technique is another alternative method applied in the previous literature to separate non-encapsulated drug from encapsulated drug in NLCs. The separation concept is correlated to the size of molecules and the pore size of the solid phase. Gel used is varying in molecules and pore size. It can be used as a solid or stationary phase in a column. Most of the researchers used Sephadex, which is a cross-linked dextran gel that used to separate the drug from the drug carrier itself. The gel should be soaked in the eluent or mobile phase for a sufficiently long period to reach the maximum swelling phase. It is important to ensure the gel reach its maximum swelling and functioning efficiently. Besides, it is necessary to ensure there is no air bubbles trapped in the column during the process of column packing. Solid phase of gel particles consisted tiny spherical beads with defined pore size on their surface. Hence, non-loaded drug with smaller size will be encapsulated or trapped in NLCs during separation process. On the other hand, NLCs loaded drug are larger in size that leads them to pass by the pore and eluted first from the column. However, this method is time consuming and causes sample dilution. As mentioned by Kumbhar and Pokharkar, the EE of NLCs was found decrease when increasing the amount of drug added in formulation without increase the

lipid composition by using this separation technique (Kumbhar & Pokharkar, 2013). In addition, Zhang and the group has determined that, the EE and DLE were 48.34 % and 8.06 %, respectively (Zhang et al., 2013). By using the same method, the other researchers found EE at 90.2 % for the separation of phenylethyl resorcinol (model drug) from NLCs. These researchers used sephadex with a difference pore size as a stationary phase in a column (Fan et al., 2014).

2.10 Drug release of NLCs

The drug release response from NLCs depends on the production temperature, emulsifier constitution and oil percentage that included in the lipid matrix (Hu et al., 2006). The drug adsorp on the outer shell or particulate surface of NLCs is released in a fast manner, while the drug incorporated in NLCs core is released in a prolonged way. The constant release of drug can be interpreted from a drug partitioning between lipid matrix and water as well as the barrier function of the interfacial membrane (Yuan et al., 2007).

The methods used in the study of *in vitro* drug release involves diffusion of drug either through Franz cell or dialysis tubing. The set-up of drug release studies should simulate the *in vivo* environment, such as temperature, ionic strength, and pH (Chen et al., 2010; Kuo & Chung, 2011; Poonia et al., 2016).

Regularly, the synthetic membrane is mounted as a barrier between donor and receptor compartment in the Franz diffusion cell (Bronaugh & Stewart, 1985). Variety type and pore size of membrane can be used in the Franz diffusion cell. The diffusion membrane should compose of inert and non-adsorbing material with receptor chamber (diffusate chamber) volumes about 0.5 – 10 mL and surface areas of exposed membrane about 0.2 – 2 cm^2. Then, it was run in a static cell (vertical or side-by-side) not in continuous flow cell. It is usually employed when evaluating drug delivery system such as sonophoresis,

iontophoresis or electroporation. Besides, the receptor fluid is continuously stirred at a certain speed and stop at the appointed time (Bartosova & Bajgar, 2012). In Franz diffusion cell, the drug release of lidocaine (active ingredient) from NLCs was noticed at 69 % and 59 % for two different NLC formulations. A burst release was also observed in the first 30 minutes for NLC formulation. It released lower compared to lidocaine solution (~97) % itself (Ribeiro et al., 2016). The cumulative drug release of isoliquiritigenin (active ingredient) from NLCs was found in the range of 17.50 % and 20.88 % after 24 hours of analysis (Noh et al., 2017). Besides, lutein (active ingredient) was released below 0.4 % at the certain parameter of Franz diffusion cell. This is because, the solid shell in NLCs could preserve and immobilize lutein in the core of lipid (Liu & Wu, 2010).

Dialysis tubing or visking tube is a type of semi-permeable membrane tubing that is used in diffusion drug release studies. A chosen medium is placed on opposite site of a dialysis membrane which contains pores of a manufactured size-range. The pore size-range of dialysis membrane is referred to the molecular weightcut-off (MWCO) of membrane. Generally, a membrane's MWCO refer to the smallest average molecular mass of a standard molecule that will not effectively diffuse across the membrane. There are various MWCO dialysis membrane have been commercially introduced, like 5000 Da, 10000 Da, 30000 Da and 50000 Da. Diffusion through dialysis membrane was adequately fast to qualify the Float-a-Lyzer for an *in vitro* release system as shown in the figure 2.11 (D'Souza & DeLuca, 2005).

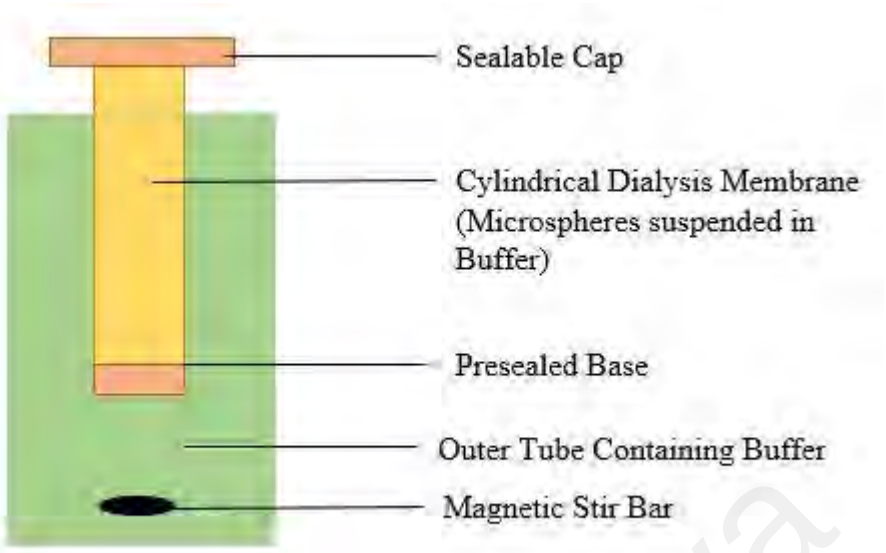

Figure 2.11: Illustration of set-up for *in vitro* release from microspheres using the Float-a-Lyzer

By using dialysis bag, the mangiferin (active ingredient) was released higher than 80 % within 20 hours analysis from NLCs into the 0.1 N HCI and phosphate buffer (medium) (Khurana et al., 2017).

By using the same technique, 14 % of brucea javanica oil (drug) was approximately released from NLCs at the first 12 hours, while, less than 60 % of the drug was released from dialysis bag within 108 hours analysis (Lv et al., 2016). As eloquently stated by Mendes and team, the miconazole (drug) was released at 22 % after 48 hours run. The rapid released drug was observed in the first half an hour (Mendes et al., 2013).

In addition, Jain and the team indicated that the quercetin dihydrate solution (drug solution) was released higher at 92 % compared to the NLC and SLN formulations in this experiment. NLC and SLN were significantly released with 55 % and 45 % at the end of 24 hours respectively. The release of quercetin dihydrate from SLN was release lower than NLC due to the looser nanoparticulate matrix of NLC with the presence of oil in the formulation (Jain et al., 2013; Nasirizadeh & Malaekeh-Nikouei, 2020).

Besides, tilmicosin was used as the active ingredients in NLC formulation. The release rate of tilmicosin from NLC was found significantly lower than tilmicosin solution at (59.96 ± 0.64) % and (81.94 ± 0.71) % respectively (Zhang et al., 2019).

According to the Gönüllü and group, the release of lornoxicam (drug used in this experiment) from NLC formulation was analyzed higher compared to SLN formulation. With the addition of liquid lipid in NLCs it will be made more easier for drug diffusion of release process from the drug system itself (Gönüllü et al., 2015).

Drug release kinetics is the mathematical model applications of drug release study. It involved the study of drug release rate, diffusion study and factors that affect the drug release rate. It is crucial to investigate the drug release pattern because it can represent the efficiency of drug formulation system. There are various mathematical models that applied in the drug release study (Taymouri et al., 2019). Examples like Korsmeyer-Peppas, Higuchi, First Order and Baker-Londale. The equation for each model has been showed in table 2.9 (Zhang et al., 2010).

Table 2.9: Equations of Mathematical Models

Mathematical Models	Equations
Korsmeyer-Peppas	$k_{KP}t^{n}$ (2.1)
Higuchi	$k_{H}t^{0.5}$ (2.2)
First Order	$100[1-e^{-kt}]$ (2.3)
Baker-Londale	$\frac{3}{2}\left[1-\left(1-\frac{F}{100}\right)^{\frac{2}{3}}\right]-\frac{F}{100}=k_{BL}t$ (2.4)

k_{KP} is a release constant incorporating structural and geometric characteristics of the drug dosage form, t is a time in hours, n is a diffusional exponent indicating the drug-

release mechanism or release exponent value, k_H is a Higuchi release, k is a first order release constant, $\frac{F}{100}$ is a fraction of drug release and $k_{BL} = [3 \times D \times C_S / (r_0^2 \times C_0)]$, where D is the diffusion coefficient, C_S is the saturation solubility, $r_0$is the initial radius for a sphere or cylinder or the half-thickness for a slab, and C_0 is the initial drug loading in the matrix.

Korsmeyer-Peppas is a simple relationship which described drug release from a polymeric system. The value of n is used to characterize a different release mechanism. First order release kinetics is a drug release rate that depends on the concentration. A graphical representation is the log of remaining drug percent versus time.

Higuchi's model represents the amount of drug released versus square root of time. It can illustrate the drug release as a diffusion process based on the Fick's Law which is square root time dependent. Its equation can be applied to other types of drug delivery systems, like controlled release transdermal patches or films for oral controlled drug delivery. Then, Baker-Londale model is for a controlled release from spherical matrix. This model also can applied for linearization of the release drug from microcapsules formulation (Paarakh et al., 2018).

Referring from the previous experiment that conducted by Choi and the team, NLC formulations were fitted well with Korsmeyer-Peppas model compared to the other kinetic models due to the highest regression coefficient value (R^2) were resulted as 0.955, 0.9372 and 0.9645 (Choi et al., 2016). The equivalent result also has been found from previous work that handled by Cunha and the team (Cunha et al., 2020).

2.11 Applications of NLCs

Table 2.10 has detailed the list of NLCs applications in the past research works.

Table 2.10: Applications of NLCs

List of Applications	Research Highlights	References
Drug carrier by topical administration	❖ NLCs assure increase penetration of drug into epidermis by close contact with stratum corneum. ❖ NLCs can be used to upgrade the occlusive properties. ❖ NLCs has lipid matrix that able to prevent the burst release in typical topical formulations.	(Aliasgharlou et al., 2016; Ghate et al., 2016)
Drug carrier by oral administration	❖ Protect the water insoluble drugs or else that were easily damaged by digestive enzymes such as antibiotics and enzymes. So, this is the reason it must incorporate in NLCs. ❖ NLCs can absorb through the lymphatic system. ❖ The controlled-release particles can slow down drug degradation and elimination. ❖ Able to enhance the bioavailability of drugs	(Puglia et al., 2008; Chen et al., 2010)
Cancer chemotherapy	❖ NLCs offered a promise to solve some of cancer chemotherapy's limitations. ❖ The limitations are poor specificity, high toxicity and responsiveness to induce the pharmaceutical resistance.	(Selvamuthukumar & Velmurugan, 2012; Di et al., 2016)

Table 2.10: Continued

List of Applications	Research Highlights	References
Drug carrier by intravenous administration	❖ NLCs has been transformed to a colloidal solution or freeze-dried powder. ❖ NLCs has achieved a sustain release and prolong the residence time of the drug in the circulatory system or target site.	(Z. Zhang et al., 2008; Prabhu et al., 2016)
Cosmeceuticals	❖ NLCs contains some properties which protect the sensitive compound against chemical degradation. ❖ It can enhance the chemical stability of active ingredients in NLCs. ❖ Increase skin hydration. ❖ Improved skin bioavailability of actives and skin targeting.	(Müller et al., 2007; Uraiwan & Satirapipathkul, 2016)
Agriculture	❖ NLCs promote photo-protection for the incorporated of active ingredient (pesticide) in it.	(Nguyen et al., 2012)

Table 2.10: Continued

List of Applications	Research Highlights	References
Food science	❖ Food grade NLCs offered interesting structures which can upgrade the stability of encapsulated bioactive, improves loading capacities and promotes sustained release profiles. ❖ Food grade NLCs must be used ingredients that reached the Generally Recognized as Safe (GRAS) status that approved by Food and Drug Administration (FDA). ❖ The formulated NLCs offered a potential application in soft beverage. The particles size was found constant in simulated beverage solutions for 2 months.	(Livney, 2015; Katouzian et al., 2017)

Among these applications, NLC presented to be particularly advantageous as carriers for topical administration of active pharmaceutical ingredient. NLC possess occlusive properties due to film formation on the skin surface. They can reduce the trans-epidermal water loss and enhance the penetration of drugs through the stratum corneum by increased hydration and consequently enhance the treatment efficiency. NLC also offer a prolonged release and improved bioavailability of the drug at the site of action.

CHAPTER 3: MATERIALS AND METHODOLOGY

3.1 Chemicals

Beeswax, *cera alba* (refined, yellow), decanoic acid, palmitic acid, kolliphor el, rosemary oil (RO), phosphate buffer saline (PBS tablet), poloxamer 407, TBHC1, and sephadex® G-50 were purchased from Sigma Aldrich. P188 and calcein were purchased from Merck. Cocoa butter from MP Biomedicals and oleic acid from Friendemann Schmidt. Virgin coconut oil from Inti Food Sdn. Bhd, isopropyl myristate from Spectrum Chemical. Ethanol was bought from R&M Chemicals. All solutions and samples were prepared by using DW with a resistivity of 18.2 MΩ.cm at 25 ˚C. All reagents used were of pharmaceutical, food and analytical grade

3.2 Formulation NLCs and SLNs

3.2.1 Melt-emulsification combined with ultrasonication method

The mixture of lipids and surfactant was preheated at 75 ± 1 ˚C (which is higher than the melting point of the BW used), homogenized, and sonicated for 4, 6, and 10 minutes using a sonic dismembrator (Model 505, Fisher Scientific, USA) at an amplitude of 20 %, 35 %, 50 %, and 70 % prior to being topped up with an appropriate amount of cold water to form an emulsion. The influence of the sonication time and amplitude percentage on the particle size of NLCs were also studied in this experiment. An excellent dispersion can be acquired by elevating the production time, stirring rate, emulsification time and stronger ultrasound power (Hou et al., 2003). However, the manufacturing of NLCs with high pressure homogenization, high temperature and high surfactant concentration will cause a burst release formulation. Therefore, the optimization of preparation method is prominent to produce NLCs with the required criteria as a drug carrier.

From previous research, 10 minutes was sufficient to obtain small sized formulations (Baek et al., 2015). Homogenization and sonication for longer than 10 minutes would likely cause metal contamination from the probe, which would decrease the quality of the

SLNs and NLCs (Liu & Wu, 2010). There is not much difference between the preparation method for SLNs and NLCs; NLCs require solid and liquid lipids heated together with a surfactant, whereas SLNs need only solid lipid heated together with surfactant.

3.2.2 Design of experiments

The effects of the relative proportions of the lipids, surfactant, and solvent on the particle size and zeta potential of the formulated lipid carriers were evaluated with an extreme vertices mixture design using JMP® 12 Statistical Discovery™ from SAS (USA). Table 3.1 shows the ranges of the investigated variables and their linear constraints, whereby the randomized design matrix is illustrated on table 3.2. Formulations in table 3.3 has been applied for the comparison of RO composition purpose.

The responses obtained were modelled with a Scheffe's quadratic polynomial as a function of relative proportion of the components, X_i that represented as equation (3.3):

$$y_i = \sum_i \beta_i X_i + \sum_{i,j} \beta_{ij} X_i X_j \quad (3.3)$$

where β_i are linear coefficients, and β_{ij} are binary interaction coefficients of components i and j ($i \neq j$).

Table 3.1: Ranges and constraints of the mixture proportions

Control variable		Composition	
		Min	Max
BW	x_1	0	0.1
RO	x_2	0	0.05
P188	x_3	0.01	0.05
DW	x_4	0	0.94
Linear constraints			
$0.05 \leq x_1 + x_2 \leq 0.1$		Equation (3.1)	
$x_1 \geq x_2$		Equation (3.2)	

Table 3.2: The designed matrix and responses

Run/Formulation	x_1	x_2	x_3	x_4	Mean particle size, y_1/nm	Mean zeta potential, y_2/ mV
F1	0.05	0.05	0.05	0.85	163 ± 2	-32 ± 5
F2	0.05	0.05	0.01	0.89	727 ± 102	-38 ± 7
F3	0.075	0	0.05	0.875	144 ± 1	-34 ± 3
F4	0.0375	0.0375	0.03	0.895	217 ± 6	-38 ± 4
F5	0.05625	0.01875	0.01	0.915	585 ± 65	-39 ± 7
F6	0.05	0.05	0.03	0.87	265 ± 4	-38 ± 5
F7	0.075	0.025	0.05	0.85	188 ± 2	-38 ± 4
F8	0.1	0	0.01	0.89	836 ± 164	-39 ± 6
F9	0.05	0	0.05	0.9	140 ± 2	-34 ± 4
F10	0.075	0.025	0.03	0.87	269 ± 7	-39 ± 5
F11	0.05	0	0.01	0.94	448 ± 73	-41 ± 6
F12	0.025	0.025	0.05	0.9	133 ± 1	-33 ± 3
F13	0.1	0	0.05	0.85	168 ± 2	-35 ± 3
F14	0.05	0	0.03	0.92	163 ± 2	-37 ± 5
F15	0.0375	0.0375	0.05	0.875	155 ± 2	-34 ± 4
F16	0.0375	0.0125	0.03	0.92	174 ± 2	-36 ± 5
F17	0.0375	0.0125	0.01	0.94	418 ± 46	-39 ± 7
F18	0.05625	0.01875	0.05	0.875	161 ± 1	-34 ± 4
F19	0.05625	0.01875	0.03	0.895	219 ± 3	-38 ± 5

Table 3.2: Continued

Run/Formulation	x_1	x_2	x_3	x_4	Mean particle size, y_1/nm	Mean zeta potential, y_2/ mV
F20	0.0375	0.0125	0.05	0.9	122 ± 2	-30 ± 4
F21	0.025	0.025	0.03	0.92	184 ± 1	-42 ± 8
F22	0.1	0	0.03	0.87	216 ± 2	-38 ± 3
F23	0.075	0.025	0.01	0.89	532 ± 63	-37 ± 6
F24	0.075	0	0.03	0.895	215 ± 2	-39 ± 5
F25	0.075	0	0.01	0.915	597 ± 104	-39 ± 5
F26	0.0375	0.0375	0.01	0.915	632 ± 76	-42 ± 7
F27	0.025	0.025	0.01	0.94	452 ± 49	-43 ± 7

Table 3.3: Formulations for the comparison of RO composition

Formulation	BW composition	RO composition	P188 composition	DW composition
F28	0.05	0.04	0.03	0.88
F29	0.05	0.03	0.03	0.89
F30	0.05	0.02	0.03	0.9
F31	0.05	0.01	0.03	0.91

3.2.3 Long-term stability studies

A stability study was implemented to evaluate the effect of storage on the average particle size, polydispersity index, and zeta potential value of the formulations. The measurement of these parameter was performed in triplicates. The formulations were stored in airtight container and kept at room temperature (27 °C) for 84 days.

3.3 Encapsulation of TBHC1 or calcein in NLCs

TBHC1 or calcein were added to the mixture of BW and RO prior heating and sonication to solubilize the drug with lipids. Hot P188 in DW at the same temperature (75 °C) was added to the mixture, which was subsequently homogenized and sonicated to form an emulsion using a sonic dismembrator. Cold water was then added to the emulsion to form NLC-encapsulated TBHC1 or calcein.

The solubility study of TBHC1 in solid and liquid lipids need to be observed since it is hydrophobic drug. It was necessary to investigate which lipid is the most compatible with TBHC1. The solubility of TBHC1 in solid lipid was tested using decanoic acid, cocoa butter, BW, and palmitic acid. It was performed by the addition of TBHC1 with increments of 2 mg into 0.1 g solid lipid, until it failed to dissolve further in the molten solid lipid (which were heated at 5 °C above their melting point) and formed a drug crystal (Baek et al., 2015). The required amount of solid lipid to solubilize TBHC1 was calculated.

Approximately 3 mL liquid lipid was poured into a centrifuge tube; the liquid lipids used were isopropyl myristate, virgin coconut oil, oleic acid, RO and kolliphor el. Subsequently, 4 mg TBHC1 was added to the liquid lipids, and the centrifuge tubes were closed tightly and shaken continuously on an orbital shaker for 72 hours at 27 °C. Afterwards, the mixtures were centrifuged for 30 minutes at 5000 rpm. The supernatant was collected and dissolved in methanol. The solubility of TBHC1 in various liquid lipids

was quantitated using a UV-Visible spectrophotometer (Cary®50) at 25 °C (Gaba et al., 2015). The concentration of TBHC1 in each oil was determined from the standard calibration curve (0.002 – 0.012 mg mL^{-1}) with an R^2 value of 0.999; and equation (3.4):

$$y = 21.8x + 0.0068 \quad (3.4)$$

3.4 Freeze-drying of NLCs and SLNs dispersion

SLNs and NLCs dispersions were frozen in a deep freezer to below -20 °C for 24 hours without the use of a cryoprotector. The samples were then transferred to a freeze-dryer (Labconco) for at least 12 hours to obtain the NLC powders. The collected samples were used for DSC and XRD analysis.

3.5 Physico-chemical properties characterization

The best NLC formulation was selected from the characterization that had been done for drug delivery study. This study included drug encapsulation efficiency, drug loading efficiency and drug release.

3.5.1 Particle size and zeta potential measurement

Determination of particle size and zeta potential of SLNs and NLCs were conducted using a Malvern Nano series Zetasiser (Malvern Instrument, UK) as shown in figure 3.1 at 25 °C with a backscattering angle of 173˚. A sample volume of 0.5 mL was diluted in 25 mL DW prior to analysis. It is imperative to prepare a highly disperse system with minimum opacity in a sample; if the sample is too concentrated, the light scattered by one particle will be scattered by another particle or interpreted as multiple scattering. This condition produces a variable and inconsistent measurement. Three measurements were performed for each sample. The sample was filled into the capillary cell as shown in figure 3.2.

Figure 3.1: Malvern Nano series Zetasizer (Malvern Instrument, UK)

Figure 3.2: Capillary cell

3.5.2 Differential scanning calorimeter (DSC)

The thermal properties of BW, P188, SLNs, and NLCs were studied by DSC (TA Instrument, Model Q20) as presented in the Figure 3.3. Sample with mass of 5–10 mg was sealed in a 40 μL aluminum sample pan and heated from 10 °C to 100 °C, at a rate of 5 °C min^{-1}. An empty aluminum pan was used as a reference. Nitrogen gas was purged to provide an inert atmosphere during sample scanning.

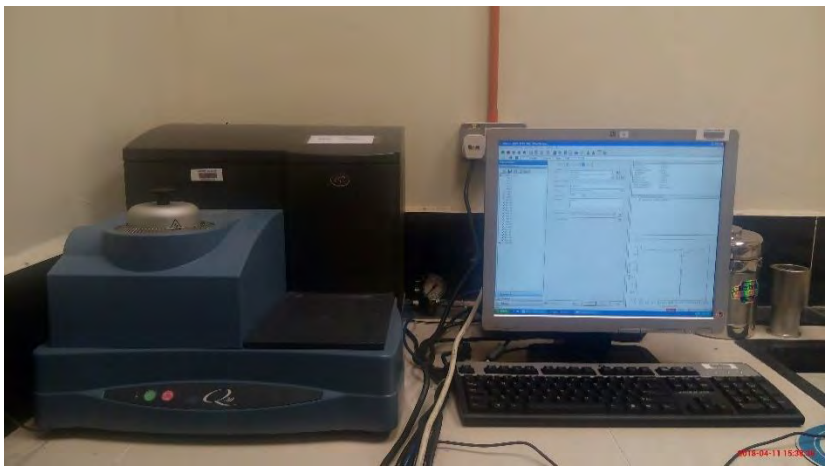

Figure 3.3: Differential scanning calorimeter

3.5.3 X-ray diffractometer (XRD)

XRD analysis of freeze-dried samples were carried out using an X-ray diffractometer (PANanalytical, Empyrean). Lyophilized sample was placed on top of sample holder and ready to be examined by XRD as shown in the figure 3.4. Samples were exposed to Cu Kα radiation at a scanning rate of 0.0263 s/step. The diffraction angle ranged, 2θ, was measured from 5 to 90°. The XRD pattern was measured at 40 kV working voltage and 40 mA current.

Figure 3.4: XRD sample

3.5.4 Field emission scanning electron microscope (FESEM)

The morphology of the NLCs was obtained using a FESEM (Hitachi, SU8220). A diluted NLCs sample was dropped onto a silicon slide. It was left air-dried before coated with platinum under vacuum condition prior examined by FESEM as represented in figure 3.5. Coating was necessary for non-conducting sample to reduce the electron charging during viewing. There were several ways that can apply during the sample preparation or analysis to reduce electron charging, which were:

1) Use low accelerating voltage
2) Coating the non-conducting sample with a thin conductive film.
3) Apply some biasing voltage to the surface of sample
4) Using low vacuum (available in some FESEM)
5) Mounting the sample with a conductive bridge that can connect between top of the sample to the sample holder by using some conductive coating or carbon tape

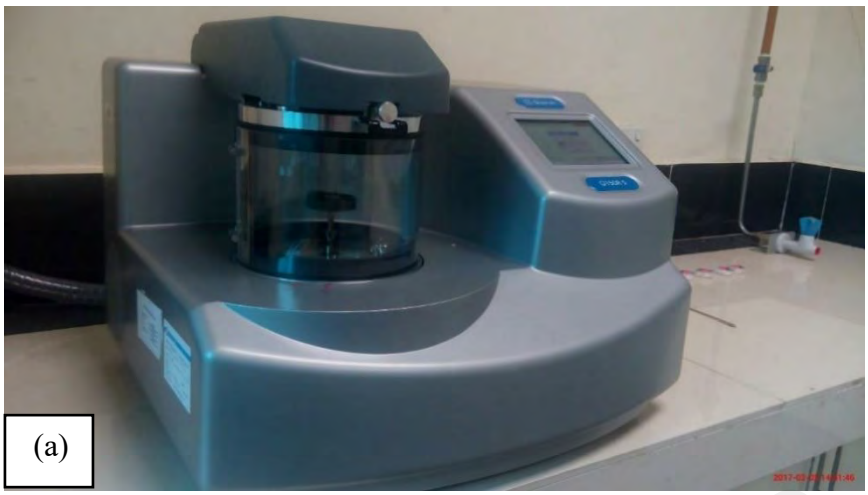

Figure 3.5 :(a) Sputter coater (b) Platinum coating process of sample

3.5.5 Transmission electron microscope (TEM)

The morphology of the NLCs was viewed under a TEM (Carl Zeiss Libra®, 120). A drop of sample solution was placed on a 400-mesh copper grid and left to adhere for 15 minutes. Excess sample solution was removed by blotting with filter paper, and the grid was then air dried and negatively stained with 1 % phosphotungstic acid. The sample was air-dried prior to visualization under TEM. An acceleration voltage of 150 kV was applied.

TEM employs a high voltage electron beam that has been emitted by a cathode. The electrons are travel through a vacuum in the column of microscope. TEM uses electromagnetic lenses to focus the electrons into a very thin beam. Afterwards, the

electron beam is transmitted through the specimen of NLCs by carrying the information. Then, this information (the "image") is magnified and focused onto an imaging device, such as a fluorescent screen, a layer of a photographic plate or a light-sensitive sensor like a charge-coupled device (CCD) camera. The image detected by CCD will display at the same time on a monitor or computer. Figure 3.6 illustrated how the TEM works to produce a micrograph.

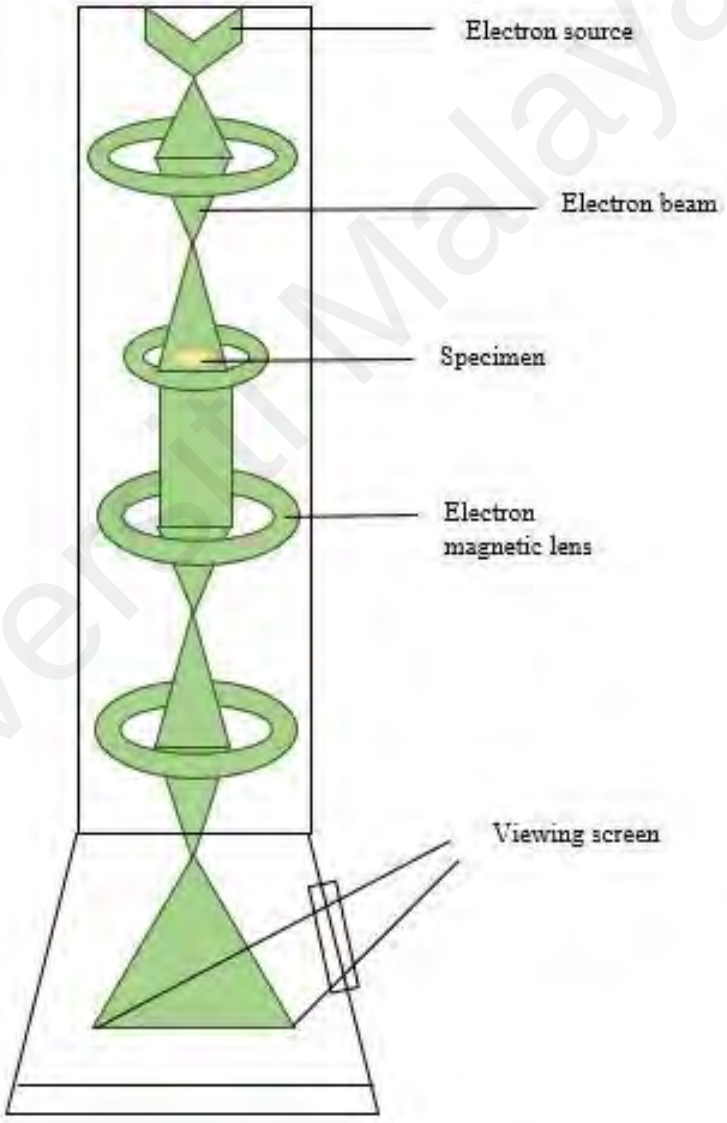

Figure 3.6: Diagram of TEM

3.6 Preparation of standard calibration curve of TBHC1 in DW for encapsulation and drug loading efficiency study

Stock solution of 0.1 mg/mL of TBHC1 in DW was prepared by dissolving 10 mg of TBHC1 in 100 mL DW. Ultrasonicator bath was employed to ensure complete dissolved of TBHC1 in DW. A series of TBHC1 solution with the concentration of 0.05 mg/mL, 0.04 mg/mL, 0.03 mg/mL, 0.02 mg/mL, 0.015 mg/mL and 0.012 mg/mL were prepared by diluting the TBHC1 stock solution. The prepared TBHC1 solutions were measured spectrophotometrically in the wavelength range of 255 to 305 nm. UV-Vis absorption spectrums of TBHC1 in DW is illustrated in figure 3.7. The maximum λ absorption of TBHC1 at 284 nm was selected to plot standard calibration curve as shown in the figure 3.8.

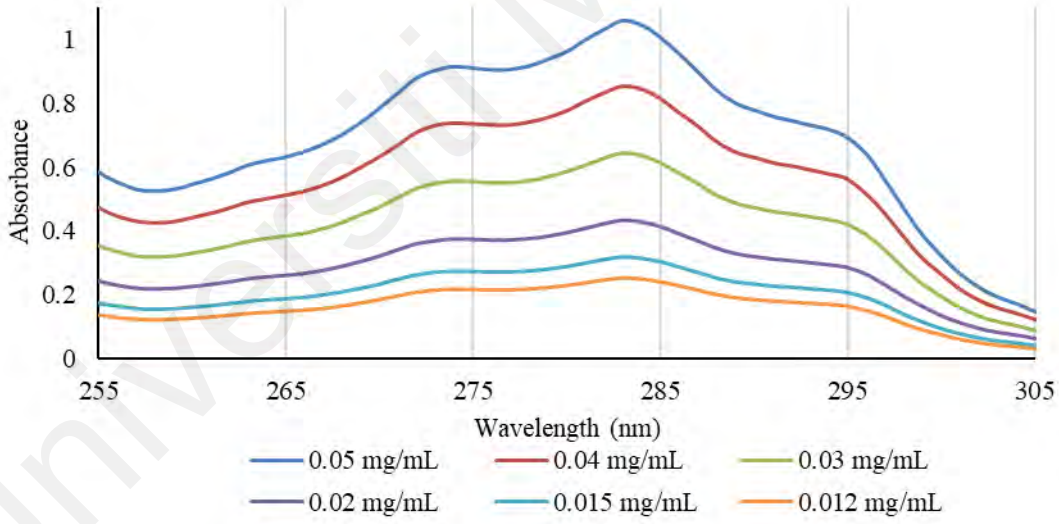

Figure 3.7: UV-VIS absorption spectrum of TBHC1 in DW

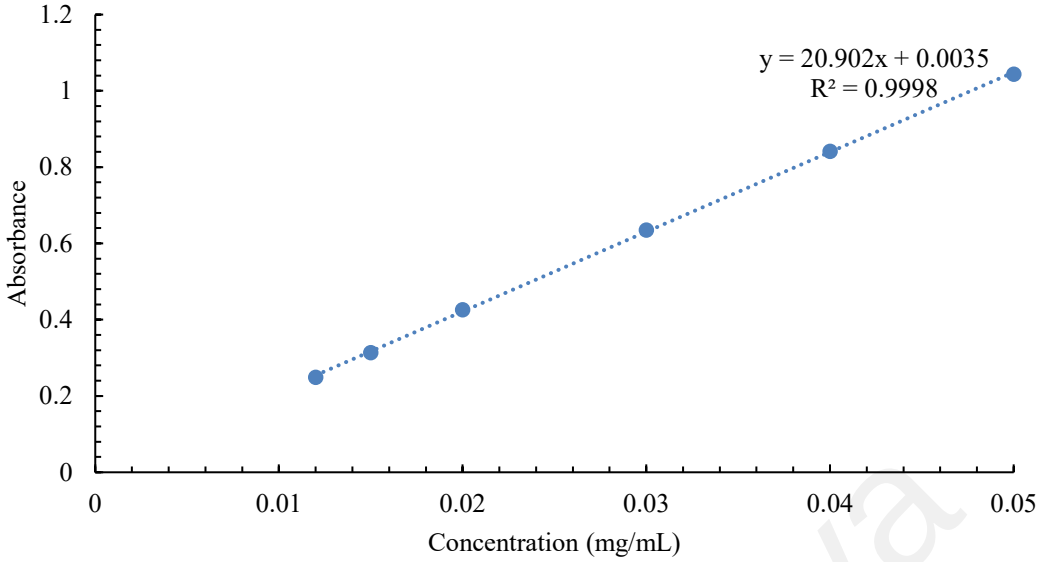

Figure 3.8: Standard calibration curve of TBHC1 in DW

3.7 Preparation of calcein standard calibration curve in DW for encapsulation and drug loading efficiency study

Stock solution of 0.02 mg/mL of calcein in DW was prepared by dissolving 2 mg of calcein in100 mL DW. Ultrasonicator bath was employed to sonicate the solution to make sure all calcein solutes dissolved in DW. A series of calcein solution with concentration of 0.006 mg/mL, 0.005 mg/mL, 0.004 mg/mL, 0.003 mg/mL, 0.002 mg/mL and 0.0001 mg/mL were prepared by diluting the calcein stock solution. The prepared calcein solutions were measured spectrophotometrically between 390 to 530 nm by using UV-Visible spectrophotometer (Cary®50). UV-VIS absorption spectrums of calcein in DW is shown in the figure 3.9. The maximum wavelength absorption of calcein at 490 nm was selected to plot standard calibration curve as shown in the figure 3.10.

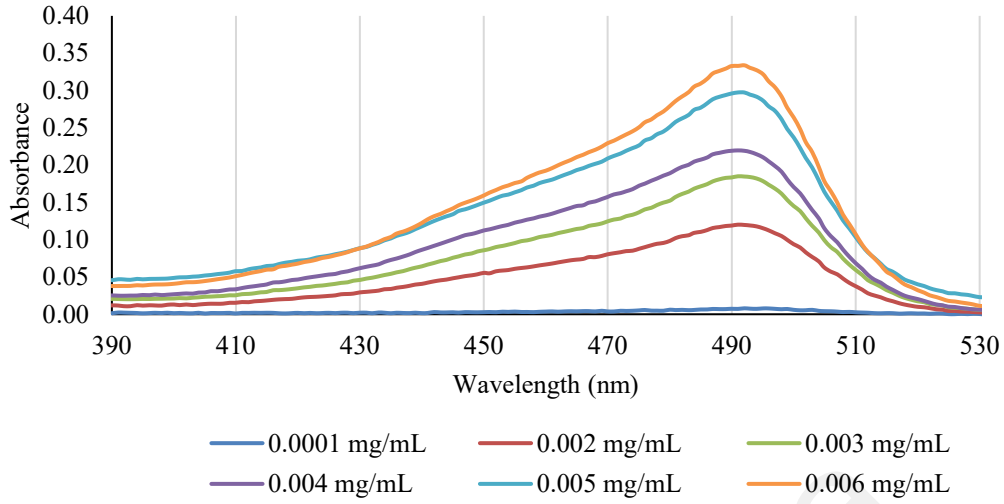

Figure 3.9: UV-VIS absorption spectrum of various calcein concentration in DW

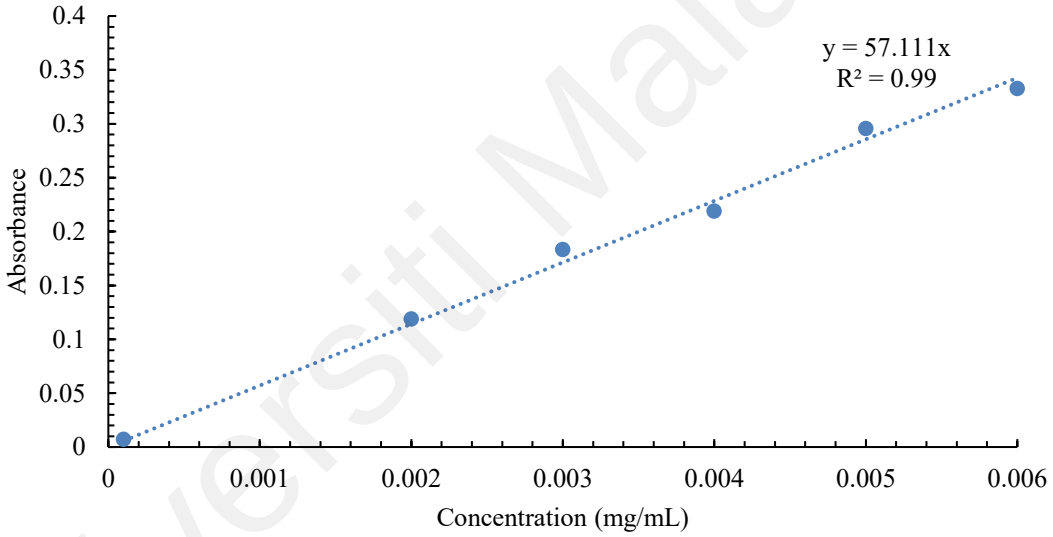

Figure 3.10: Standard calibration curve of calcein in DW

3.8 Encapsulation and drug loading efficiency of TBHC1

TBHC1 was encapsulated in the optimized formulation of NLCs. The ultrafiltration method was adapted to separate the non-encapsulated TBHCl from that encapsulated in NLCs. The concentrator body and filtrate vessel of Vivaspin® 6 compose of polycarbonate, while the membrane compose of polyethersulphone. The width and active membrane area of Vivaspin® 6 is 17 mm and 2.5 cm^2, respectively. Approximately 5 mL TBHC1 NLC dispersion was placed in the upper chamber of centrifugal filter tubes with

a 30 kDa cut-off (Vivaspin® 6, Sartorius stedim Biotech, Germany). Subsequently, the filled Vivaspin® 6 was centrifuged (Dynamica, Velocity 18R, as presented in the figure 3.11) for 1 hour 30 minutes at 7000 rpm (5182 × g) to separate the non-encapsulated TBHC1 as the filtrate. NLC-encapsulated TBHCl remained in the upper chamber of the centrifugal filter tube. Figure 3.12 shows the centrifugal filter tube (a) before and (b) after centrifuge. The supernatant in the lower part of the centrifugal tube was diluted to 5 mL with DW. The concentration of free drug in the supernatant was determined using a UV-Visible spectrophotometer (Cary®50) in a clear quartz cuvette, with a 1 cm path length, at a constant temperature of 25 °C. The concentration of drug in each sample was determined from the standard calibration curve (0.012 – 0.05 mg mL^{-1}) at wavelength of 284 nm.

Encapsulation efficiency (EE) and drug loading efficiency (DLE) were calculated by using the following equation (3.5) and (3.6), respectively:

$$\mathrm{EE} = \frac{Con._T - Con._F}{Con._T} \times 100 \quad (3.5)$$

$$\mathrm{DLE} = \frac{Con._T - Con._F}{Con._L} \times 100 \quad (3.6)$$

$Con._T$ is the weight of total drug in NLCs, $Con._F$ is the weight of free drug in supernatant and $Con._L$ is the weight of total lipid.

Figure 3.11: Centrifuge (Dynamica, Velocity 18R)

Figure 3.12: (a) Centrifugal filter tube before centrifuge and (b) centrifugal filter tube after centrifuge

3.9 Encapsulation and drug loading efficiency of calcein

Size exclusion chromatography method was applied to determine the encapsulation and drug loading efficiency of calcein in the optimized formulation of NLC. A plastic syringe with 10 cm length and 1 cm diameter was adapted in this method as a column. It was firstly packed with sephadex® G-50 as the solid phase where DW as the eluent or mobile phase. The pre-treatment of sephadex® G-50 is necessary before packing it in the column. Firstly, sephadex® G-50 was washed 3 times by DW. Afterwards, pre-saturation of sephadex® G-50 was done by soaking it in the eluent for a certain time to ensure all the sephadex® G-50 beads swell to their maximum size. Next, about 45 µL of calcein encapsulated in NLCs was introduced dropwise into the column as shown in the figure 3.13. Approximately every 0.5 mL of eluate was collected, and each fraction diluted with DW to 5 mL. Lastly, the concentration of loaded and free calcein in diluted eluent was determined spectrophotometrically by using UV-Visible spectrophotometer (Cary®50) with 1 cm path length clear quartz cuvette at constant temperature of 25 °C. The amount of calcein in each sample was determined from the standard calibration curves (0.0001 - 0.006 mg/mL) at the wavelength of 490 nm.

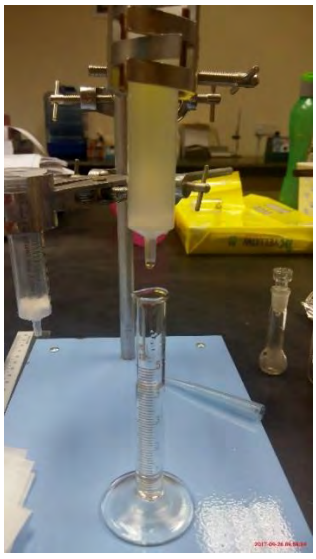

Figure 3.13: Calcein encapsulated in NLCs introduced dropwise onto the column

3.10 Preparation of TBHC1 standard calibration curve in 1:1 (v/v) ethanol: phosphate buffer saline for *In vitro* release study

Stock solution of 0.1 mg/mL of TBHC1 was prepared by dissolving 10 mg of TBHC1 in 1:1 (v/v) ethanol: phosphate buffer saline (PBS) solution. Ultrasonicator bath was employed to ensure all TBHC1 solutes dissolved completely in the solvent used. A series of TBHC1 solution with the concentration of 0.008 mg/mL, 0.005 mg/mL, 0.004 mg/mL, 0.003 mg/mL and 0.002 mg/mL were prepared by diluting the TBHC1 stock solution. The prepared TBHC1 solutions were measured spectrophotometrically between 255 to 305 nm. Besides, UV-VIS absorption spectrums of TBHC1 in ethanol: PBS (1:1) is shown in the figure 3.14. The maximum wavelength at 284 nm was selected to plot standard calibration curve as shown in the figure 3.15.

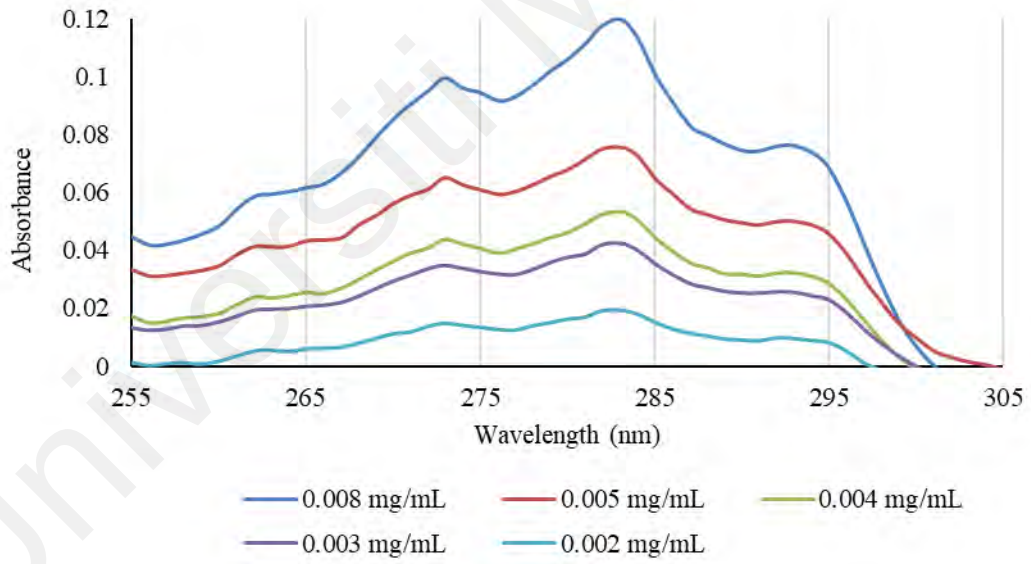

Figure 3.14: UV-VIS absorption spectrum of TBHC1 in 1:1 (v/v) ethanol: PBS solution

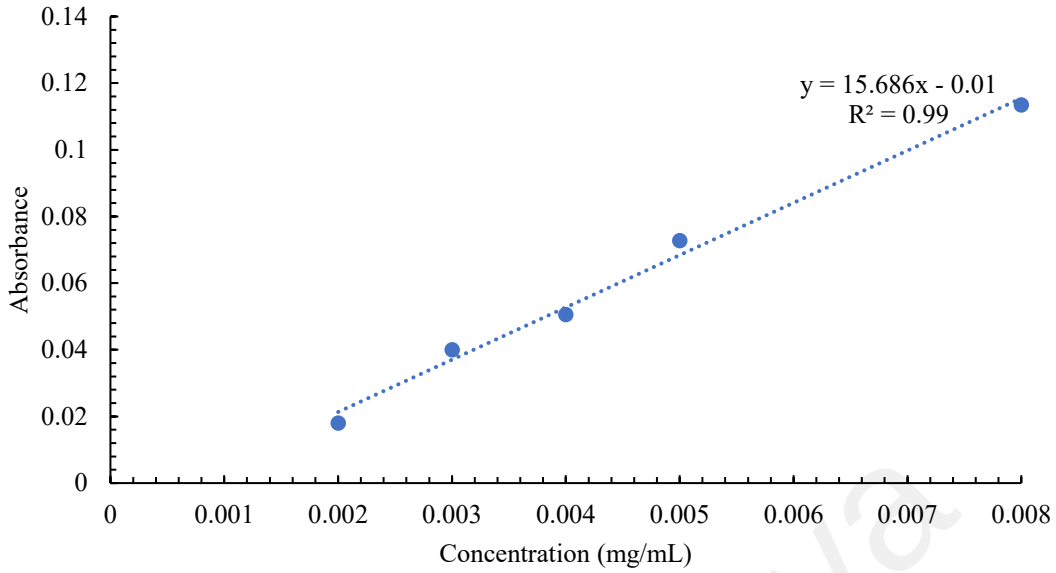

Figure 3.15: Standard calibration curve of TBHC1 in 1:1 (v/v) ethanol: PBS solution

3.11 Preparation of calcein standard calibration curve in 1:1 (v/v) ethanol: PBS solution for *In vitro* release study

Stock solution of 0.1 mg/mL of calcein was prepared by dissolving 10 mg of calcein in 1:1 (v/v) ethanol: PBS solution. A series of calcein solution with the concentration of 0.008 mg/mL, 0.005 mg/mL, 0.004 mg/mL, 0.003 mg/mL, 0.002 mg/mL and 0.001 mg/mL were prepared by diluting the calcein stock solution. The prepared calcein solutions were measured spectrophotometrically between 400 to 540 nm. UV-VIS absorption spectrums of calcein in 1:1 (v/v) ethanol: PBS solution was displayed in the figure 3.16. The maximum wavelength at 490 nm was selected to plot standard calibration curve as shown in the figure 3.17.

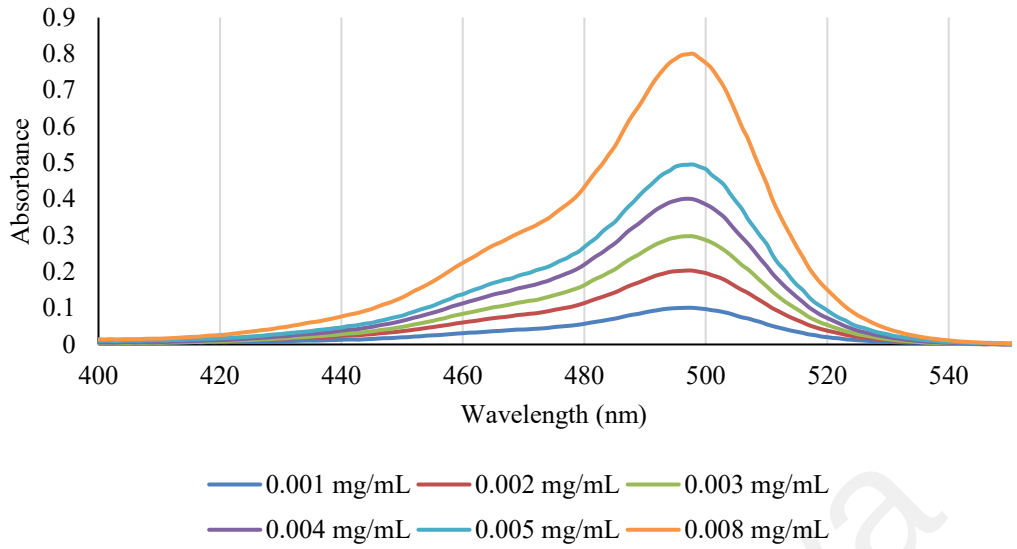

Figure 3.16: UV-VIS absorption spectrums of calcein in 1:1 (v/v) ethanol: PBS solution

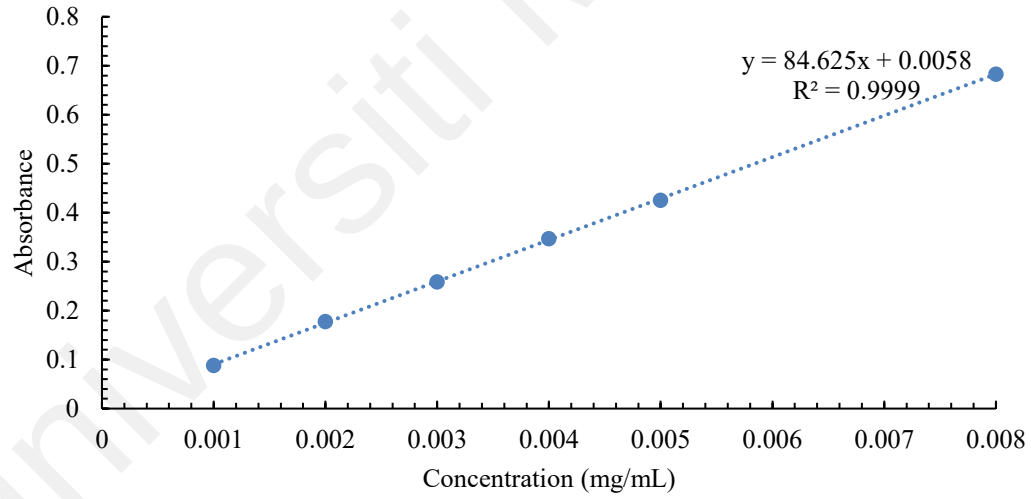

Figure 3.17: Standard calibration Curve of calcein in 1:1 (v/v) ethanol: PBS solution

3.12 *In vitro* drug release studies of TBHC1 and calcein

In vitro drug release studies were completed by using automated Franz diffusion cells (Hanson MicroettePlus™) as displayed in the figure 3.18. The diffusion system was equipped with a vertical clear glass diffusion cell of 0.9 cm orifice diameter, 1 mL donor volume and 4 mL receptor volume as showed in the figure 3.19. A cellulose dialysis

membrane with a 5 kDa cut-off was soaked in the receptor medium for at least 12 hours prior to mounting between the donor and receptor chambers. The donor chamber contained 1 mL sample dispersion, while the receptor chamber was filled with 1:1 (v/v) ethanol: PBS solution at pH 7.5, maintained at 37 °C with magnetic stirring at 400 rpm. At predetermined time intervals, the sample was automatically collected from the receptor chamber and replaced with the same volume of ethanol: PBS solution from the reservoir. The concentration of TBHC1 and calcein in the collected samples were determined using a Cary® 50 UV-Visible spectrophotometer as shown in the figure 3.20, with a 1 cm path length quartz cuvette. The amount of TBHC1 in each sample was determined from the standard calibration curve (0.002 – 0.008 mg/mL) at the wavelength of 284 nm, while, the amount of calcein in sample was determined from the standard calibration curve (0.001 – 0.008 mg/mL) at the wavelength of 490 nm. Replicates were conducted for each sample. Evaluation of the kinetic model was completed using the DDSolver software, an add-in program in Microsoft Excel that contains a mathematical model component in its library.

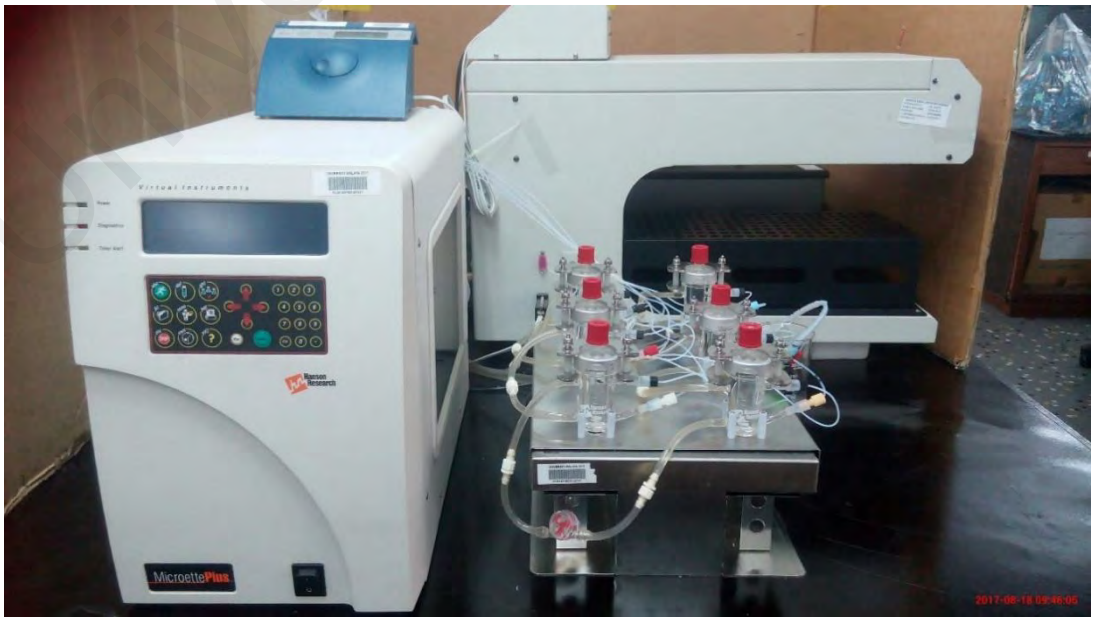

Figure 3.18: Franz diffusion cells (Hanson MicroettePlus™)

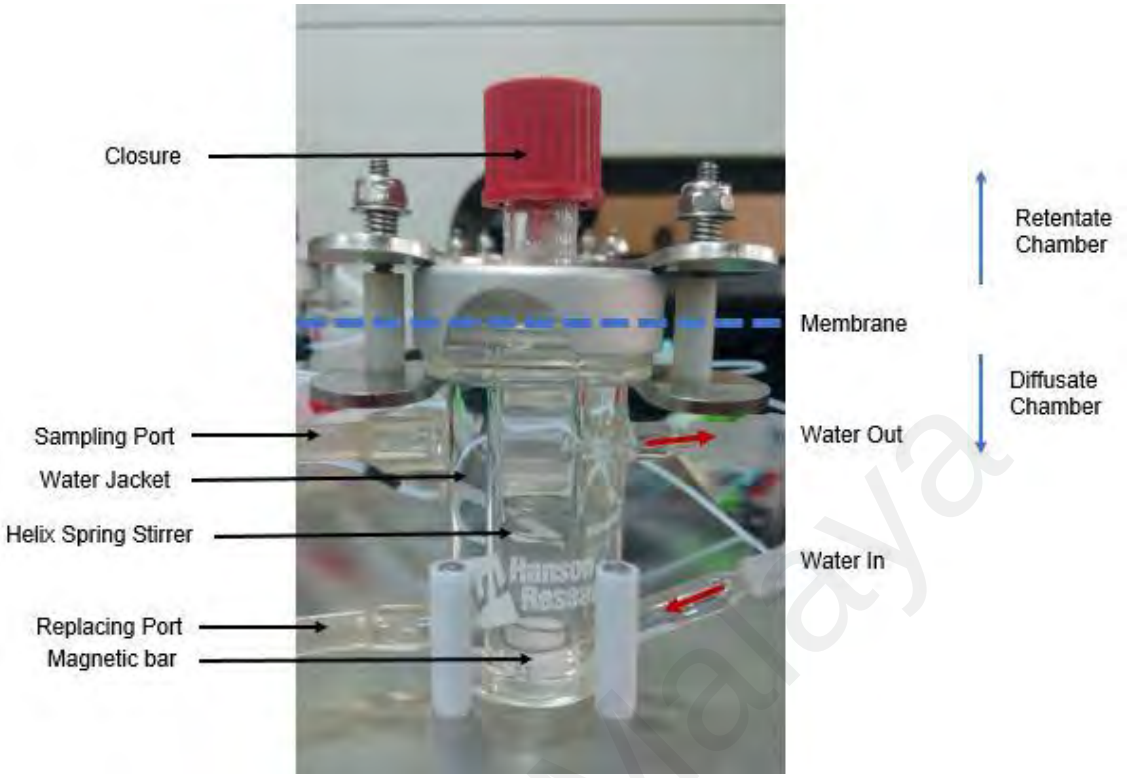

Figure 3.19: Vertical clear glass diffusion cell

Figure 3.20: Cary® 50 UV-Visible spectrophotometer

CHAPTER 4: RESULTS AND DISCUSSION

4.1 Solubility study of TBHC1 in solid and liquid lipid

The solubility studies of TBHC1 in the lipid matrix is the one factor that determine drug encapsulation and drug loading efficiency in NLCs. Hence, it is necessary to examine the solubility of TBHC1 in various solid and liquid lipids. The result of TBHC1 solubility was given in the table 4.1. Factors that affect the solubility value of TBHC1 are temperature, polarity, volume, pressure, lipophilicity of drug, pH and content of the fluid. From the result, TBHC1 displayed a highest solubility in the BW with 12 % compared to the other type of solid lipids. Furthermore, RO also presented a greatest solubility for TBHC1 with 10.78 % compared to the other liquid lipids that has been tested. Based on the result produced, BW and RO were selected to prepare NLCs due to the greatest TBHC1 solubility among the others tested lipids. It is because BW and RO has the highest lipophilicity towards the TBHC1.

Table 4.1: TBHC1 solubility in solid and liquid lipids

Solid lipids	Solubility (w/w%)	Liquid lipids	Solubility (w/v%)
Decanoic acid	6	Isopropyl myristate	0.04
Cocoa butter	8	Oleic acid	3.11
Beeswax	12	Rosemary oil	10.78
Palmitic acid	8	Kolliphor el	6.05
		Virgin coconut oil	0.07

4.2 Mixture Design

4.2.1 Modelling of the mixture design response

Scheffe's quadratic models were postulated for particle size and zeta potential responses with estimated regression coefficients as displayed in Table 4.2. The output from analysis of variance indicated that both the predictive models are statistically significant ($p < 0.0002$) with R^2 of 0.96 and 0.80, *RMSE* of 54 and 1.7, respectively. Based on the results, the corresponding particle size and zeta potential were strongly dependent on the relative proportions of their ingredient, where significant second order interactions were demonstrated between the P188 and the other ingredients.

Table 4.2: Estimated regression coefficients for particle size and zeta potential

X	Particle size			Zeta potential		
	β	s_e	p	β	s_e	p
$x_1/0.19$	1013.819	499.1611	0.0582	-35.6658	16.04827	0.0401*
$x_2/0.19$	2069.566	1217.84	0.1075	1.244193	39.15415	0.975
$(x_3 - 0.01)/0.19$	10543	1640.077	<.0001*	141.3704	52.72928	0.0158*
$(x_4 - 0.8/0.19$	112.5278	194.0146	0.5695	-41.7685	6.237663	<.0001*
$x_1 \cdot x_2$	-3049.99	1876.259	0.1224	-5.23603	60.32265	0.9318
$x_1 \cdot x_3$	-17375.8	2659.419	<.0001*	-259.697	85.5016	0.0074*
$x_2 \cdot x_3$	-17425.8	3151.682	<.0001*	-278.887	101.3281	0.0136*
$x_1 \cdot x_4$	576.7644	1314.241	0.6663	2.304943	42.25349	0.9571
$x_2 \cdot x_4$	-274.894	1881.928	0.8856	-74.147	60.5049	0.2371
$x_3 \cdot x_4$	-13823.3	1987.557	<.0001*	-145.403	63.90093	0.0361*

4.3 Particle Size

4.3.1 The effect of sonication time and amplitude percentage

The NLCs particles size was found in the range of (164 ± 4) nm to (211 ± 1) nm for 20%, 35%, 50% and 70% sonication amplitude for a period of 4, 6 and 10 minutes sonication time as presented in the figure 4.1. For 4 minutes sonication time, the particles size showed a non-significant change from 20 % to 50 % sonication amplitude. The particles size was reported at (172 ± 2) nm, (165 ± 1) nm and (174 ± 1) nm for 20 %, 35 % and 50 % sonication amplitude, respectively. However, the size of NLCs was obviously increased to (211 ± 1) nm for 70% amplitude. The equivalent pattern has also been observed for sonication time of 10 minutes. The particles size of NLCs was displayed similar, which are at (171 ± 1) nm, (170 ± 1) nm and (174 ± 3) nm for 20 %, 35 % and 50 % amplitude respectively. The NLCs particles size was clearly increased from (174 ± 3) nm to (197 ± 1) nm for 50 % to 70 % amplitude (Alam et al., 2015). Besides, the NLCs particles size was increased consistently from (164 ± 4) nm to (174 ± 2) nm from 20 % to 50 % amplitude in 6 minutes sonication time. Nevertheless, the particles size of NLCs was increased apparently to (208 ± 1) nm for 70 % amplitude in 6 minutes sonication time. The polydispersity index (PDI) value of NLCs for 20 %, 35 %, 50 % and 70 % amplitude were represented in the range of 0.16 to 0.25. It showed a nonsignificant pattern for 20 %, 35 % and 50 % amplitude. PDI value was found range between 0.16 and 0.20. As similar with the NLCs particle size, the PDI value for 70 % amplitude was also reported high at 0.25 compared to the others amplitude percentage. Hence, 70% amplitude sonication was observed most polydisperse NLCs compared to the others amplitude range. The particles size and PDI of NLCs are the highest at 70% amplitude. It is because due to the dissipated and local turbulence during sonication that has degraded the emulsifying properties of P188 (Goh et al., 2016). The sonication time did not have prominent effect on the particle size value.

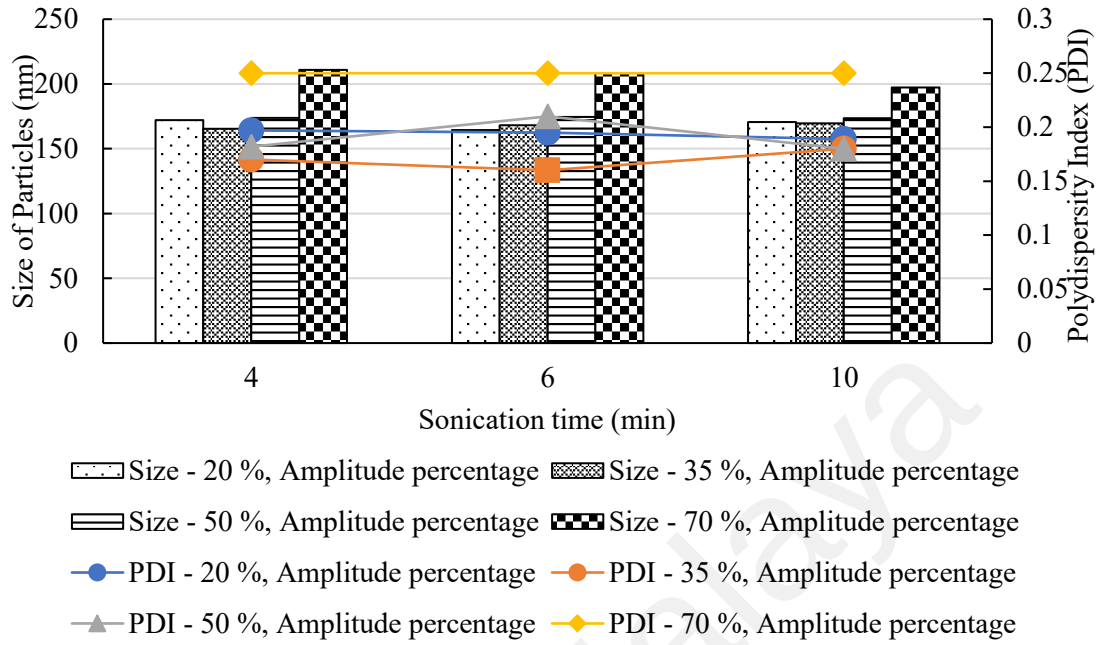

Figure 4.1: The influence of sonication time and amplitude percentage on particles size and polydispersity index of NLCs.

By applying higher amplitude percentage to the emulsion did not distribute more power to the emulsion. Inversely, it will become a resistance to the movement of the probe that determines how much power will be distributed into the emulsion. As the resistance of the probe movement increase, the additional power will be delivered by the power supply to ensure that the excursion at the probe tip remains constant. The maximum power (505 watts) of sonic dismembrator is competent or maximum limit in delivering when the resistance to the movement of the probe is high enough to draw maximum wattage. As proven from the experiment, when the higher amplitude applied, it does not interfere the NLCs size because the setting of higher amplitude will not cause the delivery of maximum power delivered to sample (Alam et al., 2015).

4.3.2 The effect of lipid and surfactant composition on the particle size of NLCs and SLNs and Polydispersity Index (PDI)

The figures 4.2 indicated that, the size of NLCs became bigger when the total lipid composition was risen from 5 % to 10 %. The total lipid was stated at the bar chart for each formulation as shown in the figure 4.2. The sonication amplitude energy was applied similar for all formulations. Therefore, it leads to the limited energy applied per total unit lipid and able to produce a bigger size of NLCs (Loo et al., 2013).

Generally, all formulations displayed in the figures 4.2 recorded a reduction in the particle size when the concentration of P188 was increased. The hydrophobic chains of P188 would adsorb on the particle surfaces as the "anchor chain", while the hydrophilic chain would extend out from the surface of particle to the aqueous medium to create a stabilizing layer. This layer covers the lipid domain of the particle and immediately helps to reduce the particle size of NLCs. In addition, the reduction of particle size might be related to the decreased of interfacial tension between lipid matrix and aqueous phase with the greater of surfactant concentration in the formulations (Zirak & Pezeshki, 2015; Fathi et al., 2018). As the concentration of P188 increased, polydispersity index (PDI) of the formulations was found reduced as shown in the figure 4.3. The range of PDI value is from 0 to 1. The large PDI value explained a very broad size distribution while, small PDI value interpreted a narrow size distribution in formulations. It is proven that, the concentration of P188 was capable to decrease the particle size and PDI value. The identical result also determined from the previous experiment that completed by Soleimanian and the group (Soleimanian et al., 2018). In addition, F16 was chosen to prepare another NLCs formulation by using poloxamer 407 as a surfactant.

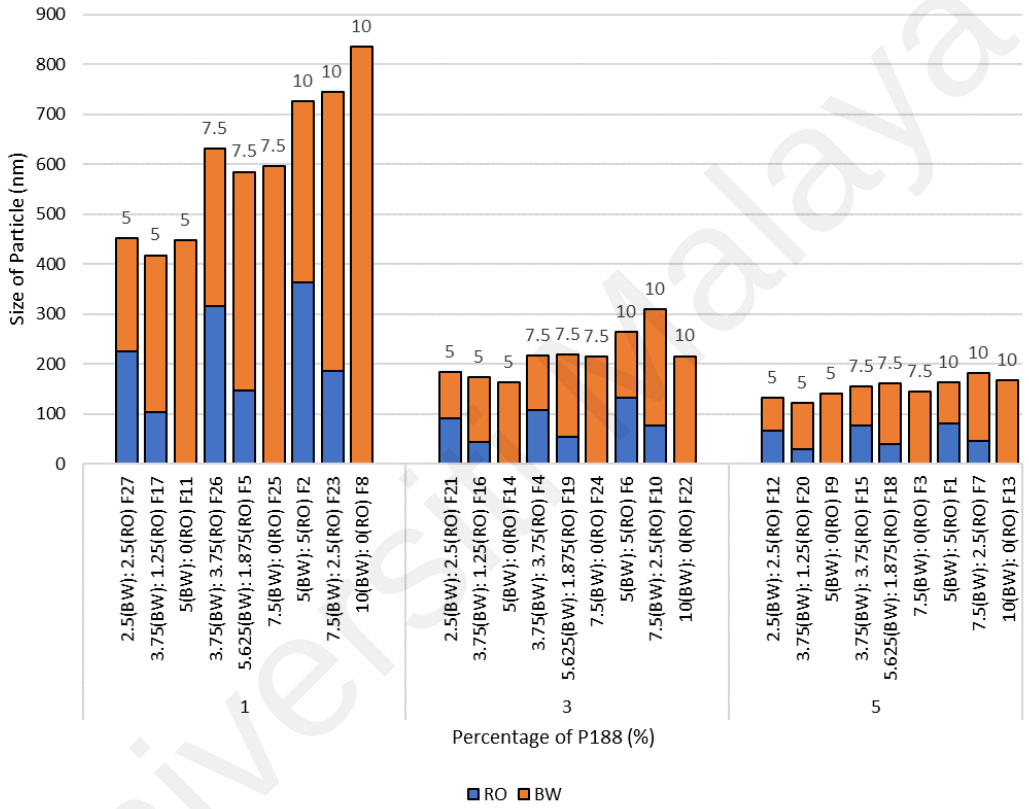

Figure 4.2: Particle size of NLCs and SLNs versus the percentage of P188

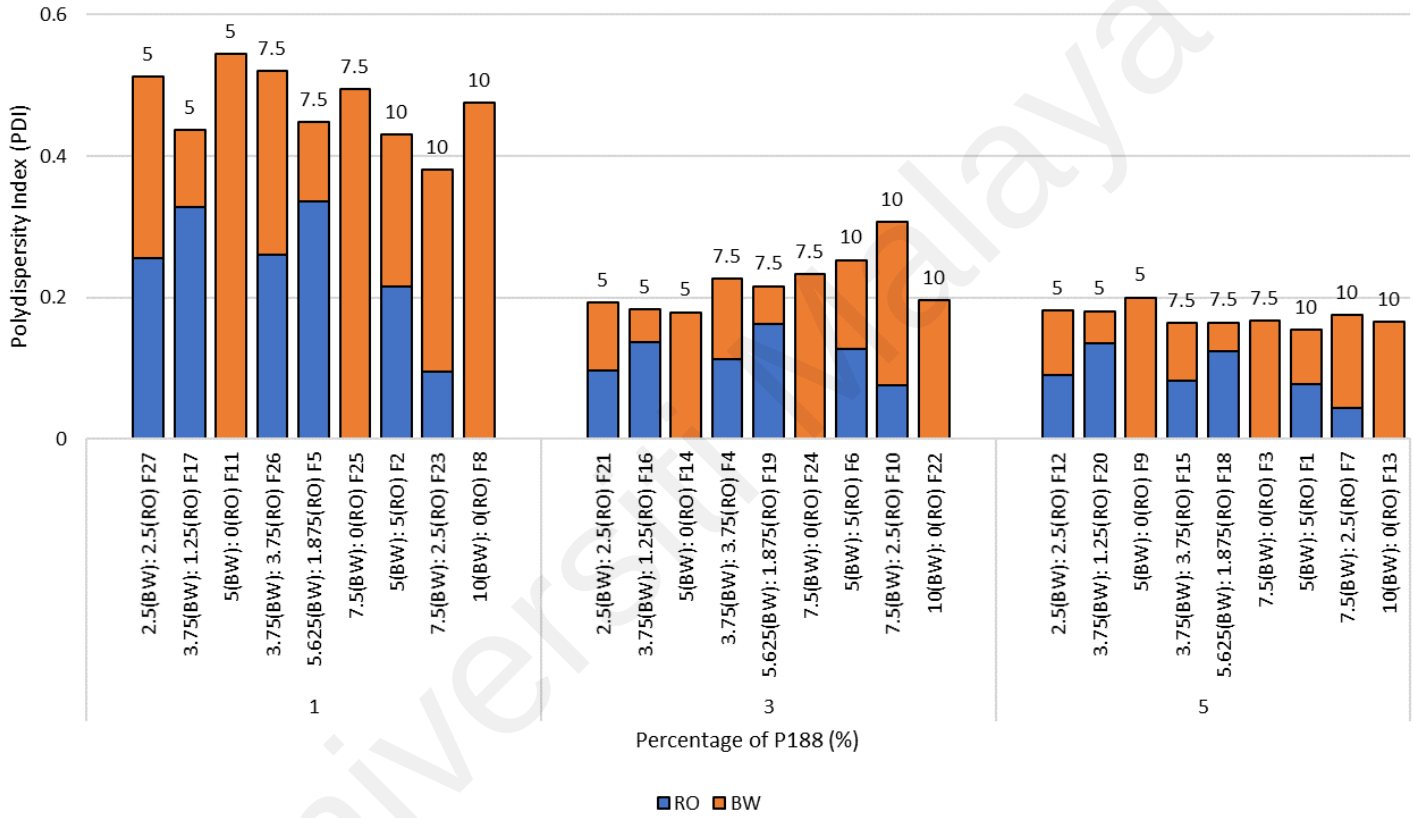

Figure 4.3: Polydispersity index (PDI) value of NLCs and SLNs versus of the percentage of P188

As known, one formulation was selected to prepare NLCs by using Poloxamer 407 in order to study the particles size differences. The NLCs size was recorded smaller (164 ± 1) nm compared to the formulation with P188 (174 ± 2) nm. Poloxamer 407 has a longer surfactant chain than P188. It can increase the hydrophobic interaction between the surfactant monomers and able to form a smaller NLCs size as compared to the shorter hydrocarbon chain.

The particle size of NLCs also became greater when the RO increased from 0 % to 4 % in NLC formulations as shown in the figure 4.4. The reason might be ascribe to swollen of the core in NLCs when more liquid oil were loaded into it (Lin et al., 2007; Dai et al., 2010). The comparable results also were noticed from the past research that completed by Kuo and the group (Kuo & Chung, 2011). However, the NLCs size was slightly decreased at 5% of RO due to the incompatible mixing between BW and RO and might be arise from a lower viscosity of the dispersed phase (Wissing et al., 2004).

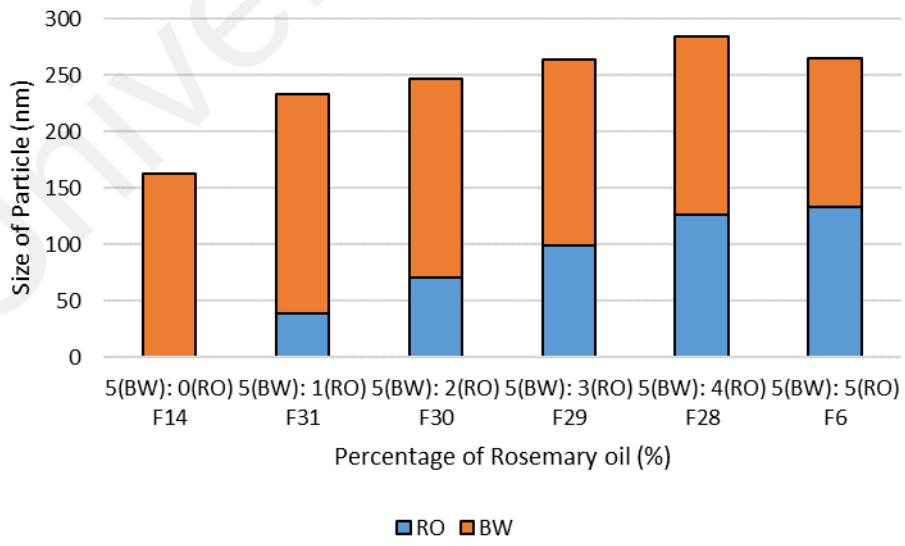

Figure 4.4: Particle size of NLCs and SLNs versus Percentage of RO

The investigation of SLNs particle size also has been done in this research. The particle size of SLNs were found increased from (140 ± 2) nm to (168 ± 2) nm when the BW's percentage was increased from 5 % to 10 % in the formulations as shown in the figure 4.5. It might be due to the high overall viscosity with an increase of solid lipid content that caused less effectiveness of homogenization during production of SLNs (Lasoń et al., 2013). Previous experiment by Shah and the group also showed the equivalent outcome. Greater percentage of stearic acid (solid lipid used) will produce a greater viscosity of the inner phase and influence the shearing capacity of the stirrer (size reduction became tough). Consequently, the particles contributed to increase in size (Shah et al., 2014).

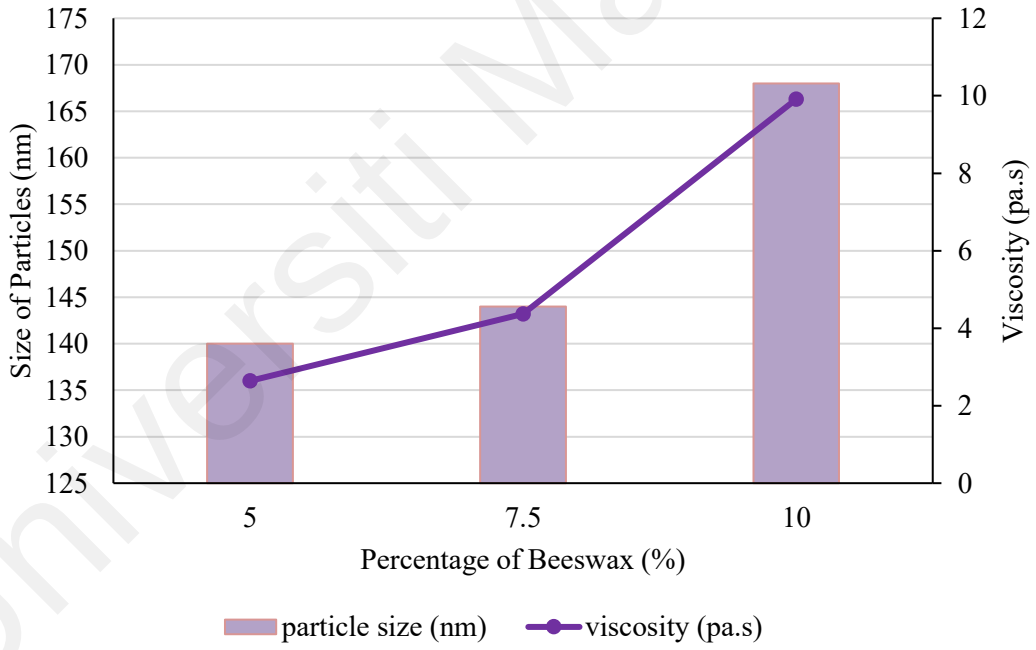

Figure 4.5: Size of particle and viscosity versus percentage of BW in SLNs. The SLNs displayed were F9 (BW (5%), RO (0%), P188 (5%), DW (90%)), F3 (BW (7.5%), RO (0%), P188 (5%), DW (87.5%)) and F13 (BW (10%), RO (0%), P188 (5%) DW (85%)).

4.4 Stability

4.4.1 Particle size and polydispersity Index (PDI)

The measurement of particle size for all formulations need to be monitored for a period of time to study their long-time storage stability. Besides, the equilibrium between surfactant at the oil-water interface and the nature of the oil phase can be influenced on the stability of oil dispersions. The PDI value ranges from 0 to 1. Particles are considered polydisperse with high value of PDI and approaching 1. Stability of oil dispersion can be obtained with the presence of sufficient surfactant in formulations (Tamjidi et al., 2013).

The presence of P188 in the formulations would help to stabilize a newly developed surface during homogenization between oil and water in NLCs and SLNs with the presence of head (hydrophilic characteristics) and tail (hydrophobic characteristics) of P188. The turbidity of particles also became lower when the percentage of P188 was raised. It is because the turbidity is related with the particles size of NLCs and SLNs. The particles size of NLCs and SLNs will be decreased when the percentage of P188 is raised in the formulation. The turbidity also can be distinguished from the figures 4.6 (a), (b) and (c). Insufficient amount of surfactant in the formulations also will cause instability and recrystallization of SLNs and NLCs. Moreover, the PDI value also displayed lower and consistent value throughout 86 days of analysis for a higher concentration of P188. It explained that the particles were in a state of monodispersity with narrow size distribution.

Figure 4.7 illustrates the effect of P188 concentration on the formation of stable of nanoparticles. Figure 4.8 to 4.15 showed the particle size of NLCs and SLNs declined as the percentage of P188 increased. Size of particles with 5% of P188 was found smaller compared to the particles with 1 % and 3 % of P188. The size of particles with 1 % of P188 had been observed fluctuated along 86 days of analysis. NLC and SLN formulation

with only 1 % of P188 caused the particles proned to aggregate and hence increased in size. This is due to the amount of P188 in the formulations of SLN and NLC were not sufficient to adsorb on the entire surface of newly formed lipid particles. Therefore, SLNs and NLCs tend to aggregate due to strong hydrophobic attraction between the particles. Then, formulation of NLCs and SLNs with the high concentration of P188 can prevent the particles from aggregation and fusion.

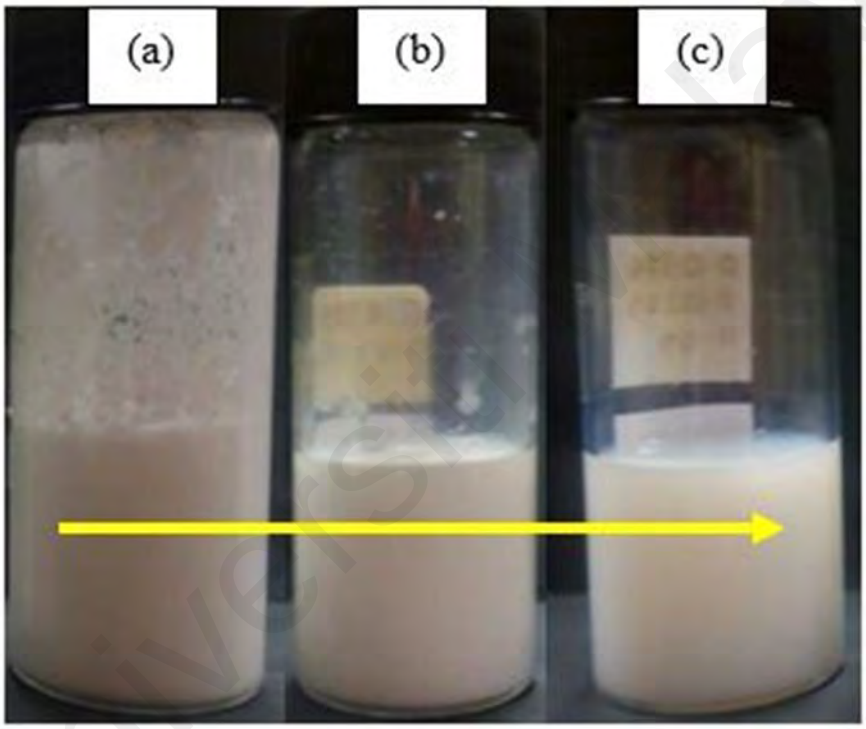

Figure 4.6: (a) F17 (BW (3.75%), RO (1.25%), P188 (1%), DW (94%)), F16 (BW (3.75%), RO (1.25%), P188 (3%), DW (92%)) and F20 (BW (3.75%), RO (1.25%), P188 (5%), DW (90%)).

By comparing the figures 4.8 to 4.15, the formulations with high lipid concentration were found physically less stable compared to the formulations with low lipid concentration due to the greater size and easily recrystallize (Loo et al., 2013).

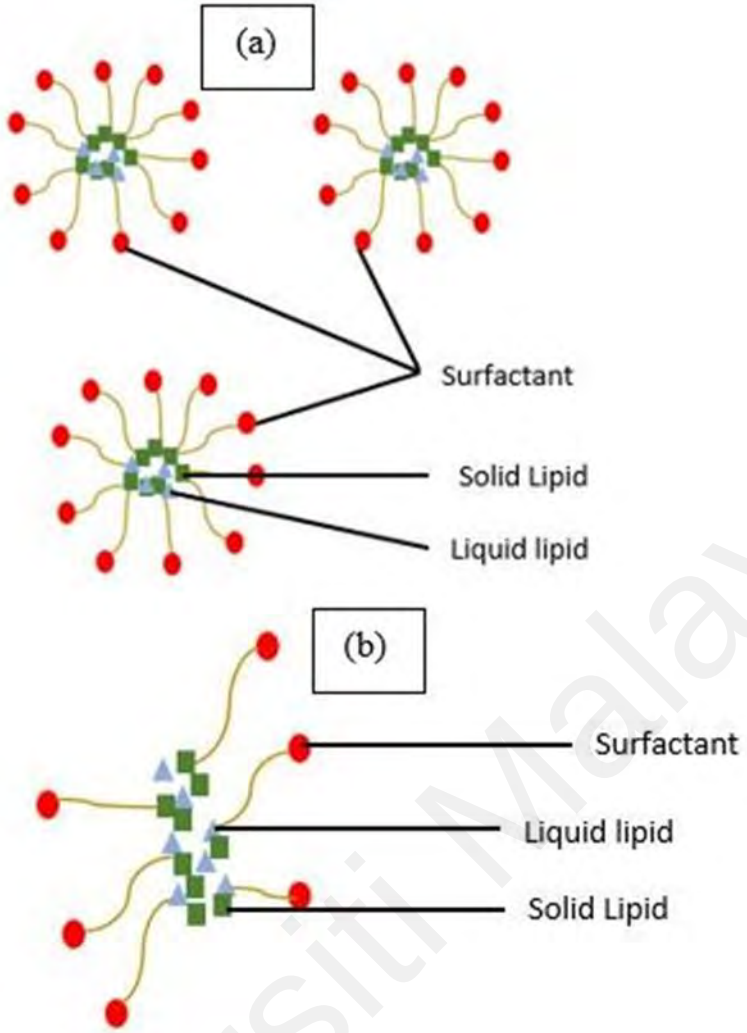

Figure 4.7: (a) Stable nanoparticles with the higher concentration of P188 (b) Less stable of nanoparticles with the lower concentration of P188.

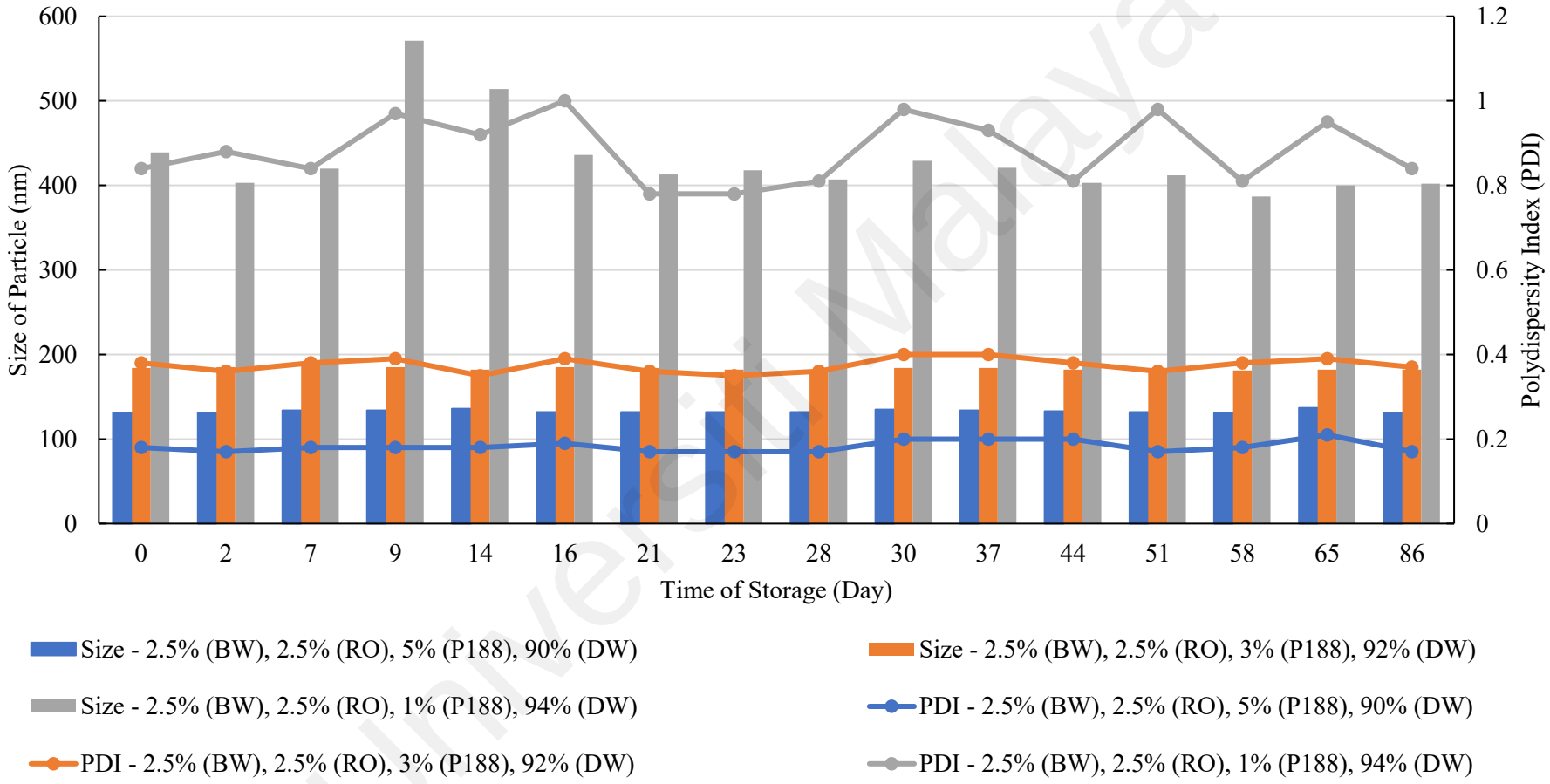

Figure 4.8: Size of particle and polydispersity index versus time of storage (day). The NLCs displayed were F27 (BW (2.5%), RO (2.5%), P188 (1%), DW (94%)), F21 (BW (2.5%), RO (2.5%), P188 (3%), DW (92%)) and F12 (BW (2.5%), RO (2.5%), P188 (5%), DW (90%)).

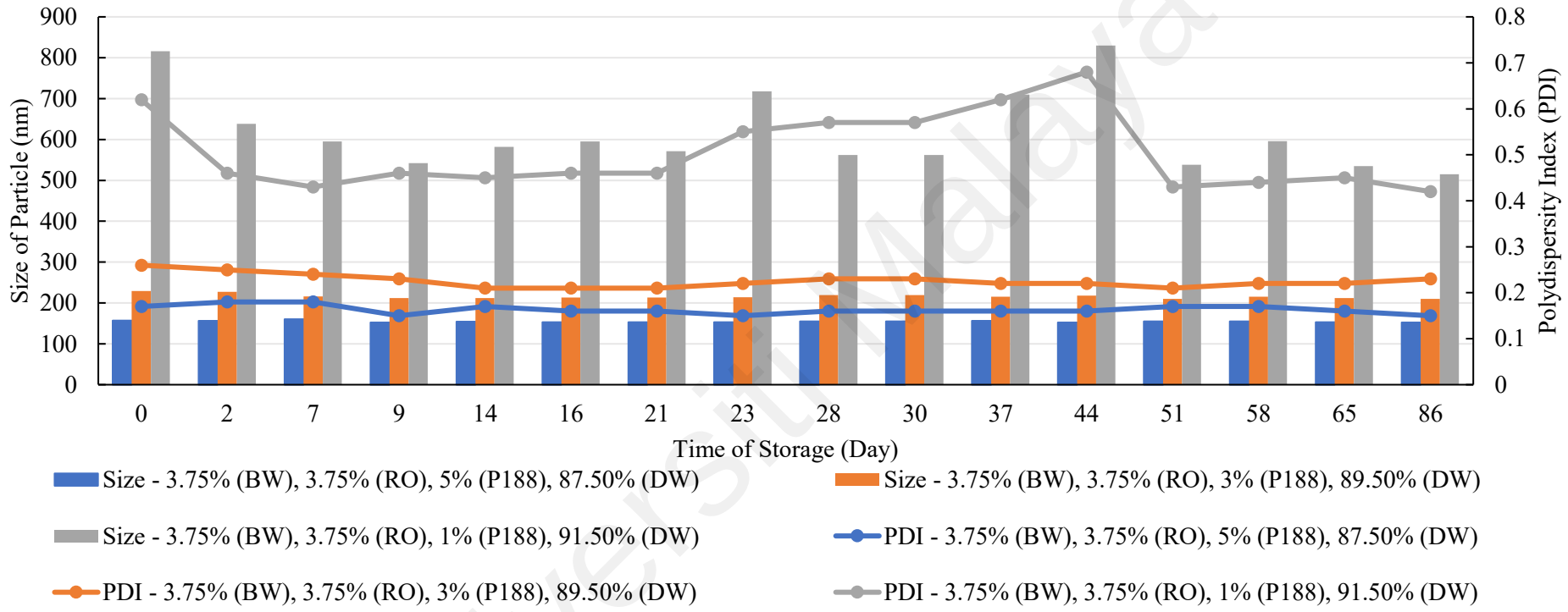

Figure 4.9: Size of particle and polydispersity index versus time of storage (day). The NLCs displayed were F26 (BW (3.75%), RO (3.75%), P188 (1%), DW (91.5%)), F4 (BW (3.75%), RO (3.75%), P188 (3%), DW (89.5%)) and F15 (BW (3.75%), RO (3.75%), P188 (5%), DW (87.5%)).

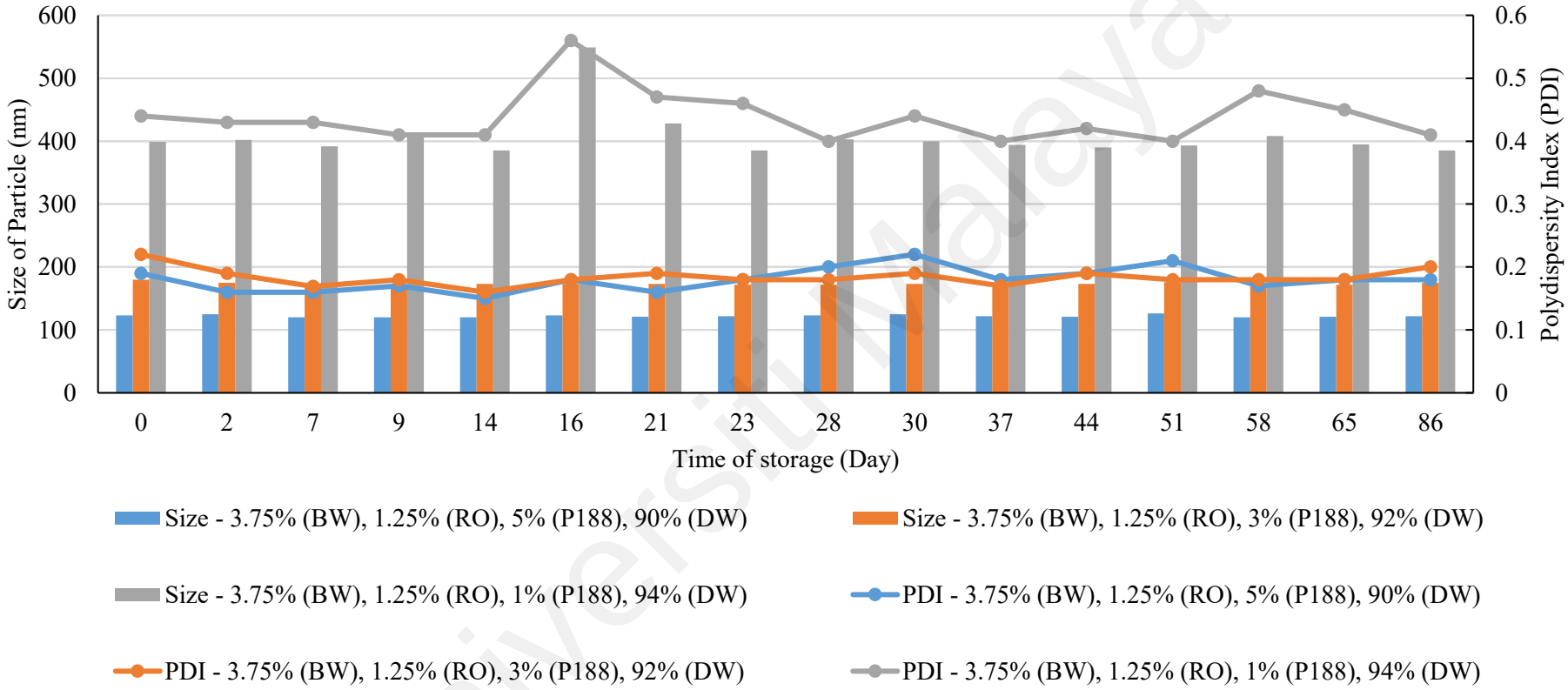

Figure 4.10: Size of particle and polydispersity index versus time of storage (day). The NLCs displayed were F17 (BW (3.75%), RO (1.25%), P188 (1%), DW (94%)), F16 (BW (3.75%), RO (1.25%), P188 (3%), DW (92%)) and F20 (BW (3.75%), RO (1.25%), P188 (5%), DW (90%)).

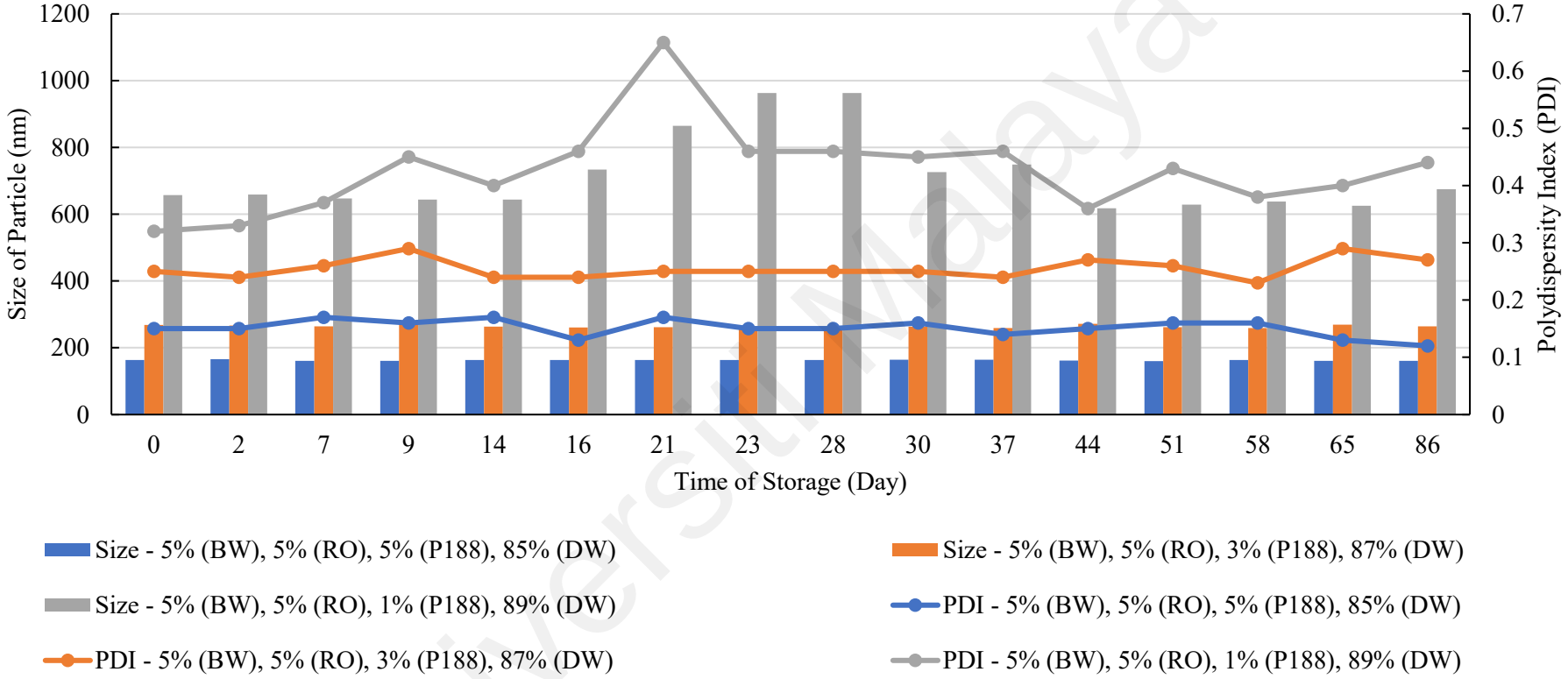

Figure 4.11: Size of particle and polydispersity index versus time of storage (day). The NLCs displayed were F2 (BW (5%), RO (5%), P188 (1%), DW (895)), F6 (BW (5%), RO (5%), P188 (3%), DW (87%)) and F1 (BW (5%), RO (5%), P188 (5%), DW (85%)).

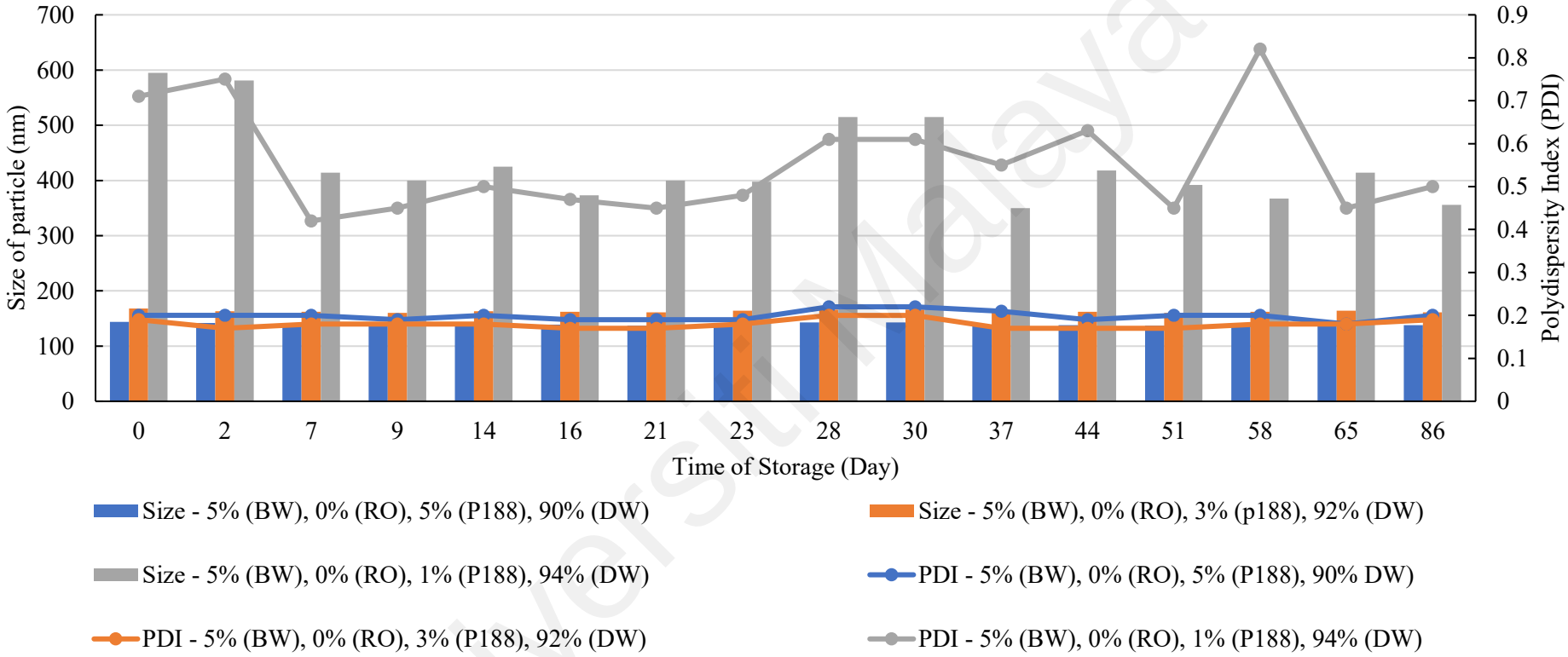

Figure 4.12: Size of particle and polydispersity index versus time of storage (day). The SLNs displayed were F11 (BW (5%), RO (0%), P188 (1%), DW (94%)), F14 (BW (5%), RO (0%), P188 (3%), DW (92%)) and F9 (BW (5%), RO (0%), P188 (5%), DW (90%)).

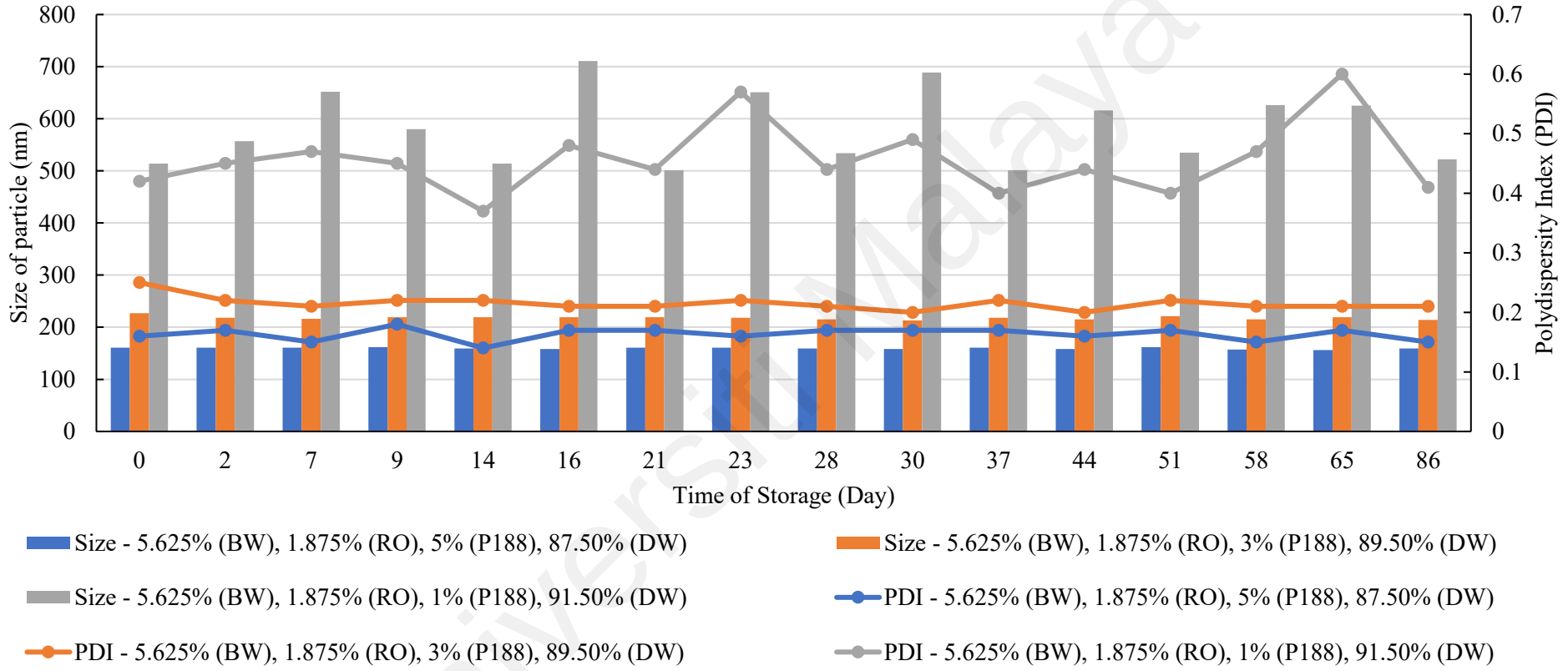

Figure 4.13: Size of particle and polydispersity index versus time of storage (day). The NLCs displayed were F5 (BW (5.625%), RO (1.875%), P188 (1%), DW (91.5%)), F19 (BW (5.625%), RO (1.875%), P188 (3%), DW (89.5%)) and F18 (BW (5.625%), RO (1.875%), P188 (5%), DW (87.5%)).

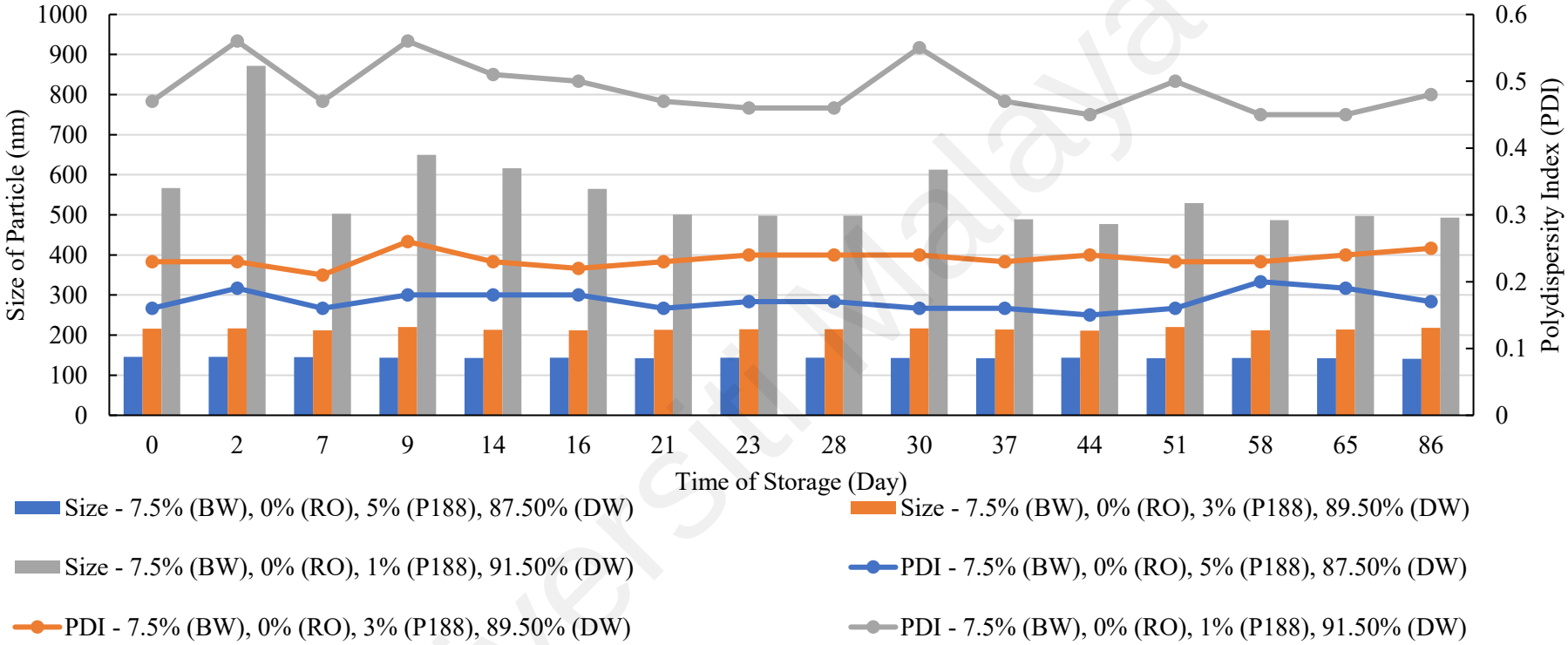

Figure 4.14: Size of particle and polydispersity index versus time of storage (day). The SLNs displayed were F25 (BW (7.5%), RO (0%), P188 (1%), DW (91.5%)), F24 (BW (7.5%), RO (0%), P188 (3%), DW (89.5%)) and F3 (BW (7.5%), RO (0%), P188 (5%), DW (87.5%)).

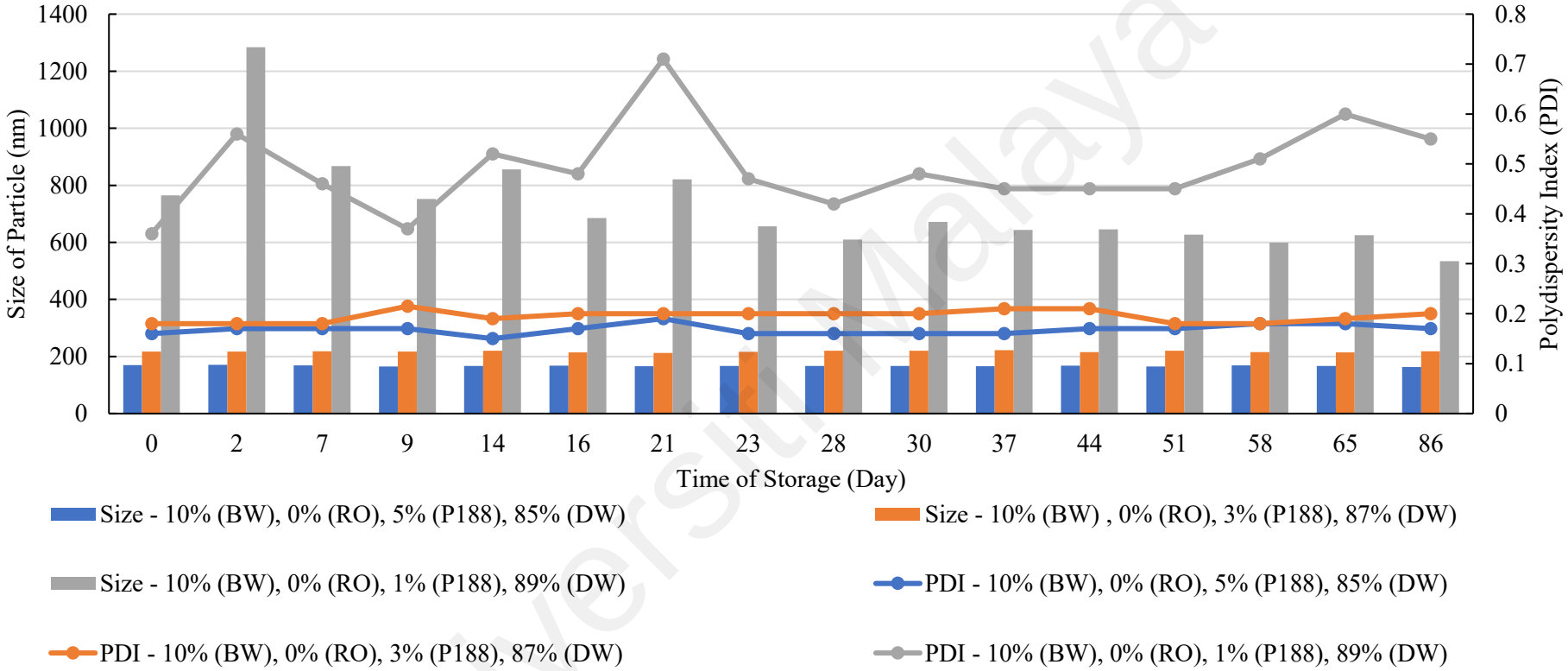

Figure 4.15: Size of particle and polydispersity index versus time of storage (day). The SLNs displayed were F8 (BW (10%), RO (0%), P188 (1%), DW (89%)), F22 (BW (10%), RO (0%), P188 (3%), DW (87%)) and F13 (BW (10%), RO (0%), P188 (5%), DW (85%)).

4.4.2 Zeta Potential

Zeta potential value enable the prediction of formulations stability. Figures 4.16, 4.17, 4.18, 4.19, 4.20, 4.21, 4.22 and 4.23 presented the zeta potential value of SLN and NLC formulations. Zeta potential value was decreased at the beginning of few days in order to stabilize the formulated NLCs and SLNs. After 86 days analysis, the range of zeta potential value was found in between -26.10 mV to -55.13 mV. As explained by Gonzalez-Mira and the team, the high zeta potential value (close to 30 mV or higher than 30 mV) whether negative or positive is considered to be a stable dispersion (González-Mira et al., 2011). Negative value of zeta potential was attained as the result of the head group polarization from non-ionic surfactant that followed by adsorption of polarized water molecules at the surface of particles (Tan et al., 2010). Zhang and the team also have found the identical results from their experiment (Zhang et al., 2017). P188 consists of a central polyoxypropylene moiety on its polar head group. Unlike ionic surfactant, P188 could not ionize in aqueous solution but it manages to induce hydroxyl ions adsorp on the polar non-ionic head group of the surfactant molecules. The water molecules layer adsorbed onto the surface of particle and formed repulsion barrier to stabilize the particles of NLCs and SLNs with the existence of steric stability on it (Ong et al., 2016; Swidan et al., 2016).

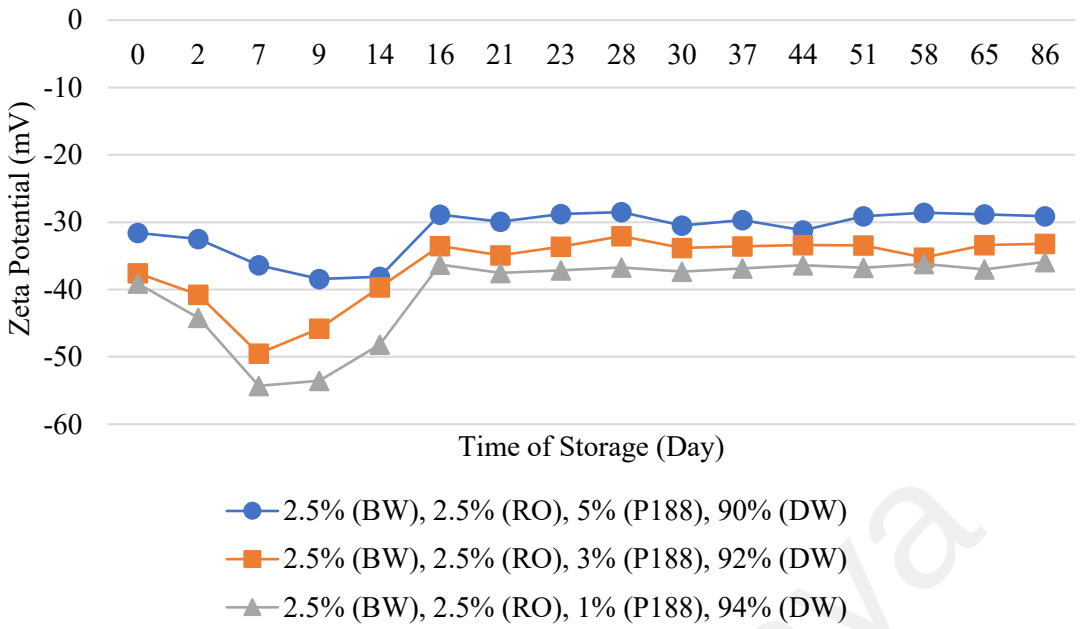

Figure 4.16: Value of zeta potential versus time of storage (day). The NLCs displayed were F27 (BW (2.5%), RO (2.5%), P188 (1%), DW (94%)), F21 (BW (2.5%), RO (2.5%), P188 (3%), DW (92%)) and F12 (BW (2.5%), RO (2.5%), P188 (5%), DW (90%)).

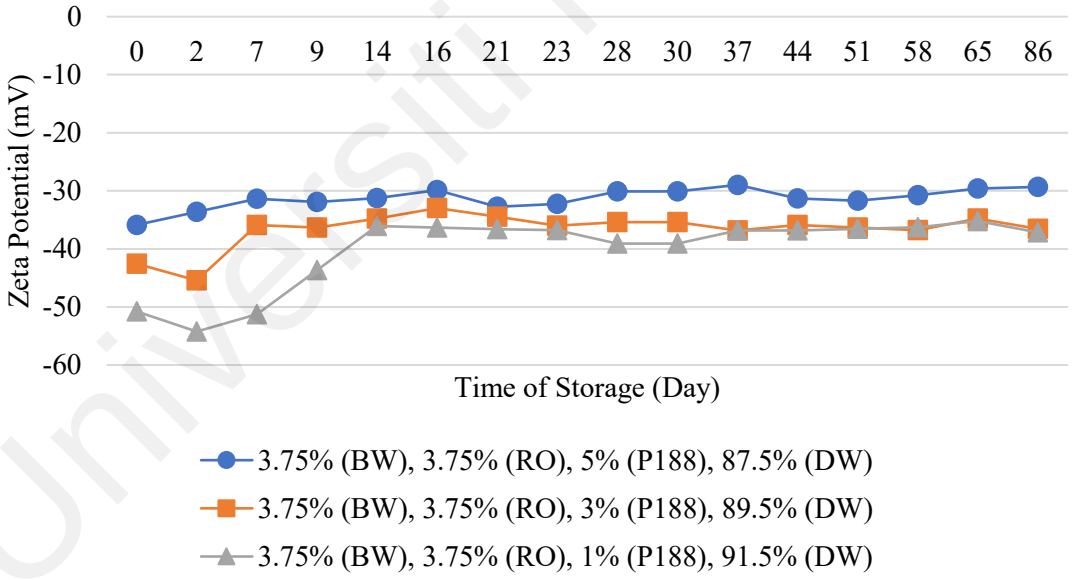

Figure 4.17: Value of zeta potential versus time of storage (day). The NLCs displayed were F26 (BW (3.75%), RO (3.75%), P188 (1%), DW (91.5%)), F4 (BW (3.75%), RO (3.75%), P188 (3%), DW (89.5%)) and F15 (BW (3.75%), RO (3.75%), P188 (5%), DW (87.5%)).

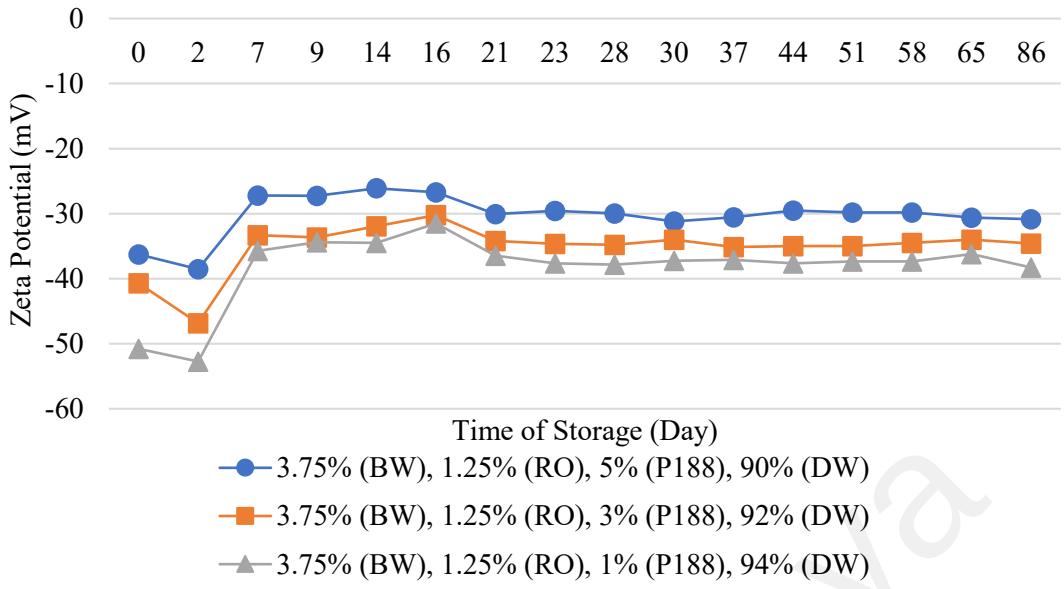

Figure 4.18: Value of zeta potential versus time of storage (day). The NLCs displayed were F17 (BW (3.75%), RO (1.25%), P188 (1%), DW (94%)), F16 (BW (3.75%), RO (1.25%), P188 (3%), DW (92%)) and F20 (BW (3.75%), RO (1.25%), P188 (5%), DW (90%)).

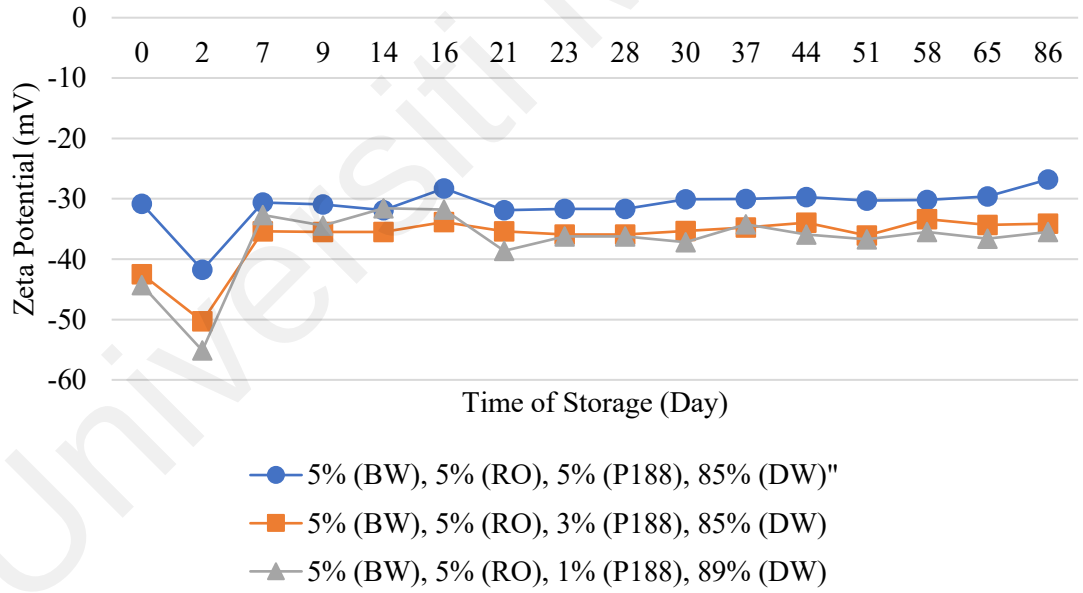

Figure 4.19: Value of zeta potential versus time of storage (day). The NLCs displayed were F2 (BW (5%), RO (5%), P188 (1%), DW (89%)), F6 (BW (5%), RO (5%), P188 (3%), DW (87%)) and F1 (BW (5%), RO (5%), P188 (5%), DW (85%)).

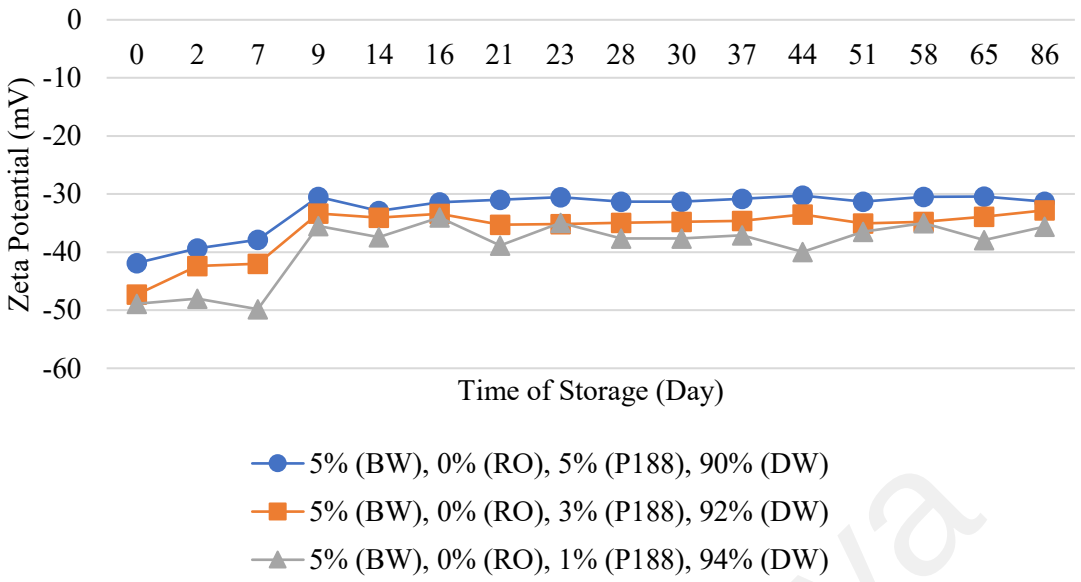

Figure 4.20: Value of zeta potential versus time of storage (day). The SLNs displayed were F11 (BW (5%), RO (0%), P188 (1%), DW (94%)), F14 (BW (5%), RO (0%), P188 (3%), DW (92%)) and F9 (BW (5%), RO (0%), P188 (5%), DW (90%)).

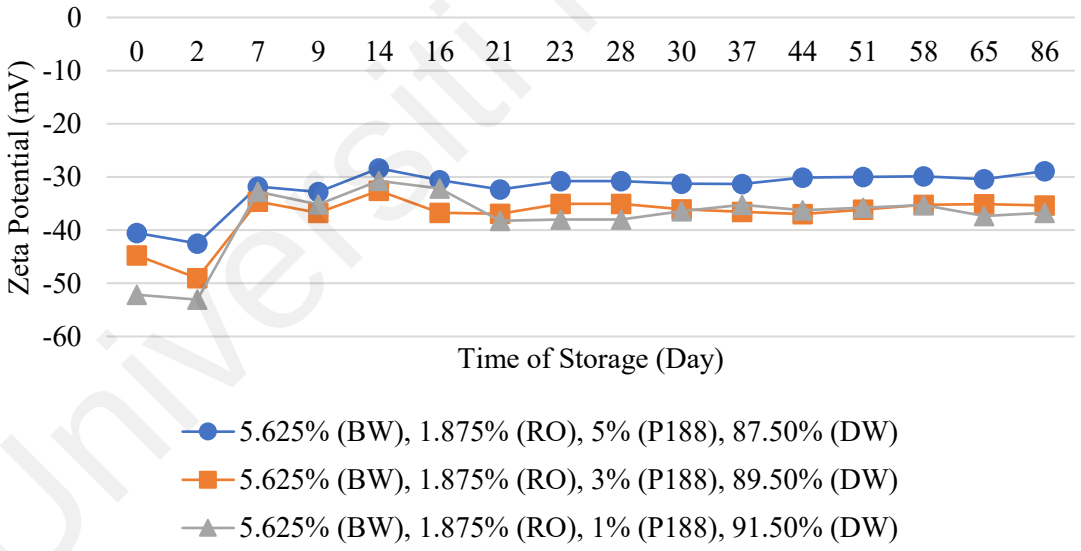

Figure 4.21: Value of zeta potential versus time of storage (day). The NLCs displayed were F5 (BW (5.625%), RO (1.875%), P188 (1%), DW (91.5%)), F19 (BW (5.625%), RO (1.875%), P188 (3%), DW (89.5%)) and F18 (BW (5.625%), RO (1.875%), P188 (5%), DW (87.5%)).

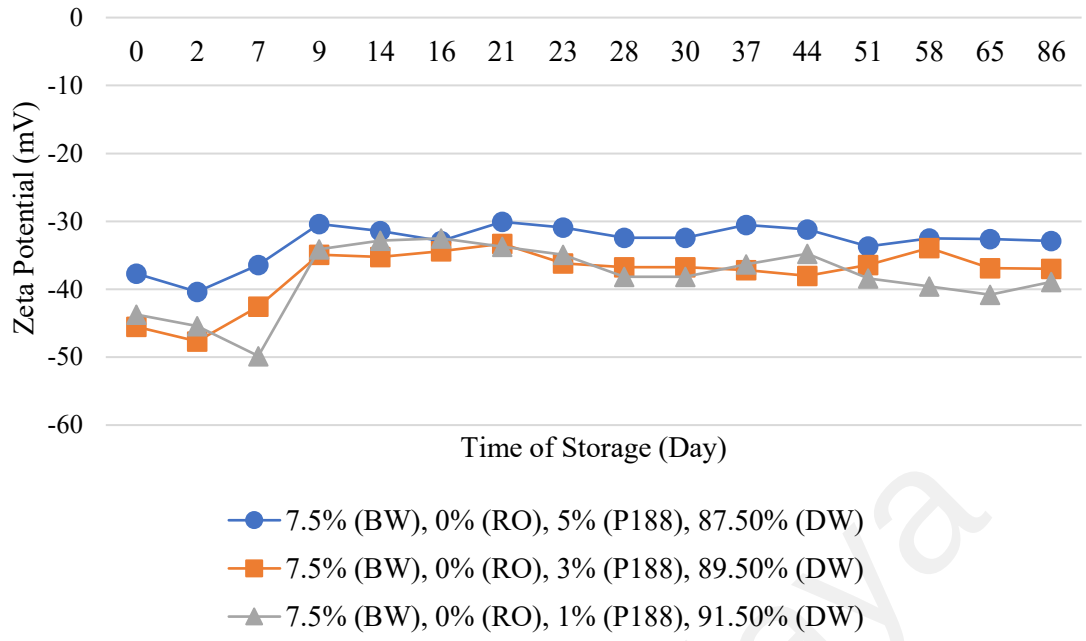

Figure 4.22: Value of zeta potential time of storage (day). The SLNs displayed were F25 (BW (7.5%), RO (0%), P188 (1%) DW, (91.5%)), F24 (BW (7.5%), RO (0%), P188 (3%), DW (89.5%)) and F3 (BW (7.5%), RO (0%), P188 (5%), DW (87.5%)).

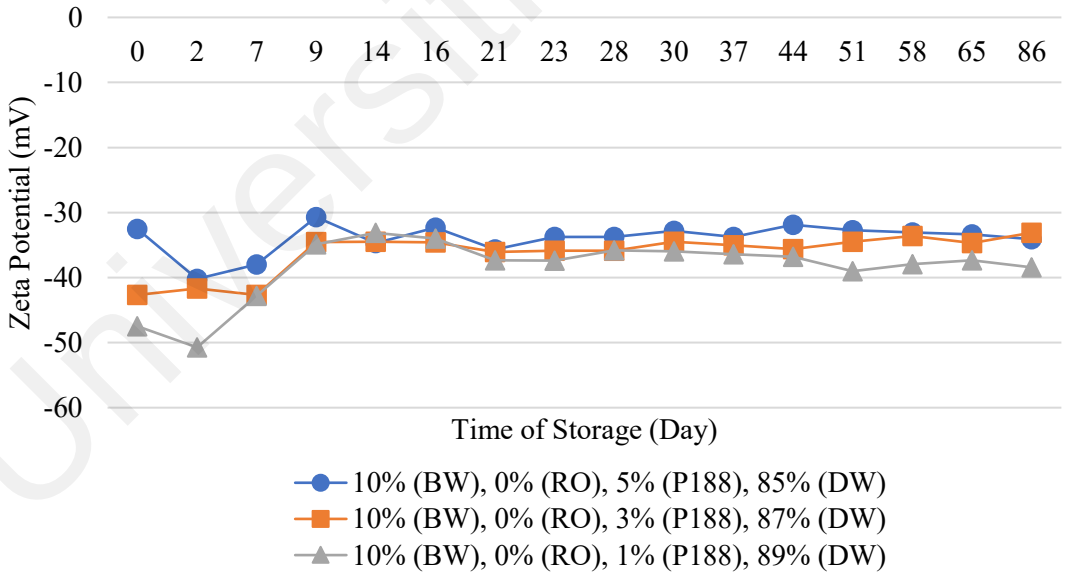

Figure 4.23: Value of zeta potential versus time of storage (day). The SLNs displayed were F8 (BW (10%), RO (0%), P188 (1%), DW (89%)), F22 (BW (10%), RO (0%), P188 (3%), DW (87%)) and F13 (BW (10%), RO (0%), P188 (5%), DW (85%)).

Generally, the zeta potential values were depressed when the percentage of P188 were greater in the all formulations as represented in the figures 4.16, 4.17, 4.18, 4.19, 4.20,

4.21, 4.22 and 4.23 (Emami et al., 2012). It is due to the adsorption of P188 onto the surface of lipid nanoparticles. The probability of P188 adsorbs on SLNs and NLCs is related to the percentage of P188 used in formulations. Increase in P188 concentration promotes a higher amount of P188 adsorb on SLNs and NLCs. Therefore, SLNs and NLCs with 1 % of P188 has a more negative value of zeta potential compared to 3% and 5 % of P188. The adsorption of 1 % P188 onto the surface of lipid nanoparticles is weaker compared to the 3 % and 5 % of surfactant in SLN and NLC formulations. Logically, 1 % of P188 was less concentrated compared to the 3 % and 5 % of P188. So, it has induced a higher zeta potential value due to the higher and effortless of particles movement that has repelled each other on the slipping plane surface, which is the boundary where the value of zeta potential was measured. The thickness of diffuse layer on the particles also has been shortened (Tan et al., 2010). For that reason, the compositional ratio has to be finely adjusted in order to ascertain NLCs with desired particle size and stability.

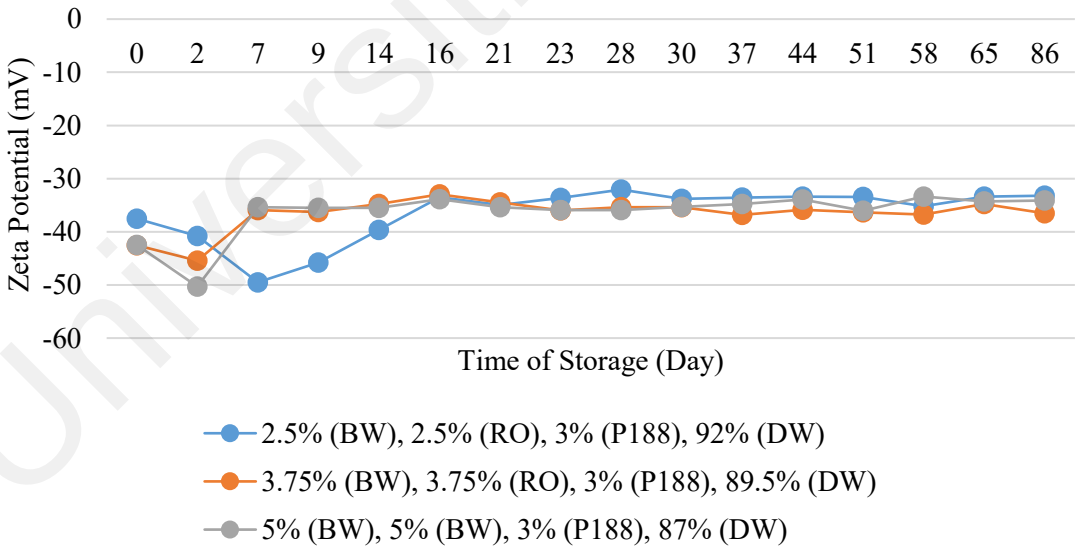

Figure 4.24: Value of zeta potential versus time of storage (day). The NLCs displayed F21 (BW (2.5%), RO (2.5%), P188 (3%), DW (92%)), F4 (BW (3.75%), RO (3.75%), P188 (3%), DW (89.5%)) and F6 (BW (5%), RO (5%), P188 (3%), DW (87%)).

After 86 days analysis, the zeta potential value of NLCs were seen almost uniform even the total of lipid composition was increased from 5 % to 10 % as represented in the figure 4.24. Hence, the total lipid in NLCs did not affect the zeta potential value in NLCs as explained by the past experiment. This is commonly due to the composition of the external surfactant phase is fixed in every batches (Kuo & Chung, 2011).

Besides, zeta potential value for the F16 in PBS medium was reported at (-18 ± 8) mV. The lower magnitude of zeta potential compared to the NLCs in deionized water (-36 ± 5) mV possibly due to charge shielding effect in PBS (Bondì et al., 2014). It was also affected from the potential compensation of ionic PBS that bound on the surface of particles. Hence, it could reduce a negativity of zeta potential magnitude. The Same formulation also has been prepared from poloxamer 407 as a surfactant. The zeta potential value was recorded at (-26 ± 4) mV and found lower compared to the zeta potential value in P188 (-36 ± 5) mV. P188 has a shorter alkyl chain than poloxamer 407. Therefore, it leads to the greater number of molecules adsorb on the NLCs due to the pack steric effect, which reflect as a more negative zeta potential (White et al., 2007).

4.5 Optimization of The Responses for NLC Formulations

For a better visualization of the effects, the predicted response domain fixed at 92 % water content is presented in a ternary contour plot (figure 4.25). Taking the constraints applied (shaded domain) into account, the simultaneous optimum responses for particle size and zeta potential were predicted to be in the range of 150-200 nm and -(36-40) mV, respectively. Furthermore, this formulation was found physically stable without formation of aggregate after a storage period of 86 days at room temperature as displayed in the figure 4.26. Hence, the formulation composing 3.75% BW, 1.25% RO and 3% P188 was selected for further study as displayed in the figure 4.25.

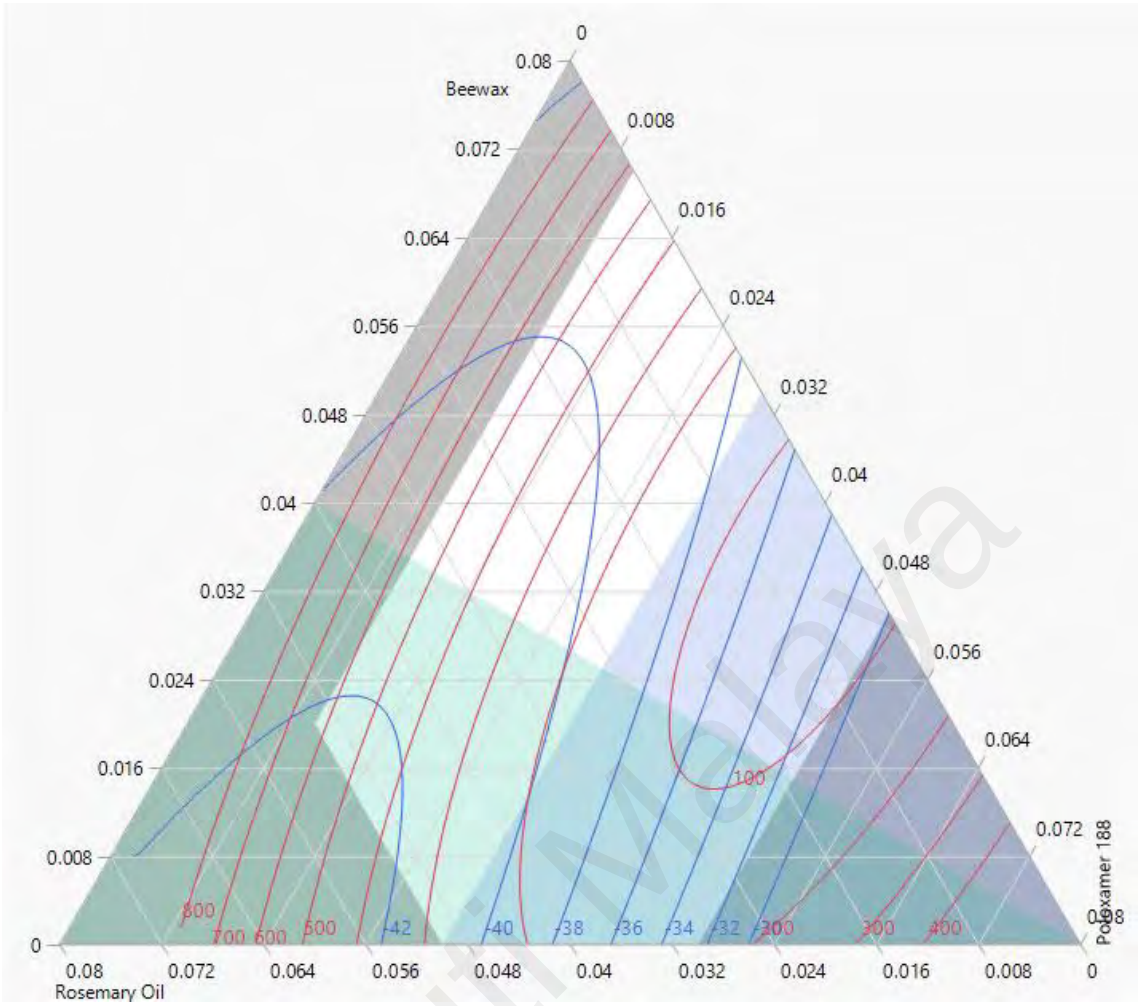

Figure 4.25: Ternary contour plot showing the effect of mixture on the particle size (red lines) and zeta potential (blue lines) of the formulated lipid carriers fixed at 92% water content.

Figure 4.26: F16 (3.75% (BW), 1.25% (RO), 3% (P188), 92% (DW))

4.6 Thermal properties analysis

Figure 4.27 and 4.28 showed the thermograms of BW, RO, P188, NLCs (F4 and F16) and SLNs (F14). The melting parameters such as melting point, onset temperature and melting enthalpy were obtained from these thermograms. The onset temperature was determined from the intersection tangent of the endothermic peak with the extrapolated baseline. Degree of Crystallinity (CD) also can be determined by calculating the ratio of sample's melting enthalpy to BW melting enthalpy as showed in equation (4.1):

$$CD = \left(\frac{Melting\ Enthalpy\ of\ Sample}{Melting\ Enthalpy\ of\ Beeswax}\right) \times 100 \quad (4.1)$$

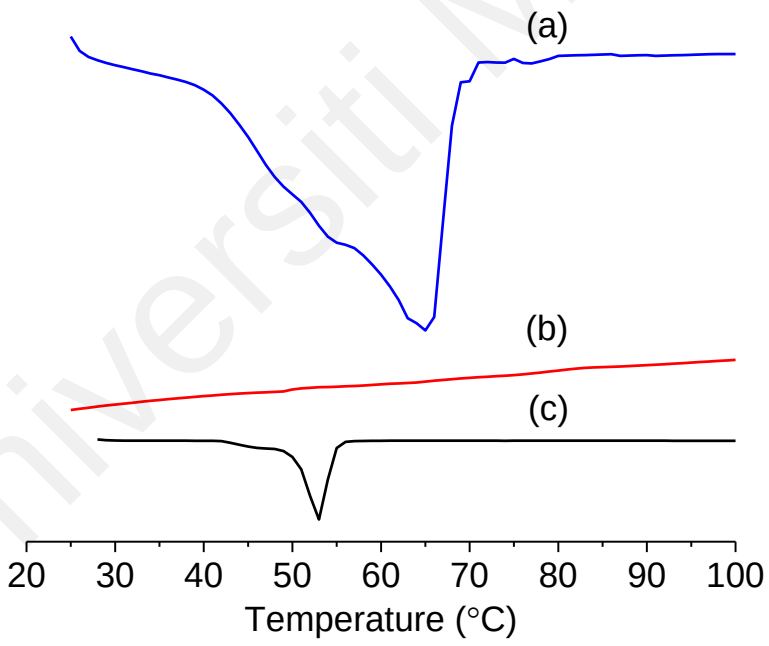

Figure 4.27: Endothermic thermogram of starting materials, (a) BW, (b) RO and (c) P188.

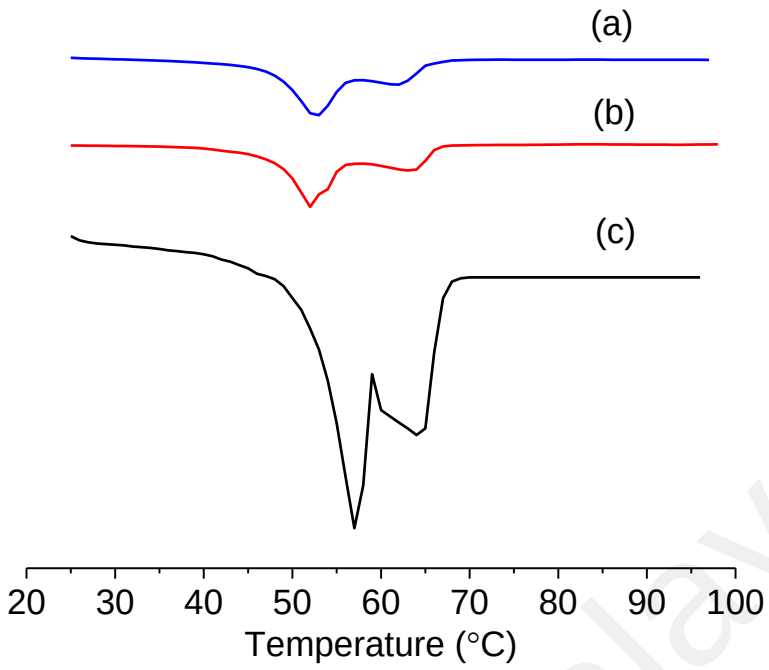

Figure 4.28: Endothermic thermogram of (a) NLCs, F4, (BW:RO, 3.75:3.75), (b) NLCs, F16, (BW:RO, 3.75:1.25), (c) SLNs, F14, (BW:RO, 5:0).

Table 4.3: Thermal properties of BW, P188, SLNs and NLCs

Samples	Onset Temperature (°C)	Melting Enthalpy (J/g)	Melting Point (°C)	Degree of crystallinity (%)
BW	61.50	16.14	65.00	-
P188	52.90	6.80	52.90	-
NLCs, F4 (3.75% (BW), 3.75% (RO), 3% (P188), 89.5% (DW))	58.46	2.38	62.00	14.75
NLCs, F16 (3.75% (BW), 1.25% (RO), 3% (P188), 92% (DW))	58.81	5.32	63.51	32.96
SLNs, F14 (5% (BW), 0% (RO), 3% (P188), 92% (DW))	59.30	8.98	64.70	55.32

The result for thermal properties were recorded in the table 4.3. From figure 4.27, RO did not show any thermal appearance due to liquid properties (existed as an oil at room temperature). Comparing with the previous research, Miglyol® 812 (triglycerides of

capric/caprylic acids) also shown a similar observation (Mendes et al., 2013). From figure 4.28, the endothermic transitions for SLNs and NLCs displayed a bimodal endothermic peak with a lower melting peaks due to the present of P188 and BW (Dora et al., 2012). Besides, NLCs (F4 and F16) recorded a lower degree of crystallinity and produced a broader peak of BW compared to the SLNs (F14) (Noh et al., 2017). However, NLCs (F4) showed the lowest degree of crystallinity with 14.75% compared to the NLCs (F16) and SLNs (F14), which were 32.96% and 55.32%, respectively. It was due to the presence of highest RO (3.75%) composition in NLCs (F4). The presence of liquid oil (RO) will disrupt the closely packing of BW in it (Lin et al., 2007). Swidan and the group found that, the more liquid lipid added in NLCs, the more crystallinity degree will be decreased (Swidan et al., 2016).

Moreover, a shift of BW's melting point peak was seen in figure 4.28 indicating the interaction of RO with the BW matrix. The Bulk material of BW exhibited a maximum peak at 65.00 °C. By referring to table 4.3, the melting point of BW in SLNs (F14, BW:RO, 5%:0%), NLCs (F16, BW:RO, 3.75%:1.25%) and NLCs (F4, BW:RO, 3.75%:3.75%) were showed lowered compared to melting point of BW. The reduced of melting point is due to the presence of surfactant and liquid lipid in the formulations (Fathi et al., 2018). The presence of liquid lipid could minimize the formation of solid lipid crystals and able to decrease the value of melting point in NLCs (Pan et al., 2016).

The melting enthalpies of SLNs (F14) and NLCs (F16 and F4) were slightly reduced compared to the BW's melting enthalpy as shown in table 4.3. This indicated a lower ordered of lattice arrangement of BW in SLNs and NLCs. The arrangement of BW in NLCs (F16 and F4) were less ordered compared to the bulk materials and SLNs (F14). The inner core of NLCs (F16 and F4) are expected composing completely amorphous compared to SLNs (F14). So, this imperfection will provide more space for drug to be accommodated in NLCs (Soleimanian et al., 2018).

In addition, the melting point of TBHC1 was observed at 209.36 °C as shown in the figure 4.29. The peak of TBHC1 in optimized NLC formulation was disappeared, suggesting that the drug was encapsulated very well and no longer in crystalline mode in NLCs (Qiua et al., 2012). Based on the past research, the peak of minoxidil (drug used) in NLCs was disappeared too. It indicated that, the minoxidil was not in the crystalline state (amorphous) but has homogenously dispersed in NLCs (Uprit et al., 2013).

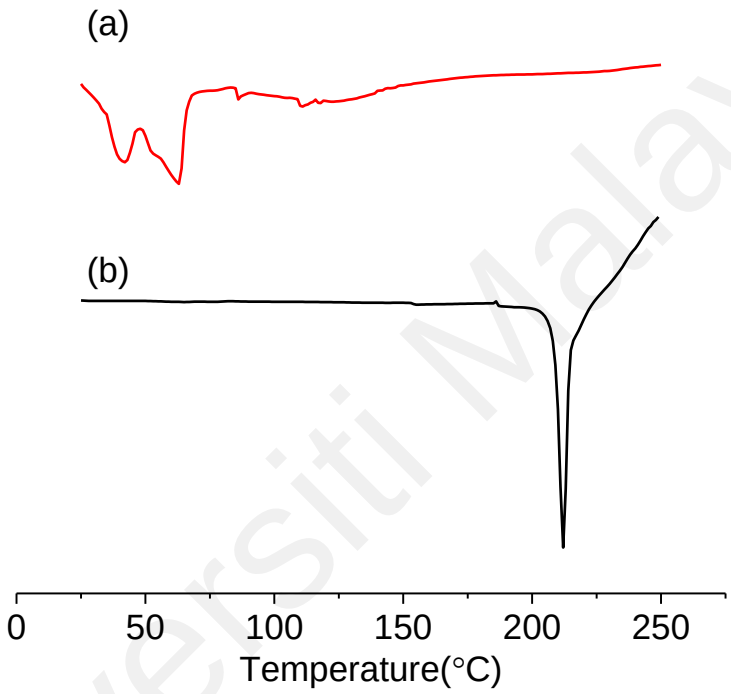

Figure 4.29: DSC thermogram of (a) Optimized NLCs loaded with TBHC1, (b) TBHC1

4.7 Crystallinity of NLCs

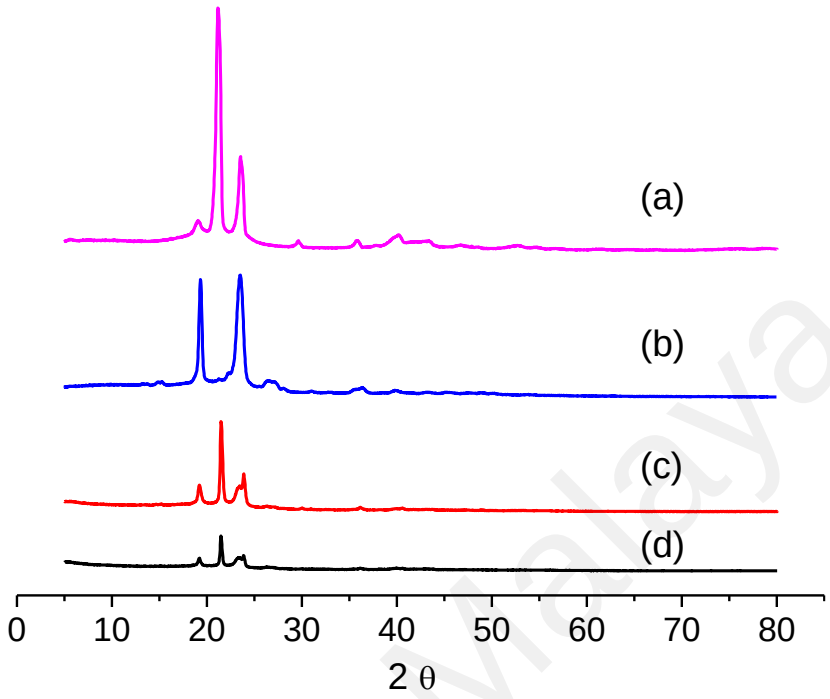

Figure 4.30: **Diffractogram of (a) BW, (b) P188, (c) SLNs, F14, (BW:RO, 5:0) (d) NLCs, F16, (BW:RO, 3.75:1.25)**

Figure 4.30 displayed the diffractograms of BW, P188, SLNs (F14) and NLCs (F16). Crystallinity degree of XRD diffractograms for each sample were measured by using Highscore Plus software. At 2θ = 21°, crystallinity degree for BW, P188, F16 (NLCs) and F14 (SLNs) were presented at 52569.00, 26339.00, 1558.06 and 2852.00, respectively. The strongest peak in BW's diffractogram was represented at 2θ = 21°. It indicated the crystalline properties of BW as a solid lipid in this experiment. By correlating with the pure lipid BW, the peak intensities for both SLNs (F14) and NLCs (F16) were found weaker. It showed that, the crystallinity of lipid decreased in nanoparticles compared to the crystallinity of pure BW. The diffractogram of NLCs (F16) showed lower crystalline properties compared to the SLNs (F14). The present of RO (with 1.25%) in NLCs (F16) did not change the position of signal but weaken its intensity. The lipid existed in NLCs (F16) caused the formation of a lower crystallinity state and less

ordered structure while, SLNs (F14) represented a higher crystallized and high ordered structure. Hence, it could demonstrate that, the presence of RO in NLCs (F16) can caused the crystallinity of BW became weaker and more drug can be loaded in it compared to the SLNs (F14) (Lin et al., 2007; Liu & Wu, 2010). The value for each sample from XRD and DSC is not comparable but showing the same pattern. When we added a liquid lipid and surfactant in the NLCs formulation, the crystallinity of sample became weaken.

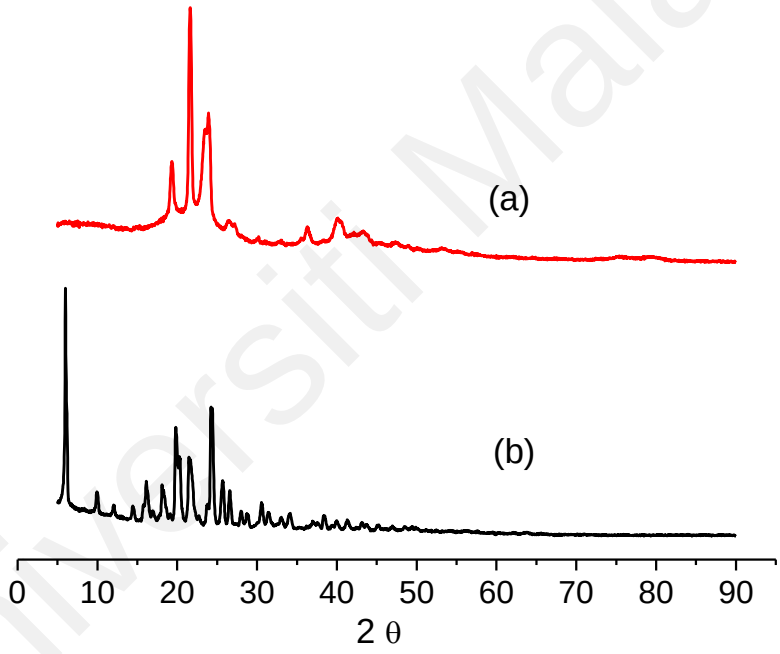

Figure 4.31: Diffractogram of (a) Optimized NLCs encapsulated with TBHC1, (b) TBHC1

Then, the diffractogram of pure TBHC1 (figure 4.31) showed the presence of several sharp peaks and the most intense appeared at 2θ = 6.4°. This peak indicated the crystalline nature of TBHC1, which is at 13507.00. However, this intense peak disappeared in the optimized NLCs (crystallinity degree at 2744.00). Therefore, the results suggested that TBHC1 was dispersed completely in NLCs and present as the form of amorphous (Liu et al., 2014; Scioli Montoto et al., 2018). The identical result also has been reported from

the past research. Rahman (2013) analyzed that, the zerumbone (drug) was no longer retained its crystallinity and became amorphous when incorporated in NLCs (Rahman et al., 2013).

In addition, the diffractograms of calcein and optimized NLCs that encapsulated with calcein was represented in the figure 4.32. Calcein's diffractogram indicated a high intensity at 2θ = 24°, which is at 3084.00 (Gao et al., 2017). The optimized NLCs encapsulated with calcein showed a lower intensity compared to the bulk BW, which displayed a weaker intensity at 2θ = 21°. Moreover, the high intensity properties of calcein at 2θ = 24° was disappeared (crystallinity degree at 524.04). These results indicated that the calcein was loaded in NLCs and hence lowered the crystalline state while represented as the form of amorphous (Aliasgharlou et al., 2016).

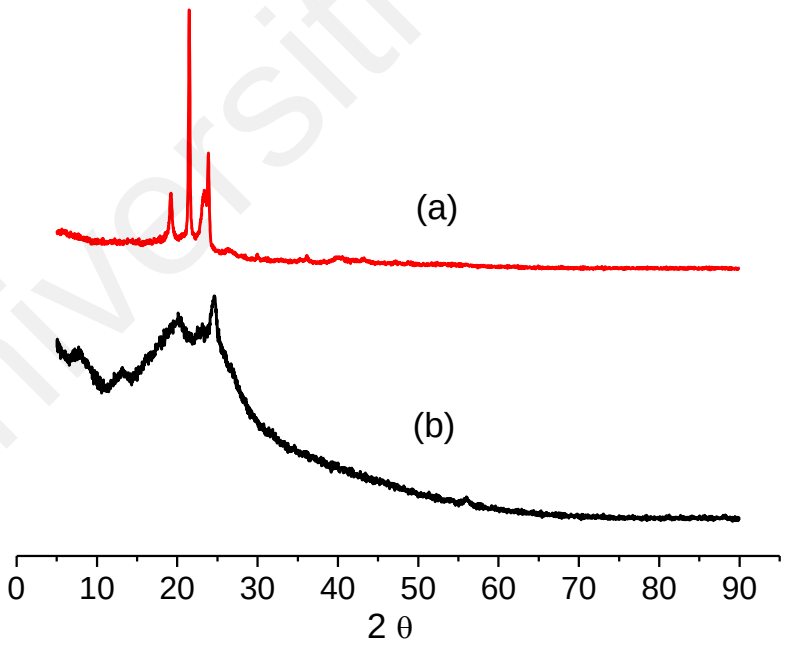

Figure 4.32: Diffractogram of (a) Optimized NLCs encapsulated with calcein, (b) Calcein

4.8 Morphology of NLCs

Figure 4.33 showed the TEM micrograph of optimized NLCs (F16). The micrograph revealed that NLCs appeared as spherical shape with a dense appearance (Poonia et al., 2016). They were presented as individual particle and non-aggregated (Kaushik, 2016). It was apparently showed the particle size obtained from TEM was in agreement with the obtained size from zetasizer (Khurana et al., 2013). While, micrograph from FESEM in figure 4.34 displayed the present of circular particles distributed on the rough surface (Babazadeh et al., 2016).

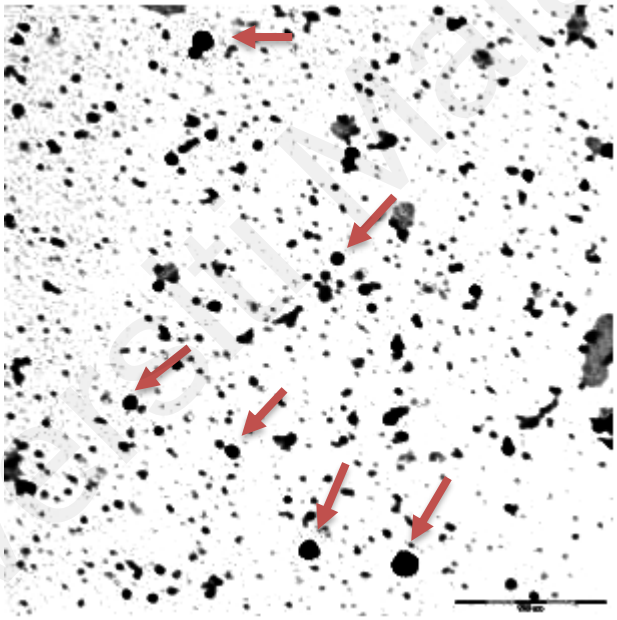

Figure 4.33: TEM Micrograph of NLCs (F16) (scale bar denotes size of 500 nm)

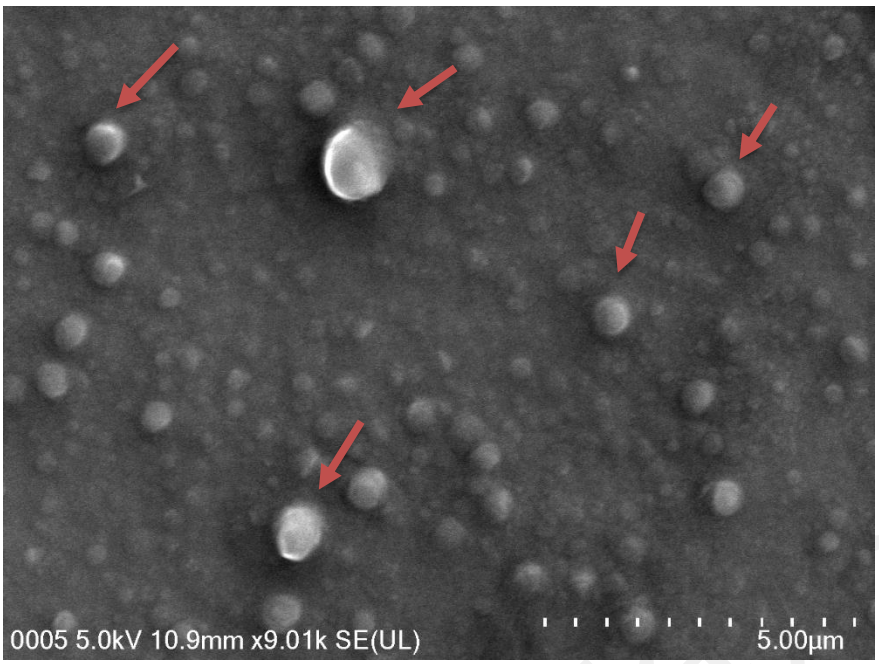

Figure 4.34: FESEM Micrograph of NLCs (F16)

4.9 Drug encapsulation and drug loading efficiency of TBHC1 in NLCs

The highest encapsulation efficiency of the optimized NLCs (F16) was found to be (99.50 ± 0.01) % at 0.04 mg/mL as indicated in the figure 4.35. The encapsulation efficiency of TBHC1 in the optimized NLCs was declined from (99.50 ± 0.01) % to (87.05 ± 0.05) % as the concentration of TBHC1 increased from 0.04 mg/mL to 0.5 mg/mL. So, the suggested optimum condition for TBHC1 encapsulation properties is (99.50 ± 0.01) % at 0.04 mg/mL. On the other hand, the drug loading efficiency of TBHC1 in NLCs increased from (0.29 ± 0.09) % to (3.20 ± 0.01) % as the concentration of TBHC1 increased from 0.04 mg/mL to 0.5 mg/mL, as revealed in figure 4.35. More efficient drug loading into the NLCs occurred as the concentration of drug increased (Yuan et al., 2007). Even though the encapsulation efficiency of the optimized NLCs was reduced with increasing concentration of drug, the drug loading efficiency was highly improved, indicating that the NLCs could be loaded with more drug. The arrangement of

lipid in NLCs became more imperfect and consequently providing sufficient space for a large amount of drug to be lodged effectively (Gaba et al., 2015).

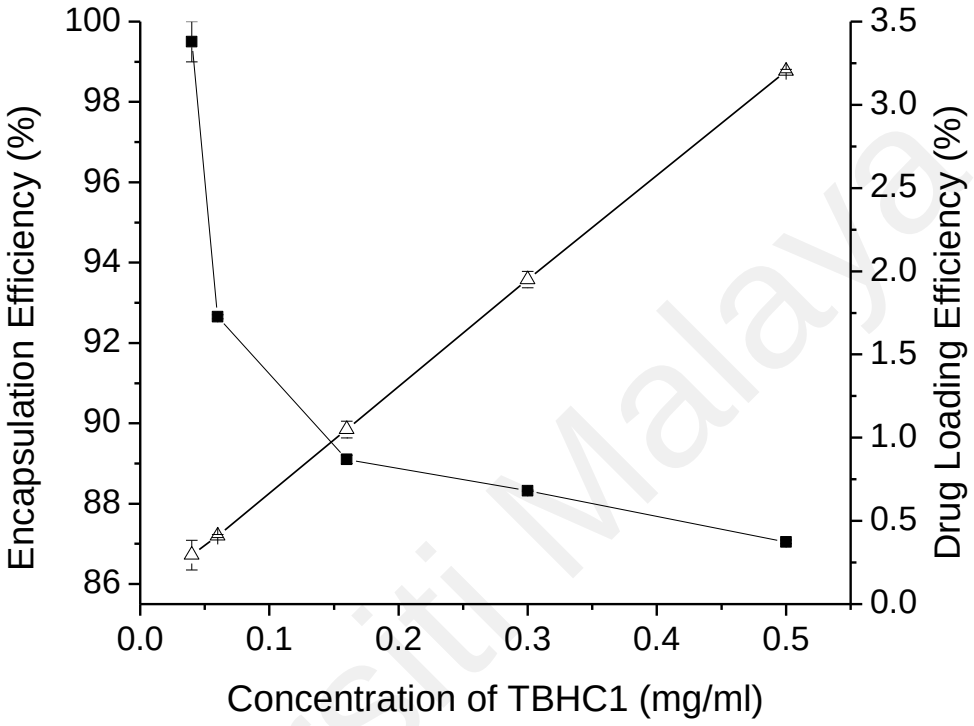

Figure 4.35: The effects of TBHC1 concentration on encapsulation efficiency (solid square) and drug loading efficiency (empty triangle)

4.10 Drug encapsulation and drug loading efficiency of calcein in NLCs

The highest encapsulation efficiency of optimized NLCs in calcein was reported to be 34.44 % at 0.04 mg/mL as stated in the figure 4.36. The encapsulation efficiency of calcein in optimized NLCs was decrease from 34.44 % to 11.44 % with the increasing of calcein from 0.04 mg/mL to 1.1 mg/mL. However, drug loading efficiency of calcein in NLCs was increased from 0.0011 % to 0.0026 % at 0.04 mg/mL to 1.1 mg/mL. Drug loading efficiency in NLCs became higher when more drug loaded into it. However, the encapsulation and drug loading efficiency of calcein in NLCs were displayed lower compared to the hydrophobic drug used (TBHC1) as explained in the previous content

(content 4.9). It is because calcein is a hydrophilic drug while TBHC1 is a hydrophobic drug. So, encapsulation and drug loading efficiency of Calcein display lowered compared to TBHC1. The similar result also has been obtained from the previous experiment that was conducted by Lipeng Qiu and the group, the EE and DLE of oxaliplatin (hydrophilic drug) was showed lower compared to the lipophilic drug used (Qiua et al., 2012). As indicated by Pimpalshende and the team, the hydrophilic drug is also tough to be encapsulated and retained in the lipid matrix due to its poor solubility in lipid and oil (Pimpalshende & Gupta, 2018). Although the encapsulation efficiency of optimized NLCs was limited, drug loading efficiency could be highly recovered with the increasing amount of drug in it. This apparently showed that NLCs could be loaded with more drug. The arrangement of lipid in NLCs became more imperfect and consequently providing a sufficient space for a large amount of drug to load it effectively (Gaba et al., 2015).

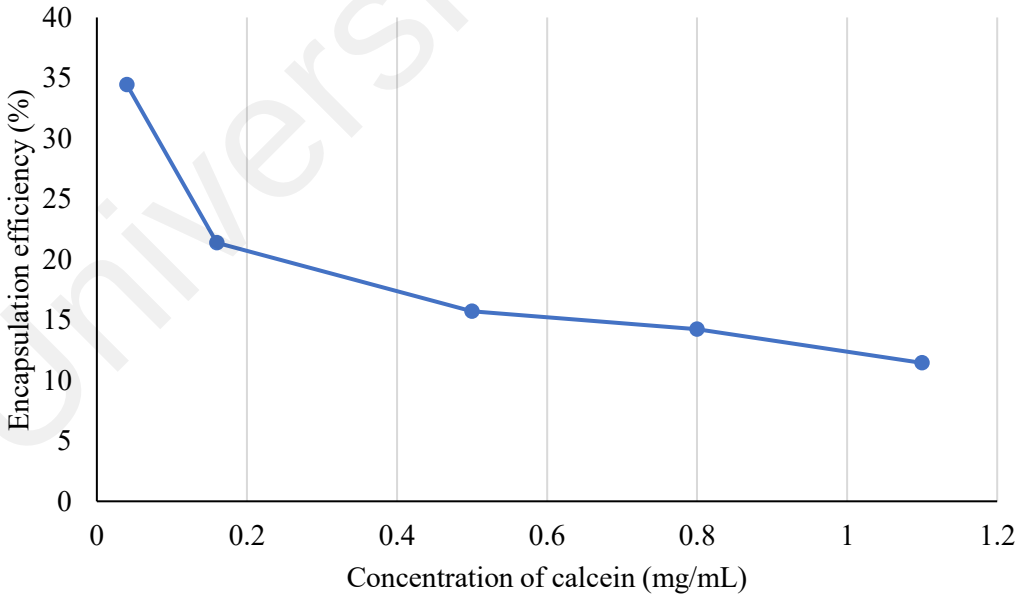

Figure 4.36: Encapsulation efficiency (%) versus concentration of calcien

4.11 *In Vitro* drug release studies of TBHC1 from NLCs

Figure 4.37 showed *in vitro* drug release of NLCs (F16), SLNs (F14) and free drug solution for 48 hours. The concentration of TBHC1 in all samples was 0.1 mg/mL. The concentration used was within the range of solubility limit for TBHC1 in deionized water (Debnath et al., 2012). This is to ensure that, total dispersed of TBHCl in the aqueous phase without formation of any sediment at the bottom of retentate. For NLCs (F16), a biphasic drug release pattern has been observed. It showed that TBHC1 was released rapidly at initial phase followed by the slow release from NLC formulation. The initial rapid release may be due to the diffuse of free drug from the aqueous phase (K_2). Next, TBHC1 was slowly and constantly released from NLCs and SLNs (K_1) as illustrated in figure 4.38. The release of TBHC1 from drug solution was very rapid (100.00± 0.07) % compared to the optimized NLCs, F16 (62.87 ± 0.04) % and SLNs, F14 (48.07 ±0.01) %. It might be due to the presence of lipid in NLCs system that can improved drug solubilizing and release potential (Gaba et al., 2015). The presence of lipid in the system will make a sustained slow drug release from NLCs compared to the free drug solution. It has the capability to produce a better release capacity by improving its effectiveness and decreases the side effects of drug that caused by the rapid release from free drug solution (Nordin et al., 2018). It could retard the release of TBHC1 into the aqueous phase. The release of TBHC1 from optimized NLCs, F16 was found higher (62.87± 0.04) % compared to SLNs, F14 (48.07 ± 0.01) %. It proved that the higher amount of drug was released from nanoparticles formulation with more content of liquid lipid. It will make the drug diffusion through liquid lipid phase faster compared to the solid lipid phase (Yuan et al., 2007). The oil content in NLCs will reduced the crystallinity structure in SLNs and spontaneously helps the drug release enhancement faster compared to SLNs (Üner et al., 2014).

In addition, the table 4.4 displayed the kinetic parameters that obtained from the fitting of TBHC1 release profiles in a different mathematical model. Based on the regression coefficient value (R^2), Korsmeyer-Peppas was fitted well followed by the Baker-Lonsdale, Higuchi and First order model. The similar results also have been found from previous experiments (Choi et al., 2016). Refer to the Korsmeyer-Peppas model, the regression coefficient values (R^2) for TBHC1 solution, NLCs (F16) and SLNs (F14) were reported as 0.98, 0.93 and 0.99, respectively. The release exponent value, n, for drug solution TBHC1, NLCs (F16) and SLNs (F14) were 0.51, 0.35 and 0.59, respectively. According to Korsmeyer-Peppas model, drug release mechanism is according to an anomalous or non-Fickian diffusion if the n value is in the range of 0.45 to 0.89. For NLCs (F16), the proposed release mechanism is according quasi Fickian diffusion since the n value is less than 0.45.

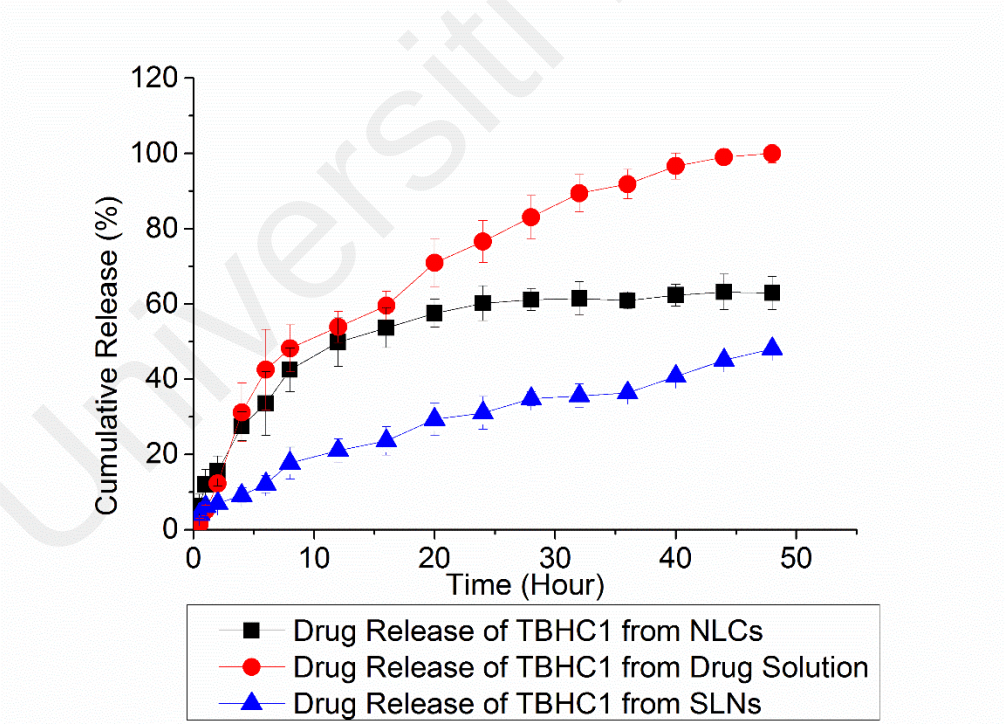

Figure 4.37: **Comparative in vitro release of TBHC1 in optimized NLCs, SLNs and free drug solution**

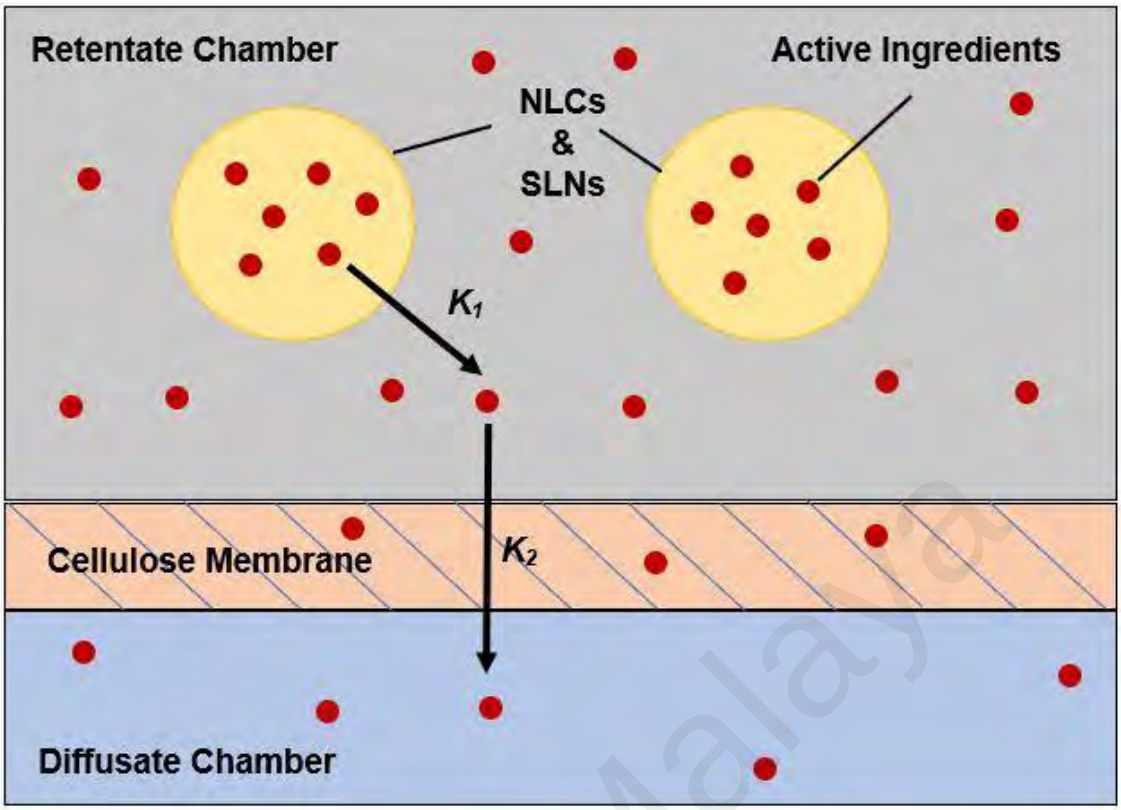

Figure 4.38: **Illustrated diagram for in vitro release mechanism of NLCs and SLNs with active ingredients in Franz diffusion cell**

Table 4.4: Kinetic data obtained by using a different mathematical model for the release of TBHC1

Kinetic model	korsmeyer-peppas		Higuchi		First-order		Baker-Lonsdale	
Parameter	K_{KP} (n)	R^2	K_H	R^2	K_1	R^2	K_{BL}	R^2
Drug solution	14.61996 (0.512456)	0.977386	15.2434	0.977107	0.069094	0.982681	0.006769	0.949957
NLCs (F16)	18.90894 (0.34663)	0.927582	11.3521	0.841112	0.03739	0.501997	0.003255	0.919019
SLNs (F14)	4.740466 (0.589583)	0.991254	6.40997	0.980242	0.014521	0.931398	0.000816	0.968484

Table 4.5: Kinetic data obtained by using a different mathematical model for the release of calcein

Kinetic model	korsmeyer-Peppas		Higuchi		First-order		Baker-Lonsdale	
Parameter	K_{KP} (n)	R^2	K_H	R^2	K_0	R^2	K_{BL}	R^2
Calcein drug solution	4.420673 (0.725676)	0.971211	9.48793	0.921005	0.02602	0.988398	0.001956	0.891018
NLCs (F16)	3.104029 (0.674665)	0.987455	5.60062	0.953746	0.012305	0.965305	0.000605	0.940931
SLNs (F14)	2.403592 (0.628486)	0.983803	3.707	0.962948	0.007437	0.924334	0.000252	0.957104

4.12 *In Vitro* drug release studies of calcein from NLCs

The *In-vitro* drug release of calcein from NLCs (F16), SLNs (F14) and free drug solution was represented in the figure 4.39. The *in-vitro* drug release was investigated for 48 hours. The calcein release from drug solution was higher (66.41 ± 0.07) % compared to the optimized NLCs, F16 (41.70 ± 0.09) % and SLNs, F14 (26.22 ± 0.06) %. It was apparently showed that, the calcein was released rapidly at initial phase followed by the slow release for NLC formulation. The initial rapid release may be due to the release of calcein from the aqueous and interfacial phase. Furthermore, the fast drug release also could be released from unentrapped drug in the dispersion and solubilization of the surfactant micelle in NLCs (Qiua et al., 2012). It might be due to the presence of lipid in NLCs system that can improved drug solubilizing and release potential (Gaba et al., 2015). With the using of same lipid composition, the release of calcein from optimized NLCs, F16 was represented greater (41.70 ± 0.09) % compared to the SLNs, F14 (26.22 ± 0.06) %. It is due the degree crystallinity of NLCs is lower compared to the SLN formulation. With the inclusion of RO (liquid lipid) in NLCs, it will be contributed to the easier drug diffusion of calcein from NLCs and explained more imperfection of it (Gönüllü et al., 2015). The identical data also has been determined from the past experiment that completed by the Kuo and the team. From this experiment, nevirapine (drug) was found slower released from SLNs compared to the NLC formulation due to the reduced thermal resistance of lipid colloids in NLCs (Kuo & Chung, 2011).

Besides, the table 4.5 was represented the kinetic parameters that determined from the fitting of calcein release profiles in a different mathematical model. By comparing the R^2 value with the others kinetic model, Korsmeyer-Peppas model has indicated the best value which were 0.97, 0.99 and 0.98 for the all samples. Then, the Korsmeyer-Peppas was displayed to be the best fitting model followed by the First order, Higuchi and Baker-Lonsdale model. The samples also has explained the ability of a system to

control a drug release from a united pattern of diffusion and erosion release mechanism (anomalous non-Fickian transport value ($0.45 \leq n < 0.89$)) in a korsmeyer-Peppas model (Üner et al., 2014). After that, the First order release kinetics has explained the drug release was depended on the drug concentration. As conducted by Choi and the team, the result has been reported identical with this experiment (Choi et al., 2016).

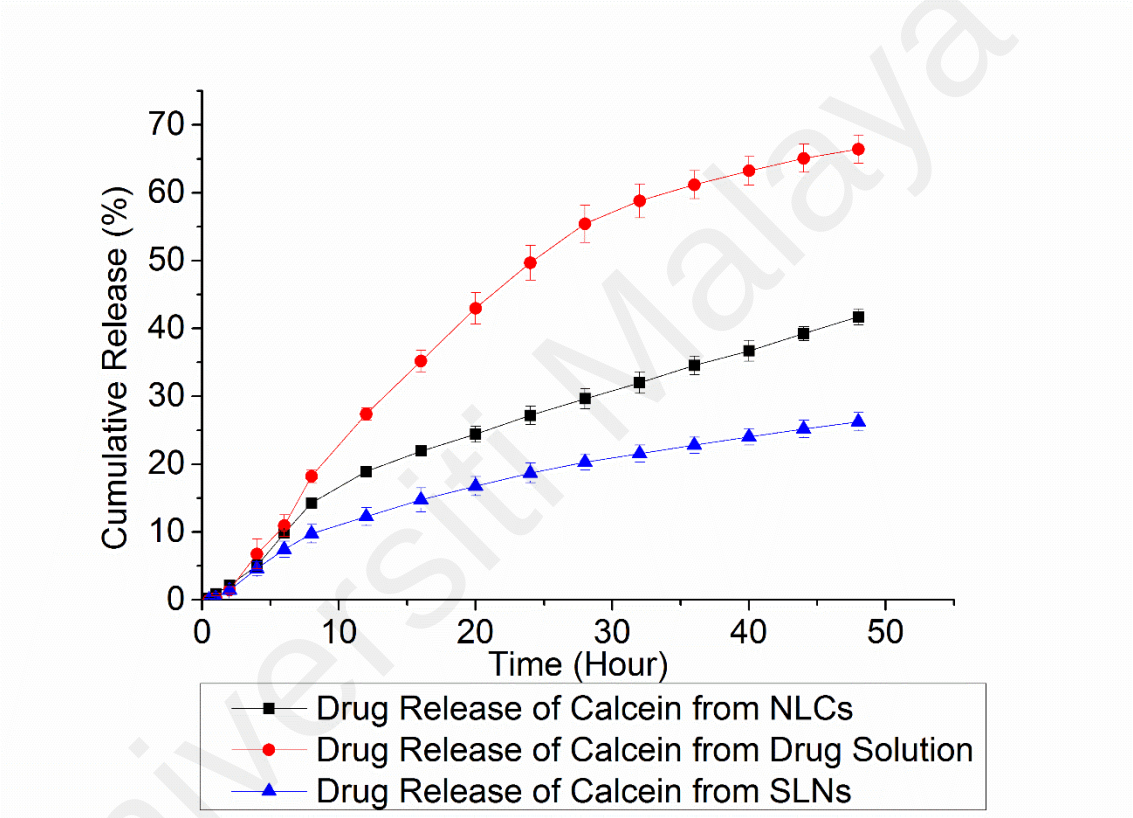

Figure 4.39: Comparative in vitro release of calcien in optimized NLCs, SLNs and free drug solution

CHAPTER 5: CONCLUSION

NLCs was successfully prepared from BW, RO and P188 in the present work. F16 consisting 3.75% (BW), 1.25% (RO), 3% (P188) and 92% (deionized water) was chosen as the optimized formulation in this research due to their physical stability for at least 86 days. The mean of particle size and zeta potential for the optimized NLCs were found at (174 ± 2) nm and (-36 ± 5) mV, respectively. NLCs showed a lower degree of crystallinity and melting enthalpy due to the present of RO. It indicated a lower ordered of lattice arrangement and more hence manage to be loaded with TBHCl and calcein. The morphology of NLCs from TEM was observed as spherical shape with a dense appearance. In addition, micrograph from FESEM displayed the circular particles spreaded on the rough surface. Moreover, drug encapsulation and drug loading efficiency of terbinafine hydrochloride was found higher compared to the calcein as hydrophilic drug in this research. Besides, NLCs promote a slow release of TBHCl and calcein compared to the drug solution. It might be due to the presence of lipid in NLCs system that can improve drug solubilizing and release potential. Hence, the results revealed from physicochemical characteristics, encapsulation efficiency, drug loading efficiency and drug release can be proven that NLCs can be a good colloidal drug delivery system. Besides, the demonstrated data from formulated NLCs could be a promising alternative vehicle to deliver various anti-fungal drugs to target tumor sites. This NLCs formulation also can be future tested on human and animal model. The other lipids also can be formulated for developing another NLCs systems with various properties. Although, further experiments need to be planned for this area.

REFERENCES

Aarabi, M. H., Chabok, H., Mirzapour, A., Ardestani, M. S., & Saffari, M. (2017). Preparation of nanoliposomes containing Rosmarinus offi cinalis L essential oil; A comparative study. *Bioscience Biotechnology Research Communications*, *10*(1), 103-108

AbdelSamie, S. M., Kamel, A. O., Sammour, O. A., & Ibrahim, S. M. (2016). Terbinafine hydrochloride nanovesicular gel: In vitro characterization, ex vivo permeation and clinical investigation. *European Journal of Pharmaceutical Science, 88*, 91-100.

Akbari, J., Saeedi, M., Farzin, D., Morteza-Semnani, K., & Esmaili, Z. (2015). Transdermal absorption enhancing effect of the essential oil of Rosmarinus officinalis on percutaneous absorption of Na diclofenac from topical gel. *Pharmaceutical Biology, 53*(10), 1442-1447.

Al-Waili, N. S. (2005). Clinical and mycological benefits of topical application of honey, olive oil and beeswax in diaper dermatitis. *Clinical Microbiology and Infection, 11*(2), 160-163.

Alam, T., Pandit, J., Vohora, D., Aqil, M., Ali, A., & Sultana, Y. (2015). Optimization of nanostructured lipid carriers of lamotrigine for brain delivery: in vitro characterization and in vivo efficacy in epilepsy. *Expert Opinion on Drug Delivery, 12*(2), 181-194.

Aliasgharlou, L., Ghanbarzadeh, S., Azimi, H., Zarrintan, M. H., & Hamishehkar, H. (2016). Nanostructured Lipid Carrier for Topical Application of N-Acetyl Glucosamine. *Advanced Pharmaceutical Bulletin, 6*(4), 581-587.

Ammar, H. O., Ghorab, M. M., Mostafa, D. M., & Ibrahim, E. S. (2016). Folic acid loaded lipid nanocarriers with promoted skin antiaging and antioxidant efficacy. *Journal of Drug Delivery Science and Technology, 31*, 72-82.

Araújo, J., Nikolic, S., Egea, M. A., Souto, E. B., & Garcia, M. L. (2011). Nanostructured lipid carriers for triamcinolone acetonide delivery to the posterior segment of the eye. *Colloids and Surfaces B: Biointerfaces, 88*(1), 150-157.

Armstrong, J. K., Meiselman, H. J., Wenby, R. B., & Fisher, T. C. (2001). Modulation of red blood cell aggregation and blood viscosity by the covalent attachment of Pluronic copolymers. *Biorheology, 38*(2, 3), 239-247.

Attama, A. A., Momoh, M. A., & Builders, P. F. (2012). Lipid nanoparticulate drug delivery systems: a revolution in dosage form design and development. *Recent Advances in Novel Drug Carrier Systems*: Intech.

Attama, A. A., Schicke, B. C., & Müller-Goymann, C. C. (2006). Further characterization of theobroma oil–beeswax admixtures as lipid matrices for improved drug delivery systems. *European Journal of Pharmaceutics and Biopharmaceutics, 64*(3), 294-306.

Attama, A. A., Schicke, B. C., & Müller-Goymann, C. C. (2007). Novel physically structured lipid matrices of beeswax and a homolipid from Capra hircus (goat fat): a physicochemical characterization for application in drug delivery. *Journal of Drug Delivery Science and Technology, 17*(2), 103-112.

Babazadeh, A., Ghanbarzadeh, B., & Hamishehkar, H. (2016). Novel nanostructured lipid carriers as a promising food grade delivery system for rutin. *Journal of Functional Foods, 26*, 167-175.

Baek, J. S., Pham, C. V., Myung, C. S., & Cho, C. W. (2015). Tadalafil-loaded nanostructured lipid carriers using permeation enhancers. *International Journal of Pharmacuetics, 495*(2), 701-709.

Bagherpour, S., Alizadeh, A., Ghanbarzadeh, S., Mohammadi, M., & Hamishehkar, H. (2017). Preparation and characterization of Betasitosterol-loaded nanostructured lipid carriers for butter enrichment. *Food Bioscience, 20*(Supplement C), 51-55.

Baig, M. S., Owida, H., Njoroge, W., Siddiqui, A.-u.-R., & Yang, Y. (2020). Development and evaluation of cationic nanostructured lipid carriers for ophthalmic drug delivery of besifloxacin. *Journal of Drug Delivery Science and Technology, 55*, 101496.

Bartosova, L., & Bajgar, J. (2012). Transdermal drug delivery in vitro using diffusion cells. *Current Medicinal Chemistry, 19*(27), 4671-4677.

Battaglia, L., & Ugazio, E. (2019). Lipid Nano-and Microparticles: An Overview of Patent-Related Research. *Journal of Nanomaterials, 2019*, 1-22.

Bechert, U., Christensen, J. M., Poppenga, R., Fahmy, S. A., & Redig, P. (2010). Pharmacokinetics of terbinafine after single oral dose administration in red-tailed hawks (Buteo jamaicensis). *Journal of Avian Medicine and Surgery, 24*(2), 122-130.

Bello, V., Mattei, G., Mazzoldi, P., Vivenza, N., Gasco, P., Idee, J. M., Robic, C., & Borsella, E. (2010). Transmission electron microscopy of lipid vesicles for drug delivery: comparison between positive and negative staining. *Microscopy and Microanalysis, 16*(4), 456-461.

Beloqui, A., Solinís, M. Á., Gascón, A. R., del Pozo-Rodríguez, A., des Rieux, A., & Préat, V. (2013). Mechanism of transport of saquinavir-loaded nanostructured lipid carriers across the intestinal barrier. *Journal of Controlled Release, 166*(2), 115-123.

Bondì, M. L., Azzolina, A., Craparo, E. F., Botto, C., Amore, E., Giammona, G., & Cervello, M. (2014). Entrapment of an EGFR inhibitor into nanostructured lipid carriers (NLC) improves its antitumor activity against human hepatocarcinoma cells. *Journal of Nanobiotechnology, 12*(1), 21.

Bronaugh, R. L., & Stewart, R. F. (1985). Methods for in vitro percutaneous absorption studies IV: The flow-through diffusion cell. *Journal of Pharmaceutical Sciences, 74*(1), 64-67.

Charcosset, C., El-Harati, A., & Fessi, H. (2005). Preparation of solid lipid nanoparticles using a membrane contactor. *Journal of Controlled Release, 108*(1), 112-120.

Chattopadhyay, P., Shekunov, B. Y., Yim, D., Cipolla, D., Boyd, B., & Farr, S. (2007). Production of solid lipid nanoparticle suspensions using supercritical fluid extraction of emulsions (SFEE) for pulmonary delivery using the AERx system. *Advanced Drug Delivery Reviews, 59*(6), 444-453.

Chen-yu, G., Chun-fen, Y., Qi-lu, L., Qi, T., Yan-wei, X., Wei-na, L., & Guang-xi, Z. (2012). Development of a Quercetin-loaded nanostructured lipid carrier formulation for topical delivery. *International Journal of Pharmaceutics, 430*(1), 292-298.

Chen, C. C., Tsai, T. H., Huang, Z. R., & Fang, J. Y. (2010). Effects of lipophilic emulsifiers on the oral administration of lovastatin from nanostructured lipid carriers: physicochemical characterization and pharmacokinetics. *European Journal of Pharmaceutics and Biopharmaceutics, 74*(3), 474-482.

Chen, Y., Chen, F., Wei, W., Zhang, X., Feng, Q., & Jin, R. (2009). Preparation of nanostructured lipid carriers loaded with supercritical carbon dioxide fluid extraction of Xionggui powder. *Zhongguo Zhong yao za zhi= Zhongguo zhongyao zazhi= China Journal of Chinese Materia Medica, 34*(2), 148-151.

Chen, Y., Yang, X., Zhao, L., Almásy, L., Garamus, V. M., Willumeit, R., & Zou, A. (2014). Preparation and characterization of a nanostructured lipid carrier for a poorly soluble drug. *Colloids and Surfaces A: Physicochemical and Engineering Aspects, 455*, 36-43.

Chime, S. A., & Onyishi, I. V. (2013). Lipid-based drug delivery systems (LDDS): Recent advances and applications of lipids in drug delivery. *African Journal of Pharmacy and Pharmacology, 7*(48), 3034-3059.

Choi, K.-O., Choe, J., Suh, S., & Ko, S. (2016). Positively Charged Nanostructured Lipid Carriers and Their Effect on the Dissolution of Poorly Soluble Drugs. *Molecules, 21*(5), 1-12.

Cirri, M., Bragagni, M., Mennini, N., & Mura, P. (2012). Development of a new delivery system consisting in "drug – in cyclodextrin – in nanostructured lipid carriers" for ketoprofen topical delivery. *European Journal of Pharmaceutics and Biopharmaceutics, 80*(1), 46-53.

Cunha, S., Costa, C. P., Loureiro, J. A., Alves, J., Peixoto, A. F., Forbes, B., Sousa Lobo, J. M., & Silva, A. C. (2020). Double Optimization of Rivastigmine-Loaded Nanostructured Lipid Carriers (NLC) for Nose-to-Brain Delivery Using the Quality by Design (QbD) Approach: Formulation Variables and Instrumental Parameters. *Pharmaceutics, 12*(7), 599.

D'Souza, S. S., & DeLuca, P. P. (2005). Development of a dialysis in vitro release method for biodegradable microspheres. *AAPS PharmSciTech, 6*(2), E323-E328.

Dai, W., Zhang, D., Duan, C., Jia, L., Wang, Y., Feng, F., & Zhang, Q. (2010). Preparation and characteristics of oridonin-loaded nanostructured lipid carriers as

a controlled-release delivery system. *Journal of Microencapsulation, 27*(3), 234-241.

Debnath, S., Kumar, G. V., & Satayanarayana, S. (2012). Design, Development and Evaluation of Novel Nanoemulsion of Terbinafine HCl. *Research Journal of Pharmacy and Technology, 5*(10), 7.

Di, H., Wu, H., Gao, Y., Li, W., Zou, D., & Dong, C. (2016). Doxorubicin- and cisplatin-loaded nanostructured lipid carriers for breast cancer combination chemotherapy. *Drug Development and Industrial Pharmacy, 42*(12), 2038-2043.

Doktorovova, S., Souto, E. B., & Silva, A. M. (2014). Nanotoxicology applied to solid lipid nanoparticles and nanostructured lipid carriers – A systematic review of in vitro data. *European Journal of Pharmaceutics and Biopharmaceutics, 87*(1), 1-18.

Dora, C. L., Putaux, J.-L., Pignot-Paintrand, I., Dubreuil, F., Soldi, V., Borsali, R., & Lemos-Senna, E. (2012). Physicochemical and morphological characterizations of glyceryl tristearate/castor oil nanocarriers prepared by the solvent diffusion method. *Journal of the Brazilian Chemical Society, 23*(11), 1972-1981.

Dubes, A., Parrot-Lopez, H., Abdelwahed, W., Degobert, G., Fessi, H., Shahgaldian, P., & Coleman, A. W. (2003). Scanning electron microscopy and atomic force microscopy imaging of solid lipid nanoparticles derived from amphiphilic cyclodextrins. *European Journal of Pharmaceutics and Biopharmaceutics, 55*(3), 279-282.

Duro, R., Gómez-Amoza, J., Martınez-Pacheco, R., Souto, C., & Concheiro, A. (1998). Adsorption of polysorbate 80 on pyrantel pamoate: effects on suspension stability. *International Journal of Pharmaceutics, 165*(2), 211-216.

El-Salamouni, N. S., Farid, R. M., El-Kamel, A. H., & El-Gamal, S. S. (2015). Effect of sterilization on the physical stability of brimonidine-loaded solid lipid nanoparticles and nanostructured lipid carriers. *International Journal of Pharmaceutics, 496*(2), 976-983.

Emami, J., Rezazadeh, M., & Varshosaz, J. (2012). Formulation of LDL targeted nanostructured lipid carriers loaded with paclitaxel: a detailed study of preparation, freeze drying condition, and in vitro cytotoxicity. *Journal of Nanomaterials, 2012*, 1-10.

Fabra, M. J., Talens, P., & Chiralt, A. (2009). Microstructure and optical properties of sodium caseinate films containing oleic acid–beeswax mixtures. *Food Hydrocolloids, 23*(3), 676-683.

Fan, H., Liu, G., Huang, Y., Li, Y., & Xia, Q. (2014). Development of a nanostructured lipid carrier formulation for increasing photo-stability and water solubility of Phenylethyl Resorcinol. *Applied Surface Science, 288*, 193-200.

Fang, C. L., Al-Suwayeh, S. A., & Fang, J. Y. (2013). Nanostructured lipid carriers (NLCs) for drug delivery and targeting. *Recent Patent of Nanotechnology, 7*(1), 41-55.

Fathi, H. A., Allam, A., Elsabahy, M., Fetih, G., & El-Badry, M. (2018). Nanostructured lipid carriers for improved oral delivery and prolonged antihyperlipidemic effect of simvastatin. *Colloids and Surfaces B: Biointerfaces, 162*, 236-245.

Fu-Qiang Hu, s.-P. J., Yong-Zhong Du, Hong Yuan, Yi-Qing YE, Su Zeng. (2005). Preparation and Chracterization of stearic acid nanostructured lipid carriers by solvent diffusion method in an aqeous system. *Colloids and Surfaces B : Biointerfaces*, 167-173.

Gaba, B., Fazil, M., Khan, S., Ali, A., Baboota, S., & Ali, J. (2015). Nanostructured lipid carrier system for topical delivery of terbinafine hydrochloride. *Bulletin of Faculty of Pharmacy, Cairo University, 53*(2), 147-159.

Ganesan, P., & Narayanasamy, D. (2017). Lipid nanoparticles: Different preparation techniques, characterization, hurdles, and strategies for the production of solid lipid nanoparticles and nanostructured lipid carriers for oral drug delivery. *Sustainable Chemistry and Pharmacy, 6*, 37-56.

Gao, S., Zhu, J., & Zhang, Y. (2017). Intercalation of calcein into layered silicate magadiite and their optical properties. *Royal Society Open Science, 4*(11), 171258.

Garcia-Orue, I., Gainza, G., Girbau, C., Alonso, R., Aguirre, J. J., Pedraz, J. L., Igartua, M., & Hernandez, R. M. (2016). LL37 loaded nanostructured lipid carriers (NLC): A new strategy for the topical treatment of chronic wounds. *European Journal of Pharmaceutics and Biopharmaceutics, 108*(Supplement C), 310-316.

Garg, T., Sharma, G., Rath, G., & Goyal, A. K. (2017). 18 - Colloidal systems: an excellent carrier for nutrient delivery. In Grumezescu (Ed.), *Nutrient Delivery* (pp. 681-712): Academic Press.

Ghate, V. M., Lewis, S. A., Prabhu, P., Dubey, A., & Patel, N. (2016). Nanostructured lipid carriers for the topical delivery of tretinoin. *European Journal of Pharmaceuticals Biopharmaceutics, 108*, 253-261.

Goh, P. S., Ng, M., Choo, Y., Amru, N. B., & Chuah, C. H. (2016). Production of tocols nanoemulsion by ultrasonication. *Journal of Oil Palm Research, 28*, 121-130.

Gönüllü, Ü., Üner, M., Yener, G., Karaman, E. F, & Aydoğmuş, Z. (2015). Formulation and characterization of solid lipid nanoparticles, nanostructured lipid carriers and nanoemulsion of lornoxicam for transdermal delivery. *Acta Pharmaceutica, 65*(1), 1-13.

González-Mira, E., Nikolić, S., Garcia, M., Egea, M., Souto, E., & Calpena, A. (2011). Potential use of nanostructured lipid carriers for topical delivery of flurbiprofen. *Journal of Pharmaceutical Sciences, 100*(1), 242-251.

Granja, A., Vieira, A. C., Chaves, L. L., Nunes, C., Neves, A. R., Pinheiro, M., & Reis, S. (2017). Folate-targeted nanostructured lipid carriers for enhanced oral delivery of epigallocatechin-3-gallate. *Food Chemistry, 237*(Supplement C), 803-810.

Grindel, J. M., Jaworski, T., Emanuele, R. M., & Culbreth, P. (2002). Pharmacokinetics of a novel surface-active agent, purified poloxamer 188, in rat, rabbit, dog and man. *Biopharmaceutics & Drug Disposition, 23*(3), 87-103.

Güngör, S., Erdal, M. S., & Aksu, B. (2013). New formulation strategies in topical antifungal therapy. *Journal of Cosmetics, Dermatological Sciences and Applications, 3*(01), 56-65.

Han, H. D., Kim, T. W., Shin, B. C., & Choi, H. S. (2005). Release of calcein from temperature-sensitive liposomes. *Macromolecular Research, 13*(1), 54-61.

Häuser, M., Langer, K., & Schönhoff, M. (2015). pH-Triggered release from surface-modified poly (lactic-co-glycolic acid) nanoparticles. *Beilstein Journal of Nanotechnology, 6(1)*, 2504-2512.

Hejri, A., Khosravi, A., Gharanjig, K., & Hejazi, M. (2013). Optimisation of the formulation of β-carotene loaded nanostructured lipid carriers prepared by solvent diffusion method. *Food Chemistry, 141*(1), 117-123.

Heurtault, B., Saulnier, P., Pech, B., Proust, J. E., & Benoit, J. P. (2003). Physico-chemical stability of colloidal lipid particles. *Biomaterials, 24*(23), 4283-4300.

Hou, D., Xie, C., Huang, K., & Zhu, C. (2003). The production and characteristics of solid lipid nanoparticles (SLNs). *Biomaterials, 24*(10), 1781-1785.

Hu, F.-Q., Jiang, S.-P., Du, Y.-Z., Yuan, H., Ye, Y.-Q., & Zeng, S. (2005). Preparation and characterization of stearic acid nanostructured lipid carriers by solvent diffusion method in an aqueous system. *Colloids and Surfaces B: Biointerfaces, 45*(3), 167-173.

Hu, F. Q., Jiang, S. P., Du, Y. Z., Yuan, H., Ye, Y. Q., & Zeng, S. (2006). Preparation and characteristics of monostearin nanostructured lipid carriers. *International Journal of Pharmaceutics, 314*(1), 83-89.

Huang, X., Young, N. P., & Townley, H. E. (2014). Characterization and Comparison of Mesoporous Silica Particles for Optimized Drug Delivery. *Nanomaterials and Nanotechnology, 4*(2)*,* 1-15.

Hung, L. C., Basri, M., Tejo, B. A., Ismail, R., Nang, H. L. L., Hassan, H. A., & May, C. Y. (2011). An improved method for the preparations of nanostructured lipid carriers containing heat-sensitive bioactives. *Colloids and Surfaces B: Biointerfaces, 87*(1), 180-186.

Iqbal, M. A., Md, S., Sahni, J. K., Baboota, S., Dang, S., & Ali, J. (2012). Nanostructured lipid carriers system: recent advances in drug delivery. *Journal of Drug Targeting, 20*(10), 813-830.

Jain, A. S., Shah, S. M., Nagarsenker, M. S., Nikam, Y., Gude, R. P., Steiniger, F., Thamm, J., & Fahr, A. (2013). Lipid colloidal carriers for improvement of anticancer activity of orally delivered quercetin: formulation, characterization and establishing in vitro-in vivo advantage. *Journal of Biomedical Nanotechnology, 9*(7), 1230-1240.

Jain, P., Rahi, P., Pandey, V., Asati, S., & Soni, V. (2017). Nanostructure lipid carriers: A modish contrivance to overcome the ultraviolet effects. *Egyptian Journal of Basic and Applied Sciences, 4*(2), 89-100.

Jia, L., Shen, J., Zhang, D., Duan, C., Liu, G., Zheng, D., Tian, X., Liu, Y., & Zhang, Q. (2012). In vitro and in vivo evaluation of oridonin-loaded long circulating nanostructured lipid carriers. *International Journal of Biological Macromolecules, 50*(3), 523-529.

Kalam, M. A., Sultana, Y., Ali, A., Aqil, M., Mishra, A. K., & Chuttani, K. (2010). Preparation, characterization, and evaluation of gatifloxacin loaded solid lipid nanoparticles as colloidal ocular drug delivery system. *Journal of Drug Targeting, 18*(3), 191-204.

Karthik, S., Raghavan, C. V., Marslin, G., Rahman, H., Selvaraj, D., Balakumar, K., & Franklin, G. (2016). Quillaja saponin: A prospective emulsifier for the preparation of solid lipid nanoparticles. *Colloids and surfaces. B, Biointerfaces, 147*, 274-280.

Katouzian, I., Faridi Esfanjani, A., Jafari, S. M., & Akhavan, S. (2017). Formulation and application of a new generation of lipid nano-carriers for the food bioactive ingredients. *Trends in Food Science & Technology, 68*, 14-25.

Kaul, S., Gulati, N., Verma, D., Mukherjee, S., & Nagaich, U. (2018). Role of Nanotechnology in cosmeceuticals: A review of recent advances. *Journal of Pharmaceutics, 2018*, 1-19.

Kaur, S., Nautyal, U., Singh, R., Singh, S., & Devi, A. (2015). Nanostructure Lipid Carrier (NLC): the new generation of lipid nanoparticles. *Asian Pacific Journal of Health Sciences, 2*(2), 76-93.

Kaushik, D. (2016). Baicalein Loaded Polysorbate 80 Nanostructured Lipid Carriers Offered Enhanced Stability and In Vitro Drug Release. *Asian Journal of Pharmaceutics (AJP), 10*(2), 128-133.

Keivani Nahr, F., Ghanbarzadeh, B., Hamishehkar, H., & Samadi Kafil, H. (2018). Food grade nanostructured lipid carrier for cardamom essential oil: Preparation, characterization and antimicrobial activity. *Journal of Functional Foods, 40*, 1-8.

Kelidari, H. R., Moazeni, M., Babaei, R., Saeedi, M., Akbari, J., Parkoohi, P. I., Nabili, M., Gohar, A. A., Morteza-Semnani, K., & Nokhodchi, A. (2017). Improved yeast delivery of fluconazole with a nanostructured lipid carrier system. *Biomedicine & Pharmacotherapy, 89*, 83-88.

Khan, S., Shaharyar, M., Fazil, M., Baboota, S., & Ali, J. (2016). Tacrolimus-loaded nanostructured lipid carriers for oral delivery – Optimization of production and characterization. *European Journal of Pharmaceutics and Biopharmaceutics, 108*(Supplement C), 277-288.

Kheradmandnia, S., Vasheghani-Farahani, E., Nosrati, M., & Atyabi, F. (2010). Preparation and characterization of ketoprofen-loaded solid lipid nanoparticles

made from beeswax and carnauba wax. *Nanomedicine: Nanotechnology, Biology and Medicine, 6*(6), 753-759.

Khurana, R. K., Bansal, A. K., Beg, S., Burrow, A. J., Katare, O. P., Singh, K. K., & Singh, B. (2017). Enhancing biopharmaceutical attributes of phospholipid complex-loaded nanostructured lipidic carriers of mangiferin: Systematic development, characterization and evaluation. *International Journal of Pharmaceutics, 518*(1–2), 289-306.

Khurana, S., Jain, N., & Bedi, P. (2013). Development and characterization of a novel controlled release drug delivery system based on nanostructured lipid carriers gel for meloxicam. *Life sciences, 93*(21), 763-772.

Kirkpatrick, W. R., Vallor, A. C., McAtee, R. K., Ryder, N. S., Fothergill, A. W., Rinaldi, M. G., & Patterson, T. F. (2005). Combination therapy with terbinafine and amphotericin B in a rabbit model of experimental invasive aspergillosis. *Antimicrobial Agents and Chemotherapy, 49*(11), 4751-4753.

Kopechek, J. A., Abruzzo, T. M., Wang, B., Chrzanowski, S. M., Smith, D. A., Kee, P. H., Huang, S., Collier, J. H., McPherson, D. D., & Holland, C. K. (2008). Ultrasound-mediated release of hydrophilic and lipophilic agents from echogenic liposomes. *Journal of Ultrasound Medicine, 27*(11), 1597-1606.

Kumbhar, D. D., & Pokharkar, V. B. (2013). Engineering of a nanostructured lipid carrier for the poorly water-soluble drug, bicalutamide: Physicochemical investigations. *Colloids and Surfaces A: Physicochemical and Engineering Aspects, 416*(Supplement C), 32-42.

Kuo, Y.-C., & Chung, J.-F. (2011). Physicochemical properties of nevirapine-loaded solid lipid nanoparticles and nanostructured lipid carriers. *Colloids and Surfaces B: Biointerfaces, 83*(2), 299-306.

Lage, O. M., Bondoso, J., & Catita, J. A. (2012). Determination of zeta potential in Planctomycetes and its application in heavy metals toxicity assessment. *Archives of Microbiology, 194*(10), 847-855.

Lakhani, P., Patil, A., Wu, K.-W., Sweeney, C., Tripathi, S., Avula, B., Taskar, P., Khan, S., & Majumdar, S. (2019). Optimization, stabilization, and characterization of amphotericin B loaded nanostructured lipid carriers for ocular drug delivery. *International Journal of Pharmaceutics, 572(2019)*, 118771-118784.

Lasoń, E., Sikora, E., & Ogonowski, J. (2013). Influence of process parameters on properties of Nanostructured Lipid Carriers (NLC) formulation. *The Journal of the Polish Biochemical Society and of the Polish Academy of Sciences, 60*(4), 773-777.

Lasoń, E., Sikora, E., Ogonowski, J., Tabaszewska, M., & Skoczylas, Ł. (2016). Release study of selected terpenes from nanostructured lipid carriers. *Colloids and Surfaces A: Physicochemical and Engineering Aspects, 510*, 87-92.

Li, H., Chen, M., Su, Z., Sun, M., & Ping, Q. (2016). Size-exclusive effect of nanostructured lipid carriers on oral drug delivery. *International Journal of Pharmaceutics, 511*(1), 524-537.

Lim, S. B., Banerjee, A., & Önyüksel, H. (2012). Improvement of drug safety by the use of lipid-based nanocarriers. *Journal of Controlled Release, 163*(1), 34-45.

Lin, W. J., & Duh, Y. S. (2016). Nanostructured lipid carriers for transdermal delivery of acid labile lansoprazole. *European Journal of Pharmaceutics and Biopharmaceutics, 108*, 297-303.

Lin, X., Li, X., Zheng, L., Yu, L., Zhang, Q., & Liu, W. (2007). Preparation and characterization of monocaprate nanostructured lipid carriers. *Colloids and Surfaces A: Physicochemical and Engineering Aspects, 311*(1), 106-111.

Liu, C.-H., & Wu, C.-T. (2010). Optimization of nanostructured lipid carriers for lutein delivery. *Colloids and Surfaces A: Physicochemical and Engineering Aspects, 353*(2), 149-156.

Liu, Y., Wang, L., Zhao, Y., He, M., Zhang, X., Niu, M., & Feng, N. (2014). Nanostructured lipid carriers versus microemulsions for delivery of the poorly water-soluble drug luteolin. *International Journal of Pharmaceutics, 476*(1), 169-177.

Livney, Y. D. (2015). Nanostructured delivery systems in food: latest developments and potential future directions. *Current Opinion in Food Science, 3*, 125-135.

Loo, C., Basri, M., Ismail, R., Lau, H., Tejo, B., Kanthimathi, M., Hassan, H., & Choo, Y. (2013). Effect of compositions in nanostructured lipid carriers (NLC) on skin hydration and occlusion. *International Journal of Nanomedicine, 2013(8)*, 13-22.

Lowe, K. C., Furmidge, B. A., & Thomas, S. (1995). Haemolytic properties of pluronic surfactants and effects of purification. *Artificial Cells, Blood Substitutes, and Biotechnology, 23*(1), 135-139.

Lv, W., Zhao, S., Yu, H., Li, N., Garamus, V. M., Chen, Y., Yin, P., Zhang, R., Gong, Y., & Zou, A. (2016). Brucea javanica oil-loaded nanostructure lipid carriers (BJO NLCs): Preparation, characterization and in vitro evaluation. *Colloids and Surfaces A: Physicochemical and Engineering Aspects, 504*, 312-319.

Maherani, B., Arab-Tehrany, E., Kheirolomoom, A., Geny, D., & Linder, M. (2013). Calcein release behavior from liposomal bilayer; influence of physicochemical/mechanical/structural properties of lipids. *Biochimie, 95*(11), 2018-2033.

Medrzycka, K. B. (1991). The effect of particle concentration on zeta potential in extremely dilute solutions. *Colloid and Polymer Science, 269*(1), 85-90.

Meland, H.-G., Røv-Johnsen, A., Smistad, G., & Hiorth, M. (2014). Studies on surface coating of phospholipid vesicles with a non-ionic polymer. *Colloids and Surfaces B: Biointerfaces, 114*, 45-52.

Mendes, A. I., Silva, A. C., Catita, J. A. M., Cerqueira, F., Gabriel, C., & Lopes, C. M. (2013). Miconazole-loaded nanostructured lipid carriers (NLC) for local delivery to the oral mucosa: Improving antifungal activity. *Colloids and Surfaces B: Biointerfaces, 111*(Supplement C), 755-763.

Mendes, I. T., Ruela, A. L. M., Carvalho, F. C., Freitas, J. T. J., Bonfilio, R., & Pereira, G. R. (2019). Development and characterization of nanostructured lipid carrier-based gels for the transdermal delivery of donepezil. *Colloids and Surfaces B: Biointerfaces, 177*, 274-281.

Michael, D., Triplett, I., & Rathman, J. (2009). Optimization of b-carotene loaded solid lipid nanoparticles preparation using a high shear homogenization technique. *Journal of Nanoparticle Research, 11*, 601-614.

Mitrea, E., Ott, C., & Meghea, A. (2014). New Approaches on the Synthesis of Effective Nanostructured Lipid Carriers. *Revista De Chimie, 65*(1), 50-55.

Montenegro, L., & Pasquinucci, L. (2017). Rosemary Essential Oil-Loaded Lipid Nanoparticles: In Vivo Topical Activity from Gel Vehicles. *Pharmaceutics, 9*(4), 1-12.

Müller, R. H., Petersen, R. D., Hommoss, A., & Pardeike, J. (2007). Nanostructured lipid carriers (NLC) in cosmetic dermal products. *Advanced Drug Delivery Reviews, 59*(6), 522-530.

Nasirizadeh, S., & Malaekeh-Nikouei, B. (2020). Solid lipid nanoparticles and nanostructured lipid carriers in oral cancer drug delivery. *Journal of Drug Delivery Science and Technology, 55*, 101458.

Negri, G., Marcucci, M. C., Salatino, A., & Salatino, M. L. F. (2000). Comb and propolis waxes from Brazil: triterpenoids in propolis waxes. *Journal of Apicultural Research, 39*(1-2), 86-88.

Nguyen, H. M., Hwang, I. C., Park, J. W., & Park, H. J. (2012). Enhanced payload and photo-protection for pesticides using nanostructured lipid carriers with corn oil as liquid lipid. *Journal of Microencapsulation, 29*(6), 596-604.

Nnamani, P. O., Hansen, S., Windbergs, M., & Lehr, C.-M. (2014). Development of artemether-loaded nanostructured lipid carrier (NLC) formulation for topical application. *International Journal of Pharmaceutics, 477*(1), 208-217.

Noh, G. Y., Suh, J. Y., & Park, S. N. (2017). Ceramide-based nanostructured lipid carriers for transdermal delivery of isoliquiritigenin: Development, physicochemical characterization, and in vitro skin permeation studies. *Korean Journal of Chemical Engineering, 34*(2), 400-406.

Nordin, N., Yeap, S. K., Zamberi, N. R., Abu, N., Mohamad, N. E., Rahman, H. S., How, C. W., Masarudin, M. J., Abdullah, R., & Alitheen, N. B. (2018). Characterization and toxicity of citral incorporated with nanostructured lipid carrier. *PeerJ, 2018(6)*, 1-19.

Oh, J.-H., Park, H.-H., Do, K.-Y., Han, M., Hyun, D.-H., Kim, C.-G., Kim, C.-H., Lee, S. S., Hwang, S.-J., Shin, S.-C., & Cho, C.-W. (2008). Influence of the delivery systems using a microneedle array on the permeation of a hydrophilic molecule, calcein. *European Journal of Pharmaceutics and Biopharmaceutics, 69*(3), 1040-1045.

Okonogi, S., & Riangjanapatee, P. (2015). Physicochemical characterization of lycopene-loaded nanostructured lipid carrier formulations for topical administration. *International Journal of Pharmaceutics, 478*(2), 726-735.

Ong, Y. S., Yazan, L. S., Ng, W. K., Noordin, M. M., Sapuan, S., Foo, J. B., & Tor, Y. S. (2016). Acute and subacute toxicity profiles of thymoquinone-loaded nanostructured lipid carrier in BALB/c mice. *International Journal of Nanomedicine, 2016(11)*, 5905-5915.

Orellana-Tavra, C., Baxter, E. F., Tian, T., Bennett, T. D., Slater, N. K. H., Cheetham, A. K., & Fairen-Jimenez, D. (2015). Amorphous metal-organic frameworks for drug delivery. *Chemical Communications, 51*(73), 13878-13881.

Orellana-Tavra, C., Marshall, R. J., Baxter, E. F., Lazaro, I. A., Tao, A., Cheetham, A. K., Forgan, R. S., & Fairen-Jimenez, D. (2016). Drug delivery and controlled release from biocompatible metal-organic frameworks using mechanical amorphization. *Journal of Materials Chemistry B, 4*(47), 7697-7707.

Özcan, İ., Abacı, Ö., Uztan, A. H., Aksu, B., Boyacıoğlu, H., Güneri, T., & Özer, Ö. (2009). Enhanced Topical Delivery of Terbinafine Hydrochloride with Chitosan Hydrogels. *An Official Journal of the American Association of Pharmaceutical Scientists, 10*(3), 1024-1031.

Paarakh, M. P., Jose, P. A., Setty, C., & Peter, G. (2018). Release kinetics–concepts and applications. *International Journal of Pharmacy Research & Technology, 8*, 12-20.

Pan, Y., Tikekar, R. V., & Nitin, N. (2016). Distribution of a model bioactive within solid lipid nanoparticles and nanostructured lipid carriers influences its loading efficiency and oxidative stability. *International Journal of Pharmaceutics, 511*(1), 322-330.

Pandita, D., Ahuja, A., Velpandian, T., Lather, V., Dutta, T., & Khar, R. (2009). Characterization and in vitro assessment of paclitaxel loaded lipid nanoparticles formulated using modified solvent injection technique. *Die Pharmazie-An International Journal of Pharmaceutical Sciences, 64*(5), 301-310.

Pardeike, J., Hommoss, A., & Müller, R. H. (2009). Lipid nanoparticles (SLN, NLC) in cosmetic and pharmaceutical dermal products. *International Journal of Pharmaceutics, 366*(1), 170-184.

Patel, D., Dasgupta, S., Dey, S., Roja Ramani, Y., Ray, S., & Mazumder, B. (2012). Nanostructured lipid carriers (NLC)-based gel for the topical delivery of aceclofenac: preparation, characterization, and in vivo evaluation. *Scientia Pharmaceutica, 80*(3), 749-764.

Paukner, S., Kohl, G., Jalava, K., & Lubitz, W. (2003). Sealed Bacterial Ghosts—Novel Targeting Vehicles for Advanced Drug Delivery of Water-soluble Substances. *Journal of Drug Targeting, 11*(3), 151-161.

Pelegri-O'Day, E. M., & Maynard, H. D. (2016). Controlled Radical Polymerization as an Enabling Approach for the Next Generation of Protein–Polymer Conjugates. *Accounts of Chemical Research, 49*(9), 1777-1785.

Pimpalshende, P. M., & Gupta, R. N. (2018). Formulation and in-vitro drug Released Mechanism of CNS Acting Venlafaxine Nanostructured Lipid Carrier for Major Depressive Disorder. *Indian Journal Of Pharmaceutical Education And Research, 52*(2), 230-240.

Pinto, F., de Barros, D. P. C., Reis, C., & Fonseca, L. P. (2019). Optimization of nanostructured lipid carriers loaded with retinoids by central composite design. *Journal of Molecular Liquids, 293*, 111468.

Poonia, N., Kharb, R., Lather, V., & Pandita, D. (2016). Nanostructured lipid carriers: versatile oral delivery vehicle. *Future Science OA, 2*(3), 1-24.

Prabhu, P., Suryavanshi, S., Pathak, S., Patra, A., Sharma, S., & Patravale, V. (2016). Nanostructured lipid carriers of artemether-lumefantrine combination for intravenous therapy of cerebral malaria. *International Journal Pharmaceutics, 513*(1-2), 504-517.

Puglia, C., Blasi, P., Rizza, L., Schoubben, A., Bonina, F., Rossi, C., & Ricci, M. (2008). Lipid nanoparticles for prolonged topical delivery: an in vitro and in vivo investigation. *International Journal Pharmaceutics, 357*(1-2), 295-304.

Qiua, L., Yanga, L., Zhoub, H., Longa, M., Jianga, W., Wanga, D., & Zhanga, X. (2012). Encapsulation of oxaliplatin in nanostructured lipid carriers-preparation, physicochemical characterization and in vitro evalulation. *Asian Journal of Pharmaceutical Sciences, 7*(5), 352-358.

Rahman, H. S., Rasedee, A., How, C. W., Abdul, A. B., Zeenathul, N. A., Othman, H. H., Saeed, M. I., & Yeap, S. K. (2013). Zerumbone-loaded nanostructured lipid carriers: preparation, characterization, and antileukemic effect. *International Journal of Nanomedicine, 2013*(8), 2769-2781.

Rajput, A. P., & Butani, S. B. (2019). Resveratrol anchored nanostructured lipid carrier loaded in situ gel via nasal route: Formulation, optimization and in vivo characterization. *Journal of Drug Delivery Science and Technology, 51*, 214-223.

Ribeiro, L. N. M., Franz-Montan, M., Breitkreitz, M. C., Alcântara, A. C. S., Castro, S. R., Guilherme, V. A., Barbosa, R. M., & de Paula, E. (2016). Nanostructured lipid carriers as robust systems for topical lidocaine-prilocaine release in dentistry. *European Journal of Pharmaceutical Sciences, 93*(Supplement C), 192-202.

Rizwanullah, M., Ahmad, J., & Amin, S. (2016). Nanostructured Lipid Carriers: A Novel Platform for Chemotherapeutics. *Current Drug Delivery, 13*(1), 4-26.

Rodriguez-Ruiz, V., Salatti-Dorado, J., Barzegari, A., Nicolas-Boluda, A., Houaoui, A., Caballo, C., Caballero-Casero, N., Sicilia, D., Bastias Venegas, J., & Pauthe, E. (2018). Astaxanthin-Loaded Nanostructured Lipid Carriers for Preservation of Antioxidant Activity. *Molecules, 23*(10), 1-12.

Rosita, N., Setyawan, D., Soeratri, W., & Mrtodihardjo, S. (2014). Physical Characterization of Beewax and Glyceryl monostearate binary system to predict characteristics of solid lipid nanoparticle (SLN) loaded Para Methoxy Cinnamic Acid (PCMA). *International Journal of Pharmacy and Pharmaceutical Sciences, 6*(2), 939-945.

Rubenick, J. B., Rubim, A. M., Bellé, F., Nogueira-Librelotto, D. R., & Rolim, C. M. B. (2017). Preparation of mupirocin-loaded polymeric nanocapsules using essential oil of rosemary. *Brazilian Journal of Pharmaceutical Sciences, 53*, 1-11.

Sadati Behbahani, E., Ghaedi, M., Abbaspour, M., Rostamizadeh, K., & Dashtian, K. (2019). Curcumin loaded nanostructured lipid carriers: In vitro digestion and release studies. *Polyhedron, 164*, 113-122.

Saez, V., Souza, I., & Mansur, C. R. E. (2018). Lipid nanoparticles (SLN & NLC) for delivery of vitamin E: a comprehensive review. *International Journal of Cosmetic Science, 40*(2), 103-116.

Safwat, S., Ishak, R. A. H., Hathout, R. M., & Mortada, N. D. (2017). Nanostructured lipid carriers loaded with simvastatin: effect of PEG/glycerides on characterization, stability, cellular uptake efficiency and in vitro cytotoxicity. *Drug Development Industrial Pharmacy, 43*(7), 1112-1125.

Schmitt, H., Andrade, J., Edwards, F., Niki, Y., Bernard, E., & Armstrong, D. (1990). Inactivity of terbinafine in a rat model of pulmonary aspergillosis. *European Journal of Clinical Microbiology & Infectious Diseases, 9*(11), 832-835.

Scioli Montoto, S., Sbaraglini, M. L., Talevi, A., Couyoupetrou, M., Di Ianni, M., Pesce, G. O., Alvarez, V. A., Bruno-Blanch, L. E., Castro, G. R., Ruiz, M. E., & Islan, G. A. (2018). Carbamazepine-loaded solid lipid nanoparticles and nanostructured lipid carriers: Physicochemical characterization and in vitro/in vivo evaluation. *Colloids and Surfaces B: Biointerfaces, 167*, 73-81.

Selvamuthukumar, S., & Velmurugan, R. (2012). Nanostructured lipid carriers: a potential drug carrier for cancer chemotherapy. *Lipids in Health and Disease, 11*(1)*,* 1-8.

Sen, M., Uzun, C., & Guven, O. (2000). Controlled release of terbinafine hydrochloride from pH sensitive poly(acrylamide/maleic acid) hydrogels. *International Journal of Pharmaceutics, 203*(1-2), 149-157.

Shah, R., Eldridge, D., Palombo, E., & Harding, I. (2014). Optimisation and Stability Assessment of Solid Lipid Nanoparticles using Particle Size and Zeta Potential. *Journal of Physical Science, 25*(1), 59-75.

Shahgaldian, P., Da Silva, E., Coleman, A. W., Rather, B., & Zaworotko, M. J. (2003). Para-acyl-calix-arene based solid lipid nanoparticles (SLNs): a detailed study of

preparation and stability parameters. *International Journal of Pharmaceutics, 253*(1), 23-38.

Shi, F., Yang, G., Ren, J., Guo, T., Du, Y., & Feng, N. (2013). Formulation design, preparation, and in vitro and in vivo characterizations of β-Elemene-loaded nanostructured lipid carriers. *International Journal of Nanomedicine, 8*, 2533.

Singh-Joy, S. D., & McLain, V. C. (2007). Safety assessment of poloxamers 101, 105, 108, 122, 123, 124, 181, 182, 183, 184, 185, 188, 212, 215, 217, 231, 234, 235, 237, 238, 282, 284, 288, 331, 333, 334, 335, 338, 401, 402, 403, and 407, poloxamer 105 benzoate, and poloxamer 182 dibenzoate as used in cosmetics. *International Journal of Toxicology, 27*, 93-128.

Singhal, G. B., Patel, R. P., Prajapati, B., & Patel, N. A. (2011). Solid lipid nanoparticles and nano lipid carriers: As novel solid lipid based drug carrier. *International Research Journal of Pharmacy, 2*(2), 20-52.

Sjöström, B., Kaplun, A., Talmon, Y., & Cabane, B. (1995). Structures of nanoparticles prepared from oil-in-water emulsions. *Pharmaceutical Research, 12*(1), 39-48.

Soleimanian, Y., Goli, S. A. H., Varshosaz, J., & Sahafi, S. M. (2018). Formulation and characterization of novel nanostructured lipid carriers made from beeswax, propolis wax and pomegranate seed oil. *Food Chemistry, 244*, 83-92.

Sorensen, K. N., Sobel, R. A., Clemons, K. V., Calderon, L., Howell, K. J., Irani, P. R., Pappagianis, D., Williams, P. L., & Stevens, D. A. (2000). Comparative efficacies of terbinafine and fluconazole in treatment of experimental coccidioidal meningitis in a rabbit model. *Antimicrobial Agents and Chemotherapy, 44*(11), 3087-3091.

Sun, M., Nie, S., Pan, X., Zhang, R., Fan, Z., & Wang, S. (2014). Quercetin-nanostructured lipid carriers: characteristics and anti-breast cancer activities in vitro. *Colloids and Surfaces B: Biointerfaces, 113*, 15-24.

Swidan, S. A., Ghonaim, H. M., Samy, A. M., & Ghorab, M. M. (2016). Comparative study of solid lipid nanoparticles and nanostructured lipid carriers for in vitro Paclitaxel delivery. *Journal Chemical, 8*(5), 482-493.

Tagavifar, M., Jang, S. H., Chang, L., Mohanty, K., & Pope, G. (2018). Controlling the composition, phase volume, and viscosity of microemulsions with cosolvent. *Fuel, 211*, 214-222.

Tamjidi, F., Shahedi, M., Varshosaz, J., & Nasirpour, A. (2013). Nanostructured lipid carriers (NLC): A potential delivery system for bioactive food molecules. *Innovative Food Science & Emerging Technologies, 19*, 29-43.

Tan, S. W., Billa, N., Roberts, C. R., & Burley, J. C. (2010). Surfactant effects on the physical characteristics of Amphotericin B-containing nanostructured lipid carriers. *Colloids and Surfaces A: Physicochemical and Engineering Aspects, 372*(1), 73-79.

Tanriverdi, S. T., & Ozer, O. (2013). Novel topical formulations of Terbinafine-HCl for treatment of onychomycosis. *European Journal of Pharmaceutial Sciences, 48*(4-5), 628-636.

Taymouri, S., Alem, M., Varshosaz, J., Rostami, M., Akbari, V., & Firoozpour, L. (2019). Biotin decorated sunitinib loaded nanostructured lipid carriers for tumor targeted chemotherapy of lung cancer. *Journal of Drug Delivery Science and Technology, 50*, 237-247.

Tetyczka, C., Griesbacher, M., Absenger-Novak, M., Fröhlich, E., & Roblegg, E. (2017). Development of nanostructured lipid carriers for intraoral delivery of Domperidone. *International Journal of Pharmaceutics, 526*(1), 188-198.

Tiwari, R., & Pathak, K. (2011). Nanostructured lipid carrier versus solid lipid nanoparticles of simvastatin: Comparative analysis of characteristics, pharmacokinetics and tissue uptake. *International Journal of Pharmaceutics, 415*(1), 232-243.

Trotta, M., Debernardi, F., & Caputo, O. (2003). Preparation of solid lipid nanoparticles by a solvent emulsification–diffusion technique. *International Journal of Pharmaceutics, 257*(1-2), 153-160.

Turasan, H., Sahin, S., & Sumnu, G. (2015). Encapsulation of rosemary essential oil. *LWT- Food Science and Technology, 64*(1), 112-119.

Uner, M. (2006). Preparation, characterization and physico-chemical properties of solid lipid nanoparticles (SLN) and nanostructured lipid carriers (NLC): their benefits as colloidal drug carrier systems. *Pharmazie, 61*(5), 375-386.

Üner, M., Karaman, E. F., & Aydoğmuş, Z. (2014). Solid lipid nanoparticles and nanostructured lipid carriers of loratadine for topical application: physicochemical stability and drug penetration through rat skin. *Tropical Journal of Pharmaceutical Research, 13*(5), 653-660.

Uprit, S., Kumar Sahu, R., Roy, A., & Pare, A. (2013). Preparation and characterization of minoxidil loaded nanostructured lipid carrier gel for effective treatment of alopecia. *Saudi Pharmaceutical Journal, 21*(4), 379-385.

Uraiwan, K., & Satirapipathkul, C. (2016). *The Entrapment of Vitamin E in Nanostructured Lipid Carriers of Rambutan Seed Fat for Cosmeceutical Uses* (Vol. 675-676), 77-80.

Vaghasiya, H., Kumar, A., & Sawant, K. (2013). Development of solid lipid nanoparticles based controlled release system for topical delivery of terbinafine hydrochloride. *European Journal of Pharmaceuticals Sciences, 49*(2), 311-322.

Weber, S., Zimmer, A., & Pardeike, J. (2014). Solid Lipid Nanoparticles (SLN) and Nanostructured Lipid Carriers (NLC) for pulmonary application: A review of the state of the art. *European Journal of Pharmaceutics and Biopharmaceutics, 86*(1), 7-22.

White, B., Banerjee, S., O'Brien, S., Turro, N. J., & Herman, I. P. (2007). Zeta-potential measurements of surfactant-wrapped individual single-walled carbon nanotubes. *The Journal of Physical Chemistry C, 111*(37), 13684-13690.

Williams, M. M., Davis, E. G., & KuKanich, B. (2011). Pharmacokinetics of oral terbinafine in horses and Greyhound dogs. *Journal of Veterinary Pharmacology and Therapeutics, 34*(3), 232-237.

Wissing, S., Kayser, O., & Müller, R. (2004). Solid lipid nanoparticles for parenteral drug delivery. *Advanced Drug Delivery Reviews, 56*(9), 1257-1272.

Woo, J. O., Misran, M., Lee, P. F., & Tan, L. P. (2014). Development of a Controlled Release of Salicylic Acid Loaded Stearic Acid-Oleic Acid Nanoparticles in Cream for Topical Delivery. *The Scientific World Journal, 2014*(1), 1-7.

Xia, D., Shrestha, N., van de Streek, J., Mu, H., & Yang, M. (2016). Spray drying of fenofibrate loaded nanostructured lipid carriers. *Asian Journal of Pharmaceutical Sciences, 11*(4), 507-515.

Yadav, N., Khatak, S., & Sara, U. V. S. (2013). Solid lipid nanoparticles-a review. *International Journal of Applied Pharmaceutics, 5*(2), 8-18.

Yuan, H., Wang, L.-L., Du, Y.-Z., You, J., Hu, F.-Q., & Zeng, S. (2007). Preparation and characteristics of nanostructured lipid carriers for control-releasing progesterone by melt-emulsification. *Colloids and Surfaces B: Biointerfaces, 60*(2), 174-179.

Zhang, C., Luo, S., Zhang, Z., Niu, Y., & Zhang, W. (2017). Evaluation of Glabridin loaded nanostructure lipid carriers. *Journal of the Taiwan Institute of Chemical Engineers, 71*, 338-343.

Zhang, K., Lv, S., Li, X., Feng, Y., Li, X., Liu, L., Li, S., & Li, Y. (2013). Preparation, characterization, and in vivo pharmacokinetics of nanostructured lipid carriers loaded with oleanolic acid and gentiopicrin. *International Journal of Nanomedicine, 8*, 3227-3239.

Zhang, Q., Yang, H., Sahito, B., Li, X., Peng, L., Gao, X., Ji, H., Wang, L., Jiang, S., & Guo, D. (2019). Nanostructured lipid carriers with exceptional gastrointestinal stability and inhibition of P-gp efflux for improved oral delivery of tilmicosin. *Colloids and Surfaces B: Biointerfaces, 187*(2020)*,* 1-8.

Zhang, X., Pan, W., Gan, L., Zhu, C., Gan, Y., & Nie, S. (2008). Preparation of a dispersible PEGylate nanostructured lipid carriers (NLC) loaded with 10-hydroxycamptothecin by spray-drying. *Chemical and Pharmaceuticals Bulletin (Tokyo), 56*(12), 1645-1650.

Zhang, Y., Huo, M., Zhou, J., Zou, A., Li, W., Yao, C., & Xie, S. (2010). DDSolver: an add-in program for modeling and comparison of drug dissolution profiles. *The AAPS Journal, 12*(3), 263-271.

Zhang, Z., Sha, X., Shen, A., Wang, Y., Sun, Z., Gu, Z., & Fang, X. (2008). Polycation nanostructured lipid carrier, a novel nonviral vector constructed with triolein for

efficient gene delivery. *Biochemical and Biophysical Research Communications, 370*(3), 478-482.

Zhao, S., Li, N., Garamus, V. M., Handge, U. A., Liu, J., Zhang, R., Willumeit-Römer, R., & Zou, A. (2016). Doxorubicin hydrochloride-oleic acid conjugate loaded nanostructured lipid carriers for tumor specific drug release. *Colloids and Surfaces B: Biointerfaces, 145*, 95-103.

Zheng, K., Zou, A., Yang, X., Liu, F., Xia, Q., Ye, R., & Mu, B. (2013). The effect of polymer–surfactant emulsifying agent on the formation and stability of α-lipoic acid loaded nanostructured lipid carriers (NLC). *Food Hydrocolloids, 32*(1), 72-78.

Zheng, M., Falkeborg, M., Zheng, Y., Yang, T., & Xu, X. (2013). Formulation and characterization of nanostructured lipid carriers containing a mixed lipids core. *Colloids and Surfaces A: Physicochemical and Engineering Aspects, 430*(Supplement C), 76-84.

Zirak, M. B., & Pezeshki, A. (2015). Effect of Surfactant Concentration on the Particle Size, Stability and Potential Zeta of Beta carotene Nano Lipid Carrier. *International Journal of Current Microbiology and Applied Science, 4*(9), 924-932.

LIST OF PUBLICATIONS AND PAPERS PRESENTED

List of Publications

1. **Latif, F. M.,** Teo, Y. Y., Misran, M., Suk, V. R. E., & Low, K. H. (2020). Formulation and physicochemical properties of nanostructured lipid carriers from beeswax and rosemary oil as a drug carrier. *Chiang Mai Journal of Science, 47*(1), 114-126.

2. Suk, V. R. E., **Latif, F. M.,** Teo, Y. Y., & Misran, M. (2020). Development of nanostructured lipid carrier (NLC) assisted with polysorbate nonionic surfactants as a carrier for l-ascorbic acid and Gold Tri. E 30. *Journal of Food Science and Technology*, 57(9), 3259-3266.

Paper Presented

1. **Latif, F. M.,** Teo, Y. Y., & Misran, M. (2017). *Formulation and characterization of nanostructured lipid carriers (NLC) for drug delivery*. Paper presented at 7th Asian Conference on Colloid and Interface Science, 8 – 11 August 2017, Kuala Lumpur, Malaysia.